MARMARA UNIVERSITY
INSTITUTE FOR GRADUATE STUDIES
IN PURE AND APPLIED SCIENCES

SYNTHESIS AND CHARACTERIZATION OF METAL FREE AND METAL PHTHALOCYANINES BEARING THYMOL MOIETIES DERIVED FROM ANTIMICROBIAL AND ANTIFUNGAL TERPENOIDS

ROVSHEN ATAJANOV

Master Thesis
Department of Chemistry
Organic Chemistry Program

THESIS SUPERVISOR
Prof. Dr. Zafer ODABAŞ

ISTANBUL, 2020

MARMARA UNIVERSITY
INSTITUTE FOR GRADUATE STUDIES
IN PURE AND APPLIED SCIENCES

SYNTHESIS AND CHARACTERIZATION OF METAL FREE AND METAL PHTHALOCYANINES BEARING THYMOL MOIETIES DERIVED FROM ANTIMICROBIAL AND ANTIFUNGAL TERPENOIDS

ROVSHEN ATAJANOV
520817906

Master Thesis
Department of Chemistry
Organic Chemistry Program

THESIS SUPERVISOR
Prof. Dr. Zafer ODABAŞ

ISTANBUL, 2020

MARMARA UNIVERSITY
INSTITUTE FOR GRADUATE STUDIES
IN PURE AND APPLIED SCIENCES

Rovshen ATAJANOV, a Master of Science student of Marmara University Institute for Graduate Studies in Pure and Applied Sciences, defended his thesis entitled **"Synthesis and characterization of metal free and metal phthalocyanines bearing thymol moieties derived from antimicrobial and antifungal terpenoids"**, on … January 2020 and has been found to be satisfactory by the jury members.

Jury Members

Prof. Dr. Zafer Odabaş   (Advisor)

Marmara University ………………………………………… …………………

Prof. Dr. Ümit SALAN   (Jury Member)

Marmara University …………………………………………

Assoc. Prof. Dr. Mevlüde Canlıca   (Jury Member)

Yıldız Technical University ………………………………… ……………………

APPROVAL

Marmara University Institute for Graduate Studies in Pure and Applied Sciences Executive Committee approves that Rovshen ATAJANOV be granted the degree of Master of Science in Department of Chemistry, Organic Chemistry Program on January 22 2020. (Resolution no: 2020/.03-.02…….).

Director of the Institute

Prof. Dr. Bülent EKİCİ
Enstitü Müdürü

ACKNOWLEDGEMENTS

My journey as a Master of Science student is one that I will never forget nor the people who were a part of it. First of all, I would like to introduce my sincere thanks to my Thesis Supervisor Prof. Dr. Zafer Odabaş. He has motivated, encouraged and supported me whenever I needed help. His support and guidance were the biggest reason for me to be able to finish this thesis. Memories of his kind friendship will always remain with me.

I am very grateful to Prof. Dr. Mahmut Durmuş for his useful discussion and helpful advices whilst our research on photophysical and photochemical characterization of phthalocyanine compounds at Gebze Technical University. It was a privilege working with him.

My profound thanks to Prof. Dr. Andreas Schmidt, Daniel Grosch and Harun Tas from Clausthal University of Technology for their kind hospitality and big support during my Erasmus+ student exchange program.

My special thanks to my friend PhD candidate Safinaz Şahin for her generous assistance in our laboratory during my thesis work.

I would also like to acknowledge the entire Chemistry Department staff for their kindness, helpfulness and tolerance.

My family have provided so much support wherever I have been. This thesis could not have been written without their support. I would like to express my sincerest gratitude towards my parents, my sisters and my little brother.

Last, but not least, tremendous thanks go to my friends.

January 2020   Rovshen Atajanov

I

DECLARATION

The present work was carried out from September 2018 until January 2020 under the supervision of Prof. Dr. Zafer Odabaş at the Institute for Graduate Studies in Pure and Applied Sciences of Marmara University. Author has accomplished this research subject by himself and used only the indicated sources and auxiliary aids. The thesis is the work of the author except where acknowledged by reference and has not been submitted for any other degree.

STATEMENT OF COPYRIGHT

January 2020   Rovshen Atajanov

TABLE OF CONTENTS

ABSTRACT

SYNTHESIS AND CHARACTERIZATION OF METAL FREE AND METAL PHTHALOCYANINES BEARING THYMOL MOIETIES DERIVED FROM ANTIMICROBIAL AND ANTIFUNGAL TERPENOIDS

Phthalocyanines (Pcs) are tetrapyrrolic macrocycles with 18 delocalized π-electrons and are synthetic analogues of naturally occurring porphyrins. Along with their chemical and physical stability, their architectural flexibility and broad spectroscopic properties attract the interest of chemists, physicists and industrial scientists since the discovery of their synthesis. Modifications in axial or peripheral positions of Pc ring yield wide distribution of physical and chemical characteristics [1].

Thymol is phenolic monoterpenoid compound obtained from essential oils of *Thymus vulgaris*, *Monarda puctata* [2] and various other kinds of plants. It shows wide biological activities against cancerogenous cells [3], microbial diseases [4] and also has been known to exhibit anti-inflammatory [5] and anti-oxidative effects [6].

In this work, nucleophilic substitution and azo coupling reactions were carried out between thymol and phthalonitrile compounds. Using the starting compounds obtained from these reactions, new metallo- and metal-free Pcs were synthesized in order to investigate their potential applications suitable with their chemical and physical characteristics. Furthermore, photophysical and photochemical properties of some of newly synthesized Pcs were investigated for photodynamic therapy (PDT) studies.

The structures of new compounds were determined based on the results of spectroscopic methods such as FT-IR, UV-*vis*, NMR and MALDI TOF MS.

Throughout this thesis it has been shown that phthalocyanines are among the most versatile and interesting compounds within molecular materials. Although technological applications based on these compounds already exist in the market, the design of phthalocyanines with suitable properties for specific applications will continue to be studied due to the possibilities of improvement and the appearance of new properties and applications of these compounds.

January 2020   Rovshen Atajanov

ÖZET

ANTİMİKROBİYAL VE ANTİFUNGAL ÖZELLİKLİ TERPENOİDLERDEN OLAN TİMOL VE TÜREVİ BiLEŞİKLERDEN METALLİ VE METALSİZ FTALOSİYANİNLERİN SENTEZİ VE KARAKTERİZASYONU

Ftalosiyaninler (Pcs), 18 tane delokalize π elektronuna sahip tetrapirol makrohalkalı bileşikler olup, doğal bileşikler olan porfirinlerin sentetik türevleridir. Kimyasal ve fiziksel dayanıklılıklarının yanı sıra tasarım esneklikleri ve geniş spektroskopik özellikleri, sentezlerinden bu yana kimyagerlerin, fizikçilerin ve endüstriyel bilim insanlarının ilgisini çekmektedir. Pc halkasının aksiyal veya periferal konumlarında yapılan değişiklikler bu bileşiklere çok geniş yelpazede fiziksel ve kimyasal özellikler kazandırabilir [1].

Timol, monoterpenoid sınıfı fenol bileşiklerinden olup *Thymus vulgaris, Monarda puctata* [2] ve birçok farklı bitkilerin esansiyel yağlarından elde edilir. Timol, kanser hücrelerine [3] ve mikrobiyal hastalıklara [4] karşı geniş bir aktivite göstermekle beraber, anti oksidatif [6] ve iltihaplanmaya karşı [5] etkileri vardır.

Bu çalışmada, timol ve ftalonitril bileşikleri arasında nükleofilik sübstitüsyon ve azo kenetleme reaksiyonları gerçekleştirilmiştir. Bu reaksiyonlardan elde edilen bileşiklerden, fiziksel ve kimyasal özelliklerine göre potansiyel kullanım alanlarını incelemek üzere metalli ve metalsiz Pc bileşikleri sentezlenmiştir. Ayrıca, bazı bileşiklerin Fotodinamik Terapi (PDT) çalışmaları için, fotofiziksel ve fotokimyasal özellikleri araştırılmıştır.

Sentezlenen yeni bileşiklerin yapıları FT-IR, UV-*vis*, NMR ve MALDI TOF MS gibi metotlarla analiz edilmiş ve aydınlatılmıştır.

Bu tez boyunca Pc'lerin moleküler materyaller arasında en çok yönlü ve ilginç bileşikler olduğu gösterilmiştir. Bu bileşiklere dayanan teknolojik uygulamalar halihazırda piyasada mevcut olsa da spesifik uygulamalar için uygun özelliklere sahip Pc'lerin tasarımı, bu olasılıkların iyileştirilmesi ve yeni özelliklerinin ve uygulamalarının ortaya çıkarılması amacıyla incelenmeye devam edecektir.

Ocak 2020   Rovshen Atajanov

LIST OF SYMBOLS

Ac$_2$O	Acetic anhydride
AcONa	Sodium acetate
Bu	Butyl
^{o}C	Cercius Degree
CDCl$_3$	Deutero Chloroform
(CH$_3$COO)$_2$O	Acetic anhydride
CHCl$_3$	Chloroform
CH$_2$Cl$_2$	Dichloromethane
cm^{-1}	1/Cantimeter (Wave number)
^{13}C-NMR	Carbon Nuclear Magnetic Resonance Spectroscopy
CoPc	Cobalt (II) phthalocyanine
CuPc	Copper (II) phthalocyanine
d$_6$-DMSO	Deuterated Dimethylsulfoxide
d	Day
ΔE	Energy difference
ε	Extinction coefficient, dm^3 mol^{-1} cm^{-1}
FePc	Iron phthalocyanine
G	Gram
^{1}H-NMR	Proton Nuclear Magnetic Resonance Spectroscopy
H$_2$Pc	Metal free phthalocyanine

InOAcPc	Indium (III) acetate phthalocyanine
K$_2$CO$_3$	Potassium carbonate
kj	kilo joule
L	Ligand
LiOMe	Lithium methoxide
LiOPent	Lithium pentoxide
LuOAcPc	Lutetium (III) acetate phthalocyanine
M	Metal or Molar
MeOH	Methanol
mL	Milliliter
min	Minutes
MgPc	Magnesium (II) phthalocyanine
MnPc	Manganese (II) phthalocyanine
MPc	Metal phthalocyanine
NaNO$_2$	Sodium nitrite
-NH$_2$	Amino group
NH$_4$OH	Ammonium hydroxide
Nm	Nanometer
-NO$_2$	Nitro group
OAc	Acetyl
Si	Silicon
SOCl$_2$	Thionyl chloride

t-Bu	Tertiary butyl
TiO$_2$	Titanium dioxide
Zn(OAc)$_2$	Zinc (II) acetate
ZnPc	Zinc (II) phthalocyanine

LIST OF ABBREVIATIONS

BAM-SiPc®   Bisamino silicon (IV) phthalocyanine, SiPc[$C_3H_5(NMe_2)_2O$](OMe)

DBU   1,8-diazabicyclo[5.4.0]undec-7-ene (basic solvent)

DBN   1,5-diazabicyclo[4.3.0]non-5-ene (basic solvent)

DCM   Dichloromethane

DMF   Dimethylformamide

DMSO   Dimethylsulphoxide

DPBF   1,3-diphenylisobenzofuran

DSSC   Dye Sensitized Solar Cells

FT-IR   Fourier-transform infrared spectroscopy

HOMO   Highest Occupied Molecular Orbital

HCl   Hydrochloric acid

LUMO   Lowest Unoccupied Molecular Orbital

MeOTPD   N,N,N′,N′-Tetrakis(4-methoxyphenyl)benzidine

MALDI TOF MS   Matrix Asisted Laser Desorption Ionization Time of Flight Mass
Spectroscopy

MPc   Metallo phthalocyanine

NIR   Near Infrared

NLO   Nonlinear optics

NMR   Magnetic Resonance spectroscopy

OFET   Organic Field Fffect Tansistors

OLED	Organic Light-Emitting Diode
Pc	Phthalocyanine
PDT	Photodynamic Therapy
PS	Photosensitizer
SubPc	Pc analogs that consists of 3 isoindole units instead of 4
THF	Tetrahydrofuran
TLC	Thin Layer Chromatography
TMS	Tetrametylsilane
UV	Ultraviolet
UV-*vis*	Ultra violet – visible spectroscopy

LIST OF FIGURES

XIV

XV

XVI

LIST OF SCHEMES

CHAPTER 1. INTRODUCTION

Pcs have been major source of interest since the discovery of their unexpected synthesis in the beginning of the last century [7]. The reason for such intense interest to these macrocycles was because of their high stability, architectural flexibility and unique spectral properties [8]. Due to the ease of the modifications on the Pc ring, optional adjustments can be made to improve their properties. For example, Pc aggregation can be decreased and solubility can be enhanced by introducing bulky groups with alkyl chains to the axial and peripheral positions of the Pcs. On the other hand, while the hydrogen atoms in the Pc core can be replaceable by more than 70 different metals and metalloids, this advantage offers additional features for synthetic organic chemists to optimize the physical responses of the Pcs [9].

Pcs are highly colored, planar and 18π electron cyclic oligopyrrole aromatic systems composed of four iminoisoindoline units where the pyrrole groups are conjugated to benzene rings and bridged by nitrogen atoms [10]. Since these heteroaromatic macrocycles are typical near infrared (NIR) dyes and have a strong blue and green color, they have been used extensively in dye and pigment industry [11]. By introducing various chromophores into the Pc core, to broader spectral range of absorption can be reached and higher extinction coefficients can be achieved [12].

Based on these attributes, Pc properties can be improved for the potential applications. In this thesis work, we introduced biologically active thymol compounds to phthalocyanine ring with either oxo and azo bridges. We observed that the absorption bands of azo bridged Pcs considerably red shifted compared to their oxo bridged derivatives. We have also investigated photophysical and photochemical properties of some of our newly synthesized oxo bridged phthalocyanines.

CHAPTER 2. GENERAL INFORMATION

2. 1. Brief history of phthalocyanines

The discovery of the Pcs that have become known for their color brilliance and scope, dates back to the early twentieth century. Although the importance of this discovery was not yet known at the time, A. Braun and J. Tcherniac from South Metropolitan Gas Company (London) were able to synthesize small amounts of a blue, alcohol insoluble residue as a by-product during the melting of o-cyanobenzamide [13]. Only a few years later, more precisely in 1927, scientists Henri de Diesbach and Edmond von der Weid from University of Freiburg (Switzerland) published a paper on the behavior of o-dinitriles towards copper salts and pyridine. Upon boiling a mixture of o-dibromobenzene and copper cyanide in pyridine, they obtained an indigo blue solid that was not soluble in water, alcohol, or ether. Elemental analyses were used to perform at least a crude determination of the molecular formula, but a detailed structure could not be determined [14]. The most important step in the discovery of Pc achieved a year later on the premises of Scottish Dyes LTD, during the industrial production of phthalimide from phthalic acid. At a broken point of the enameled iron kettle, a blue-green solid separated, which, after further investigation, was characterized as being a highly stable and insoluble dye [15,16]. Three employees recognized the potential of the new color pigment and patented both the manufacturing process and its production. Application for the company acquired in 1928 by ICI (Imperial Chemical Industries). For its part, the ICI was keen to explore the structure of the new color pigment and sent a sample to J. F. Thorpe at Imperial College in London. This transferred the enlightenment of the structure to an emerging scientist named R. P. Linstead [16]. The resulting collaboration between ICI and Linstead proved fruitful cooperation. Already in 1934 Linstead was able to determine the structures of H_2Pc and some MPc by means of elemental analysis and characterization of decomposition products. In the MPc investigations, Linstead concentrated mainly on the central atoms magnesium and iron, but was also able to report derivatives with the transition metals including cobalt, nickel and copper [16-22]. The structure proposal for the phthalocyanine scaffold, which dates from 1933, was completed in 1936 with the help of X-ray examinations (Figure 1) by JM Robertson be assured [23].
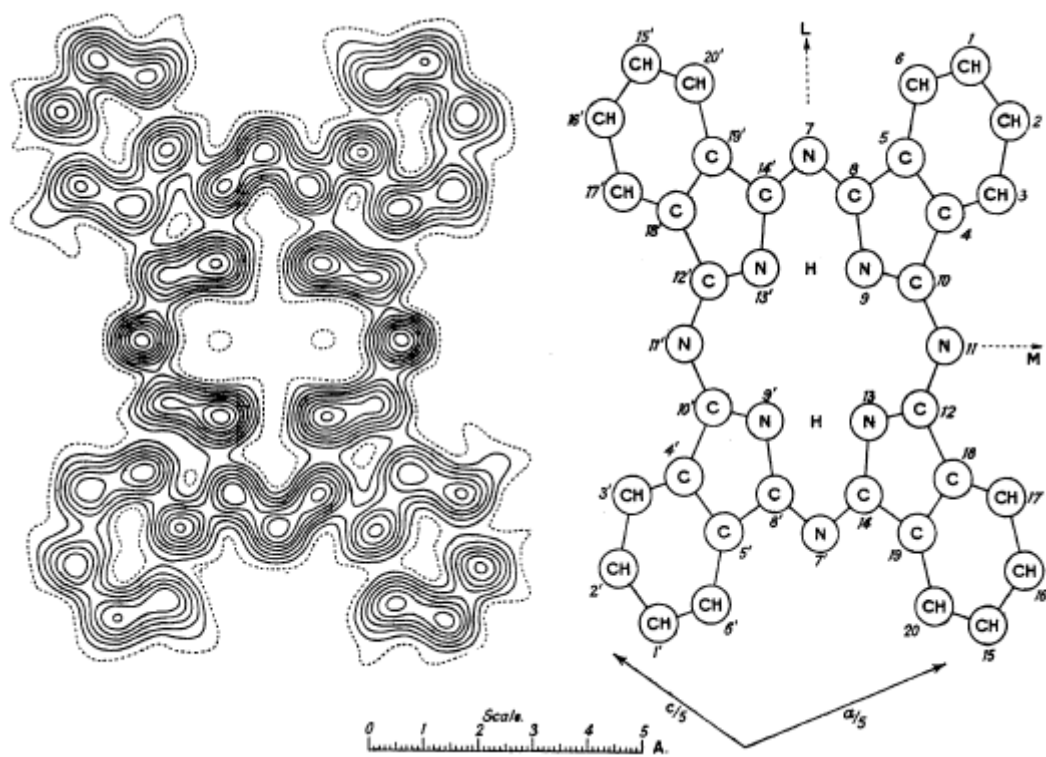
Figure 2.1. X-ray structure analysis of the H_2Pc molecule dates back to 1936.

2. 2. Structure and nomenclature

Porphyrins are derived from the main body porphine by substitution of hydrogen atoms of the tetrapyrrole skeleton by organic residue groups. They have a cyclic conjugated π-electron system and they have known for their metal complexes with Mg^{2+} (chlorophyll, leaf pigment of green plants), Fe^{2+} (heme, component of proteins for the oxygen transport of vertebrates) and Co^{3+} (vitamin B12) in nature [24]. The Pcs, that are not available in nature, can be described as tetrabenzotetraazaporphines (Figure 2). The four benzopyrrole units are linked by nitrogen bridges. The planar heteroaromatics are characterized by a high thermal and chemical stability. The phthalocyaninato dianion can act as a tetradentate ligand for metal cations and form extremely stable metal complexes. The four metal-nitrogen bonds are equivalent and are predominantly covalent in the case of 3d metals, at least from manganese to copper [25]. In tri- or quadruple-positive metal ions, one or two axial ligands are bound to the central metal atoms. For complexing, more than 70 elements are suitable [26a]. Pcs, through their

delocalized 18-electron system (Figure 2.2) have specific electronic and optical properties that can be further influenced by variation of metal cation and substituents.

Porphyrin   **Phthalocyanine**
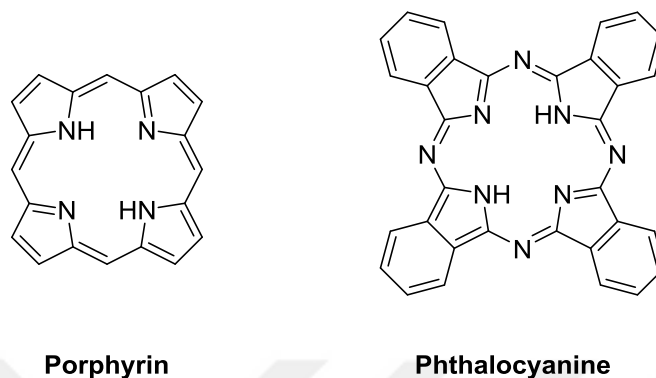
Figure 2.2. Structures of porphyrin and phthalocyanine

The name phthalocyanine proposed by Linstead is derived from the prefix *phthalo*, which describes the relationship to phthalic acid and is complemented by the root word *cyanos* (greek: blue), which reflects the deep blue character of the unsubstituted compounds. According to IUPAC recommendation, these macrocyclic compounds named as 29H,31H-tetrabenzo[b, g, l, q]-5,10,15,20-azaporphyrin [26b].

Pcs are a class of macrocyclic compounds with an alternating carbon-nitrogen ring system. With its 42 π electrons, of which 18 π-electrons form a planar, continuous cycle, the dianionic (doubly negatively charged) phthalocyanine fulfills the Hückel rule (4n+2), which is crucial for aromaticity, and thus its structure closely related to porphyrin, which, for example, is a vital constituent of hemoglobin [27a]. Replacing the four bridging methine carbon atoms of the porphyrinoid macrocycle with nitrogen atoms leads to porphyrazine, the direct precursor of phthalocyanine. Anellation of four benzoic arene units to the aromatic porphyrazine skeleton yields the colorful Pc macrocycle. Extending the existing aromatic system by another four benzoic arene units yield another structural derivative of phthalocyanine, the naphthalocyanine [27b]

As shown in Figure 2.3, 16 free positions on the backbone are available for the modification of phthalocyanine. The carbon atoms 2, 3, 9, 10, 16, 17, 23, 24 are

generally referred to as peripheral (p) positions and the atoms 1, 4, 8, 11, 15, 18, 22, 25 are designated as nonperipheral (np) positions. If either all peripheral and non-peripheral positions are substituted, an octa-substituted phthalocyanine is obtained, which is identified by the abbreviation (o). Further variations are possible through the incorporation of various cations. In this case, the embedded central atom (M) originating from the periodic table is preceded by the abbreviation Pc, which stands for the Pc, hence the name MPcs. Metal-free Pcs are described with H_2Pc. For compounds with axial (a) ligands, the metal is preceded by the corresponding substituent in brackets. The compound 2,3,9,10,16,17,23,24 octapentyloxyphthalocyaninato-silicon-dichloride would be referred to briefly as a-$(Cl)_2$Si-op-OC_5H_{11}, the OC_5H_{11} designating the alkoxy carbon chain [27b].
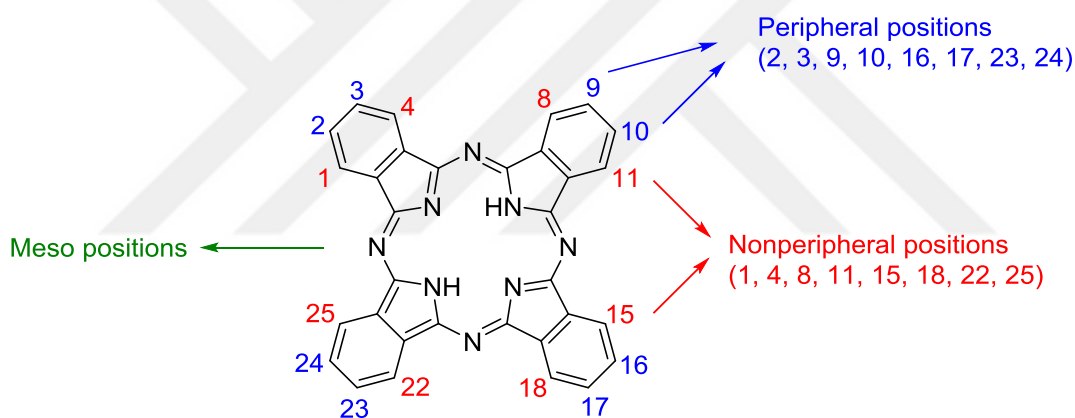
Figure 2.3. Numbering of phthalocyanines as recommended by IUPAC

2. 3. Synthesis of phthalocyanines

The literature describes a variety of synthetic routes to MPcs, which are summarized in Scheme 2.1. The most important methods are reductive cyclotetramerizations of phthalonitrile (PN) or diiminoisoindoline [28]. Phthalic acid, phthalic anhydride, phthalimide, 2-cyanobenzamide or o-dibromobenzene can also be used as starting materials. However, phthalonitrile and diiminoisoindoline are thought to be formed *in situ* during the reaction of these compounds, and thus they are responsible for the actual

cyclization [29]. In all of these reactions, typically four equivalents of the phthalic acid derivative are reacted with one equivalent of the corresponding metal or metal salt at temperatures above 150 °C in the melt or in high boiling solvents. Often also ammonia sources such as urea are added, which favor the in-situ formation of diiminoisoindolin. As a rule, these synthetic strategies can also be applied to substituted phthalic acid derivatives for the formation of substituted Pc. Furthermore, MPcs can be obtained by metalation of H_2Pc or labile metallophthalocyanines [PcM'] such as [PcLi$_2$] or [PcK$_2$].
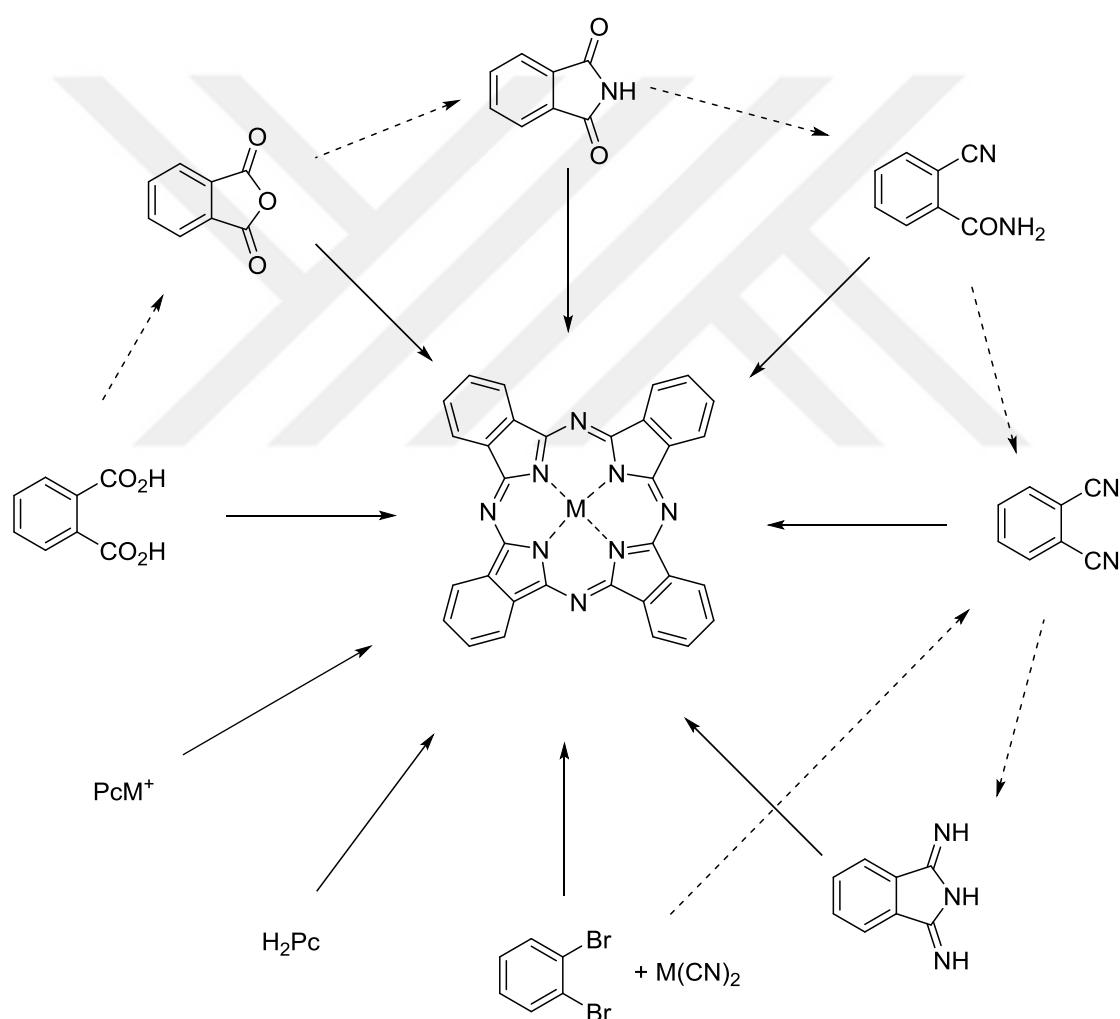
Scheme 2.1. Synthetic methods for metallophthalocyanines

One of the widely used methods in the preparation of substituted Pcs is synthesis from phthalonitriles in 1-pentanol [30]. In this method, a suitable lithium or sodium or potassium alcoholate was initially added and the resulting phthalocyaninato complex subsequently demetalated [31]. The use of strong organic bases and the alcohol instead of metal alcoholates allows the synthesis of phthalocyanines under milder reaction conditions and with higher yields. 1,8-diazabicyclo [5.4.0] undec-7-ene (DBU) is used in the preparation of MPcs and 1,5-diazabicyclo [4.3.0] non-5-ene (DBN) (Figure 2.4) for H_2Pc. Weaker bases than DBU or DBN lead to lower yields or contaminated products. It is assumed that the formation of a balance between alcohol and alcoholate. The yield of MPcs is lower when using alcohols with lower boiling point than 1-pentanol [32].

DBU **DBN**

Figure 2.4. Structures of 1,8-diazabicyclo [5.4.0] undec-7-ene (DBU) and 1,5-diazabicyclo [4.3.0] non-5-ene (DBN)

The Pc formation does not proceed according to a uniform mechanism, since many different routes lead to Pcs. The mechanisms have not fully understood, because the cyclotetramerization reaction is highly exothermic and takes place under drastic conditions, which complicates mechanistic studies [33]. However, several intermediate steps have been isolated and targeted experiments carried out [34].

Alkoxides serve as "catalysts" in the reaction described in alcohol. They activate a phthalonitrile molecule (**I**) by binding to a nitrile carbon atom. The then negatively charged nitrogen atom nucleophilically attacks the carbon atom of the vicinal nitrile group to form a five-membered ring. **II** is a 1-alkoxy-3-iminoisoindole derivative. Next, the negatively charged nitrogen atom of **II** attacks another phthalonitrile molecule (**I**). Analogous ring closure to the isoindole skeleton yields **III**, which could be isolated

from nitrosubstituted phthalodinitriles. Reaction with two other phthalonitriles (**I**) leads to **IV**. It is also conceivable that two **III** ions form **III'** upon coordination to a metal (Scheme 2.2) [34b].

In addition to the activation of the phthalonitrile, the alkoxide group also has crucial importance in the ring closure favored by the template effect. The imino group attacks the aryl ether nucleophilically. In this case, an aldehyde cleaved rather than an alkoxide [34b, 35]. A two-electron reduction of the macrocycle followed by Hückel aromaticity $(4n + 2)$ for the inner conjugated system. The protons released during the oxidation of the alcoholate to the aldehyde are also trapped by alcoholation [34b].

However, alkoxides are reactive compounds and may react with intermediates during cyclotetramerization. It has been shown that the yield of phthalocyanine increases when the alcoholic ions are trapped after the initial activation of the phthalonitrile with water [34b].
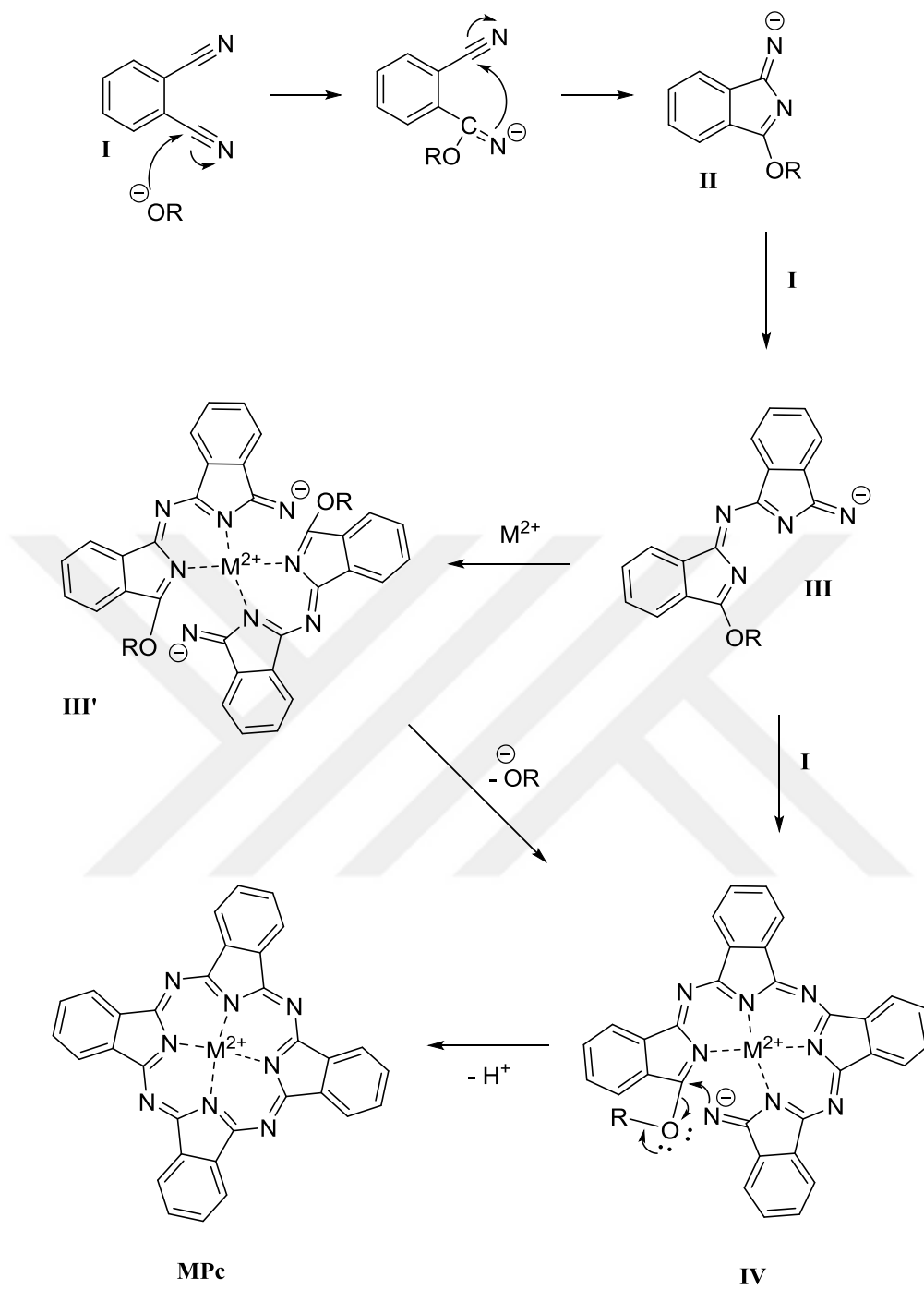
Scheme 2.2. Mechanism of phthalocyanine formation

2. 4. Subphthalocyanines

More than 20 years since its initial synthesis and structural elucidation [36], no further research on subphthalocyanines has been reported because of their difficult synthesis and purification [37]. It was not until their application to prepare unsymmetrical phthalocyanines by a ring-extension reaction of a subphthalocyanine and their nonlinear optical properties that they became interesting again [38]. Subphthalocyanines [37a, 38, 39] are the smallest homologues of Pcs and consist of three iminoisoindole units, which coordinate a trivalent boron atom. Subphthalocyanines with elements other than boron are not known. Subphthalocyanines, in contrast to most metal phthalocyanines, are not planar but have a dome-shaped structure. In addition to steric reasons, this is because the boron is coordinated tetrahedrally. With their delocalized 14 π-electron system, subphthalocyanines are aromatic, although they lack a planar structure [27c,39,40].

An anionic, axial ligand must be bound to the sp^3-hybridized B^{3+} ion. Subphthalocyanines are synthesized in a cyclotrimerization reaction of a phthalonitrile in the presence of a boron compound; often, a boron trihalide BX_3 is used. Accordingly, a subhalophthalocyanine with an axial halide ligand, which can be substituted by nucleophiles such as alcohols, is obtained. This ligand substitution opens the way for the functionalization of subphthalocyanines. Although the chemical and thermal stability of subphthalocyanines is sufficient for the chemical modification of their peptides, they are reactive compounds that are less stable than their phthalocyanine homologues [27c,40].

Although the first synthesis took place in 1972, a comprehensive study on the optimization of reaction conditions was not published until 2003 [41]. A mechanistic study of the formation of chlorido-subphthalocyaninato boron (III) showed that presumably first an adduct of the two educts phthalonitrile (**I**) and BCl_3 is formed, which undergoes a rearrangement to the intermediate **V**. This intermediate **V** cyclotrimerized to the sub-phthalocyanine parent structure. This is then reduced by transferring two electrons to the macrocycle in a presumably BCl_3-catalyzed elimination of chlorine (Scheme 2.3) [42]. Alkylaromatics in the reaction medium, eg. solvents such

as xylene and toluene can partially prevent the formation of by-products such as peripherally halogen-substituted subphthalocyanines [43].
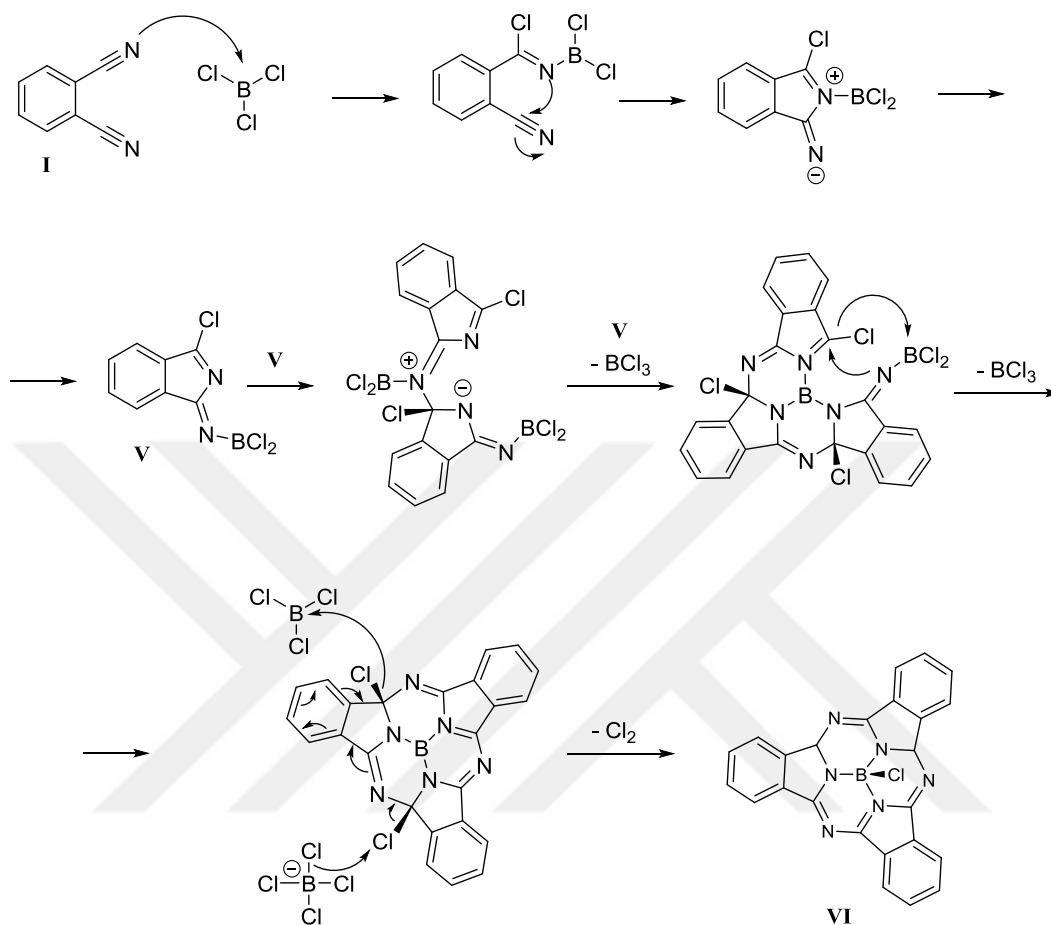
Scheme 2.3. Mechanism of SubPc formation

The UV-*vis* spectra of subphthalocyanines are dominated by the Q and B bands, as in Pcs. These are hypsochromically displaced by the smaller conjugated electron system (14 instead of 18 π electrons) compared to MPcs and the absorption coefficients are slightly lower [44,45]. Peripheral donor and acceptor substituents lead to a red shift of the Q band, while the influence of axial ligands is negligible [45].

In addition to the synthesis of unsymmetrical Pcs and the investigation of nonlinear optical properties, subphthalocyanines are still interesting objects for potential applications, i. a. as liquid crystals, in supramolecular assemblies, in donor-acceptor combinations for photovoltaic systems, and in molecular sensors and OLEDs [45,46]. In

particular, the nonplanarity of an aromatic system continues to make them scientifically interesting [46]. In addition, subphthalocyanines are not centrosymmetric; together with its dome-shaped structure, this results in chirality in the isomer mixture of a synthesis with unsymmetrically substituted dinitriles [27c,45,46].

2.5. Structural considerations

2.5.1. Structure types depending on the central atom

Due to the large number of metallic and non-metallic cations, which are suitable as a central atom for the Pc macrocycle, only a few examples can be shown in this section. These should help to get a rough overview of the structure types of Pcs depending on the central atom. In general, many of the metals are capable of forming several types of structures depending on the metal salt and reaction conditions chosen. A detailed discussion of the individual types can be found in the relevant literature [47]. With their four coordinating nitrogen atoms, Pcs are particularly well suited as ligands for metal ions. While metal-free Pcs form only one structure, the MPcs generate not only simple coordination compounds (PcM) but also structures with complex symmetries (see Figures 2.5 and 2.6). Decisive for which of these structures arises is the oxidation state of the corresponding metal. Since the phthalocyanine itself is in the -2 oxidation state, it requires either two cations with the oxidation state +1 or a cation with the formal oxidation number +2 to obtain its charge neutrality. If the metal is present in a higher oxidation state than +2, multiple coordination by the macrocycle (Pc_2M, Pc_3M_2) or additional ligands are necessary to ensure charge neutrality of the whole molecule. Complexes (PcM_2) with cations of oxidation +1 are known from the metals lithium [48, 49], sodium [50] and potassium [50]. Structures of composition PcM are e.g. of the divalent metals magnesium, zinc, cobalt, nickel, lead, iron, copper, cadmium, etc [51]. So-called Pc_2M sandwich compounds or Pc_3M_2 triple-decker structures are mainly formed by the lanthanides yttrium [52], lanthanum [53], cerium [54, 55] or gadolinium [53]. The individual structure types are shown in Figure 2.5.

PcM

PcM$_2$

Pc$_2$M

[PcM]$_n$, Pc$_3$M$_2$ (n=1)

Stapled Pc$_2$M

Bicyclic PcM
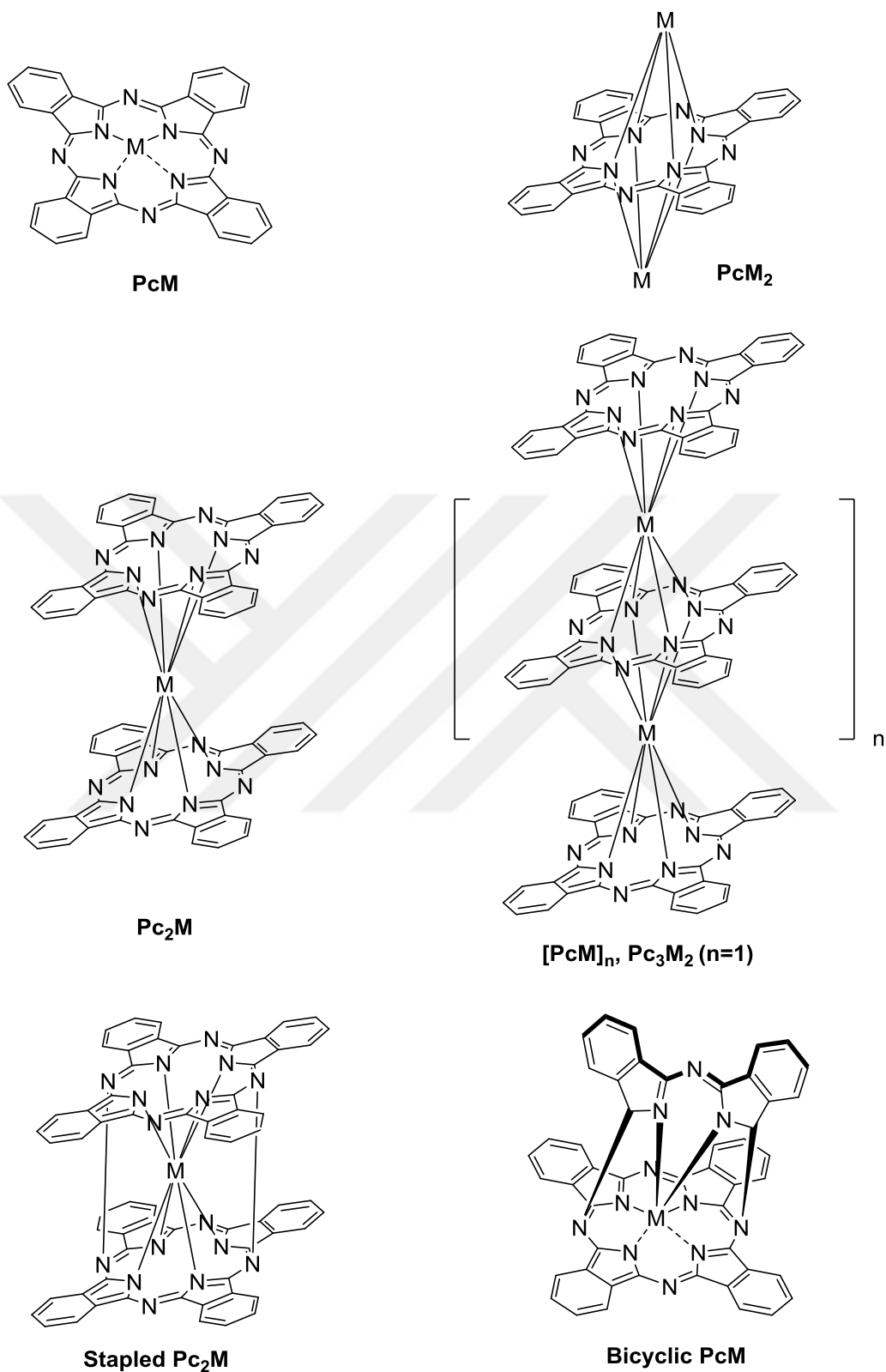
Figure 2.5. Structures of various metal-phthalocyanine complexes

13
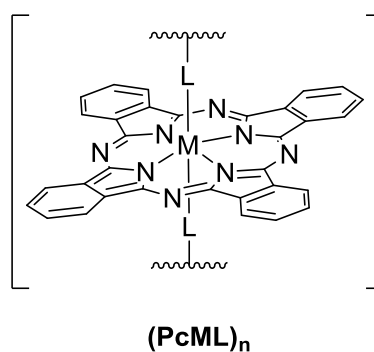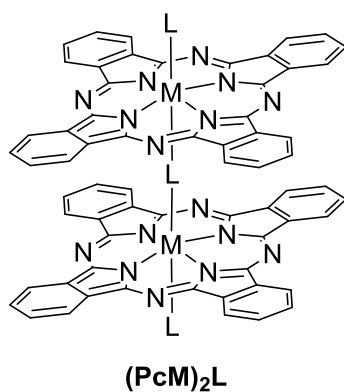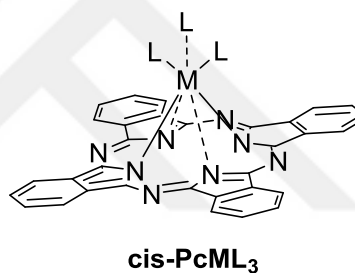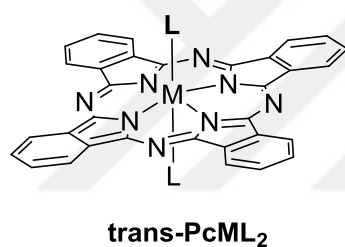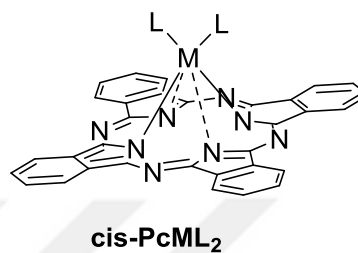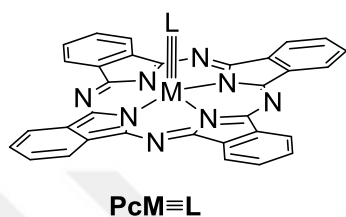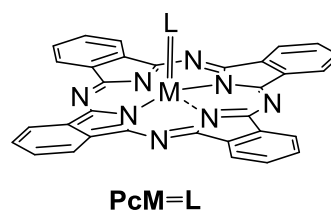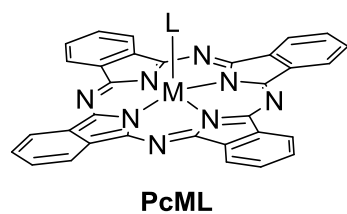
Figure 2.6. Structures of various metal phthalocyanine complexes with additional ligands.

In addition to the compounds just described with monovalent or divalent cations as well as the sandwich compounds, there are also numerous MPcs with high-value central atoms. Due to the increasing charge on the metal (oxidation states greater than +2), the Pc macrocycle alone is no longer able to achieve the desired charge neutrality, as a result of which additional ligands are needed to compensate for the additional charge. Halides [56-58], oxides [59] and hydroxides [60] as well as coordinating heterocycles such as pyridine [61] are used as additional ligands. Particular preference is given to the coordination compounds with halides as counterions, which are easily accessible in view of their diversity and high availability. An overview of known structures of metal phthalocyanine complexes with additional ligands is shown in Figure 2.6. Structures of the PcML type are formed, for example, by the elements of the 3rd main group of the periodic table, such as aluminum [56], gallium [56] and indium [57].

The elements boron and uranium occupy a special position. Boron does not form a classical Pc structure but occurs as subphthalocyanine. The subphthalocyanine formally consists of only three benzopyrrole units, which are also linked via azo bridges (Figure 2.7) [62]. Uranium is able to form a superphthalocyanine in addition to the conventional Pc structures, which formally consists of five benzopyrrole units (Figure 2.7) [63].
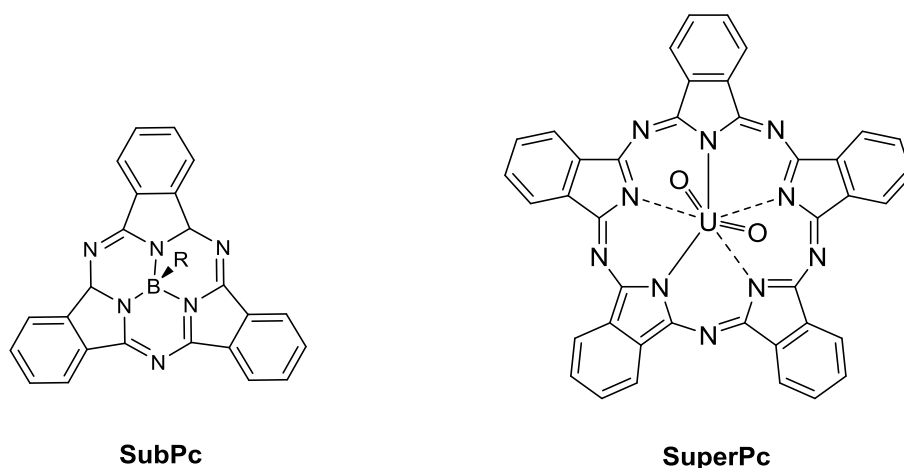
SubPc   **SuperPc**

Figure 2.7. Structures of subphthalocyanine (SubPc) and superphthalocyanine (SuperPc)

2.5.2. Symmetrical and asymmetrical substitution of macrocycles

Structural variations involving the ligand are generally determined by the dinitrile precursors used in the cyclization. Depending on the substitution and symmetry of the precursor, a large number of isomeric, symmetrical and unsymmetrically substituted phthalocyanines can be obtained [64]. Scheme 2.4 shows the four possible regioisomers which can be obtained by cyclization of a 4-position monosubstituted dinitrile [65].
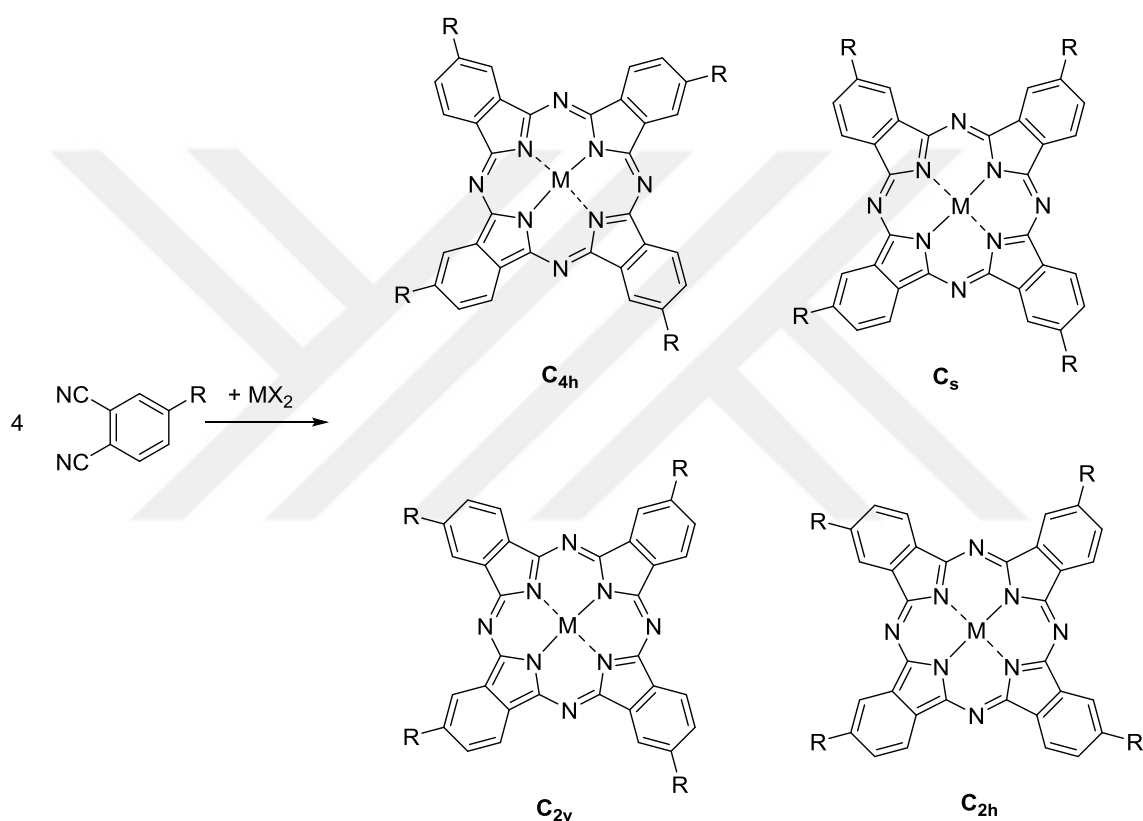
Scheme 2.4. Regioisomers of tetrasubstituted metal phthalocyanines.

The different symmetries of the isomers have an influence on the optical properties of the Pcs. If the symmetry is further reduced by the presence of one or more axial ligands on the metal, different enantiomers must also be taken into account because of the axial chirality. Due to the identical molecular weight and the similar polarities of the isomers, mixtures are generally difficult or impossible to separate. If two different dinitriles **A** and **B** are used for the cyclization, depending on the ratio used, heterogeneously

assembled hybrid macrocycles of different symmetry are obtained in addition to the uniform A4 and B4 systems (Figure 2.8) [65,66]. The asymmetric introduction of substituents yields various benefits, such as increasing solubility due to decreased aggregation. For specific applications, the introduction of a certain number of functional groups at specific sites of the ligand may also be useful. The most important reason for the synthesis of such A_nB_m Pcs is because of the change in the photophysical properties, which is achieved by changing the polarity and polarizability of the macrocycles. For example, A_3B_S systems are interesting materials in nonlinear optics (NLO) [67].
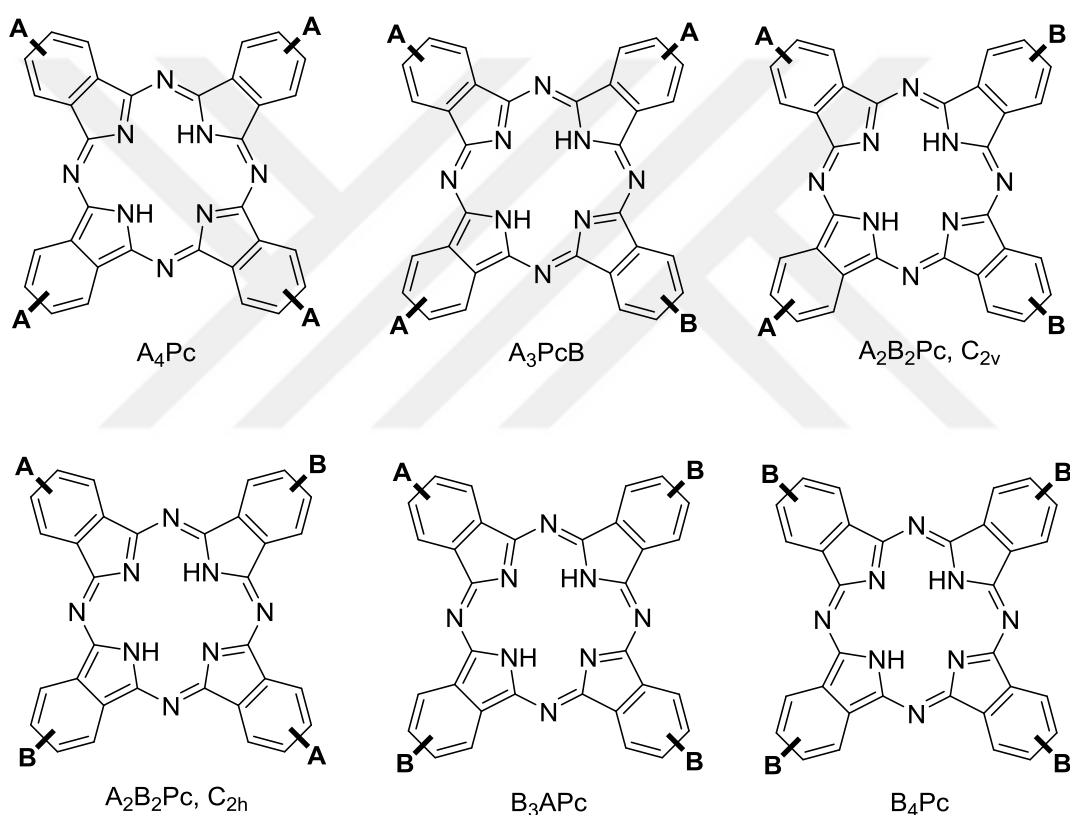
Figure 2.8. Different A_nB_n Phthalocyanines.

The synthesis of unsymmetrically substituted Pcs can be achieved by random co-cyclization of the corresponding dinitrile precursors, wherein the product mixture obtained can be separated by chromatography in the case of soluble phthalocyanines. Selective methods for the preparation of A_3B systems include the ring expansion of subphthalocyanines by diiminoisoindolines [68] (Scheme 2.5) and polymer-assisted

methods [69]. Depending on the synthetic effort required to prepare the desired materials as well as the separability of product mixtures, it must be considered in each case whether the selective methods provide an advantage over statistical co-cyclization. In general, it should be noted that for insoluble Pcs the selective methods are to be preferred since chromatographic purification is not possible. In the case of soluble, substituted Pcs, the chromatographic separation of the products is often less expensive than, for example, the preparation and purification of the corresponding subphthalocyanines and diiminoisoindolines.
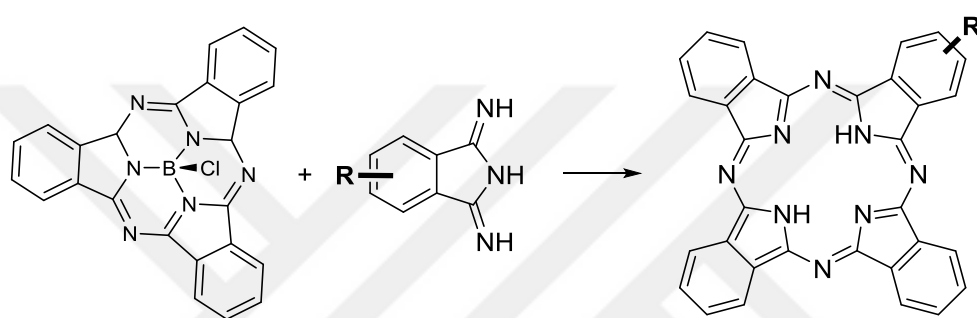
Scheme 2.5. Selective preparation of an A_3B phthalocyanine by ring extension on a subphthalocyanine.

C_{2v}-symmetric A_2B_2 Pcs are potential candidates for NLO applications because of their polarizability, similar to A_3B Pcs. *NOLAN et al.* developed a selective synthetic strategy starting from "semi-phthalocyanines" (Scheme 2.6) [70]. "Semi-phthalocyanines" are first prepared from the corresponding phthalonitrile and LiOMe in methanol. In the subsequent cyclization they are stirred with an excess of the second dinitrile in dimethylaminoethanol with a metal salt at 60 °C. The low reaction temperature prevents the homocyclization of the second dinitrile, so that C_{2v}-symmetric A_2B_2 Pcs selectively formed.
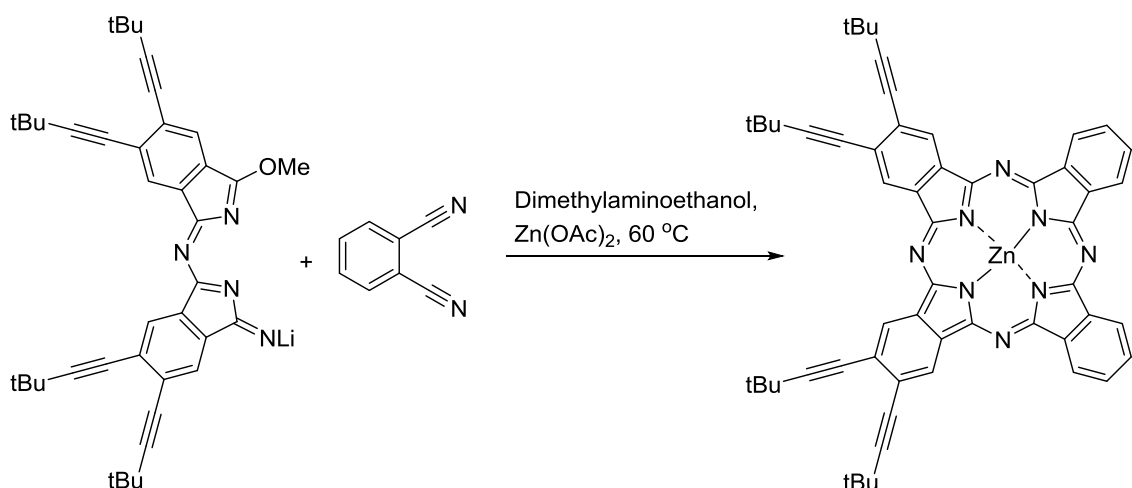
Scheme 2.6. Selective preparation of A_2B_2 phthalocyanines.

2.6. Properties of phthalocyanines

2.6.1. Absorption behavior

Due to the internal 18π electrons of the ring system, the Pcs have a large number of delocalized electrons, which is why they show interesting absorption properties. The Pcs are deeply colored compounds, in the solid state they have a blue-violet to dark-green color depending on the modification, in the solution they show a blue to green color [71]. In the UV/*vis* range, the metal-containing Pcs have two absorption bands, the intense Q band and less intense Soret band, which are due to $\pi \rightarrow \pi^*$ and $n \rightarrow \pi^*$ transitions, respectively [72] (Figure 2.9).
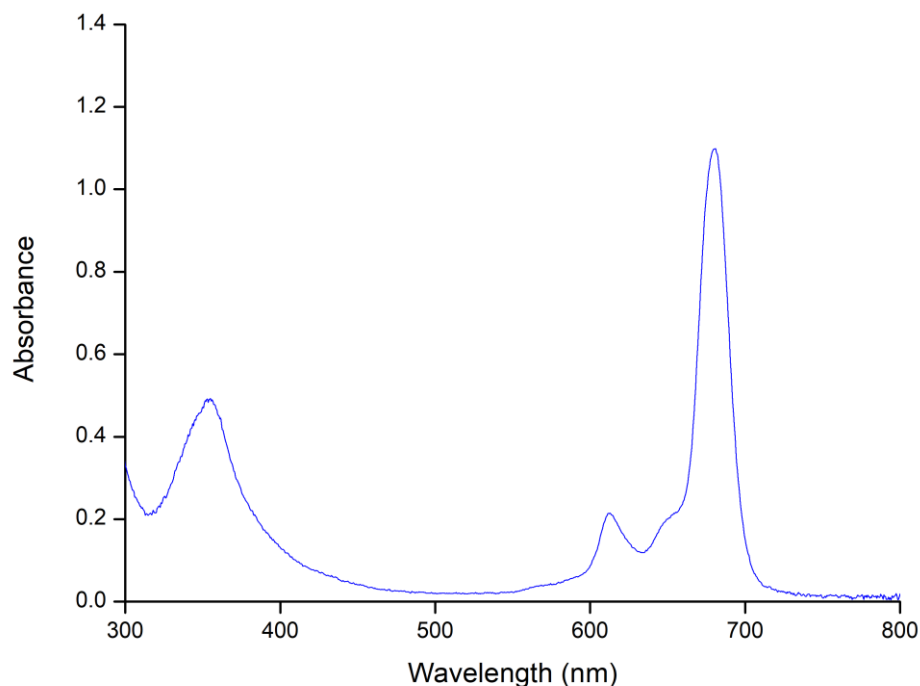
Figure 2.9. UV-*vis* spectrum of ZnPc in DCM

The $\pi \rightarrow \pi^*$ transition corresponds to the HOMO-LUMO transition and is referred to as Q Band. The energy difference between HOMO and LUMO depends on the size of the aromatic system [73]. In the series porphyrin, phthalocyanines, naphthalocyanine, the aromatic system is extended by four fused benzene rings. This reduces the HOMO / LUMO energy difference and follows bathochromic shift of the Q band with increasing intensity. Thus, porphyrins have an absorption maximum in the range of 560 to 630 nm [74], the Pcs in the range of 660 to 740 nm and naphthalocyanines in the range of 750 to 850 nm [75].

In the metal-free Pcs, takes place the splitting of the Q band [76] (Figure 2.10). This is due to the non-degenerate LUMOs involvement. Introduction of the metal ion increases the symmetry from D2h to D4h. As a result, the orbitals are degenerate and no splitting occurs.
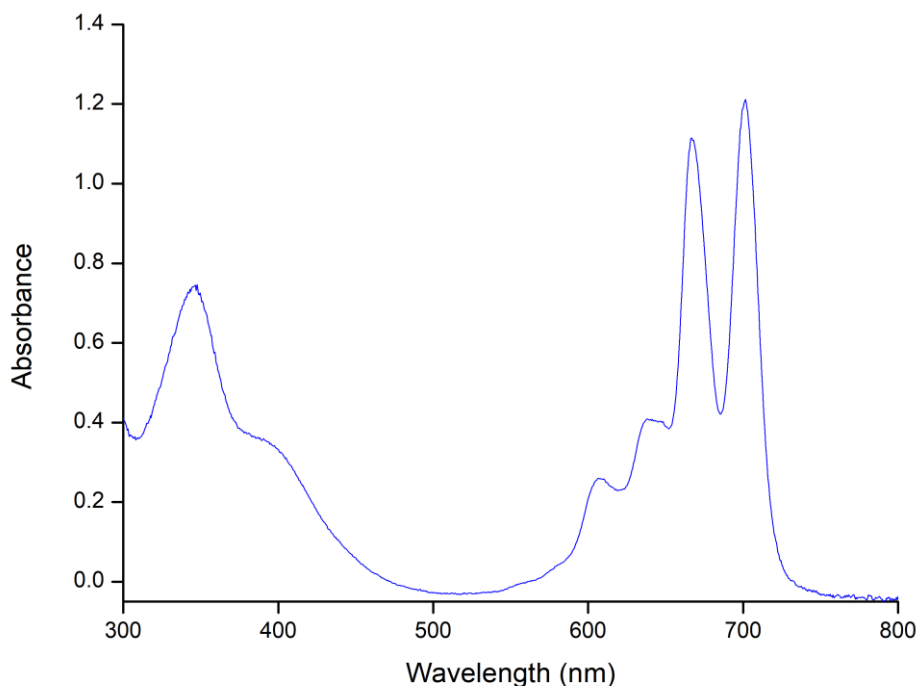
Figure 2.10. UV-*vis* spectrum of H$_2$Pc in DCM

The intensity and location of the absorption bands are not limited by the size of the aromatic system, but also by the nature and position of the substituents. At the same position on the ring system, electron-donating substituents, such as alkoxy groups lead to a redshift and electron-withdrawing groups, such as carboxy, cyano and nitro groups lead to a blue shift [77].

In addition to the nature and number of substituents, the solvent plays an important role in the absorption properties. In the solution, the macrocycles tend to aggregate. This behavior is particularly pronounced in very polar solvents, such as water. The formation of aggregates is shown in the UV-*vis* spectrum by the decrease in the extinction of the Q band and broadening of the entire band range [78]. At the same time, the intensity of the Soret band is increasing. The van der Waals interactions between the π systems and the formation of hydrogen bonds are some of the reasons for aggregate formation. Aggregation may interfere with triplet-triplet quenched excited states on the photochemical properties.

21

2.6.2. Phthalocyanine organization

Pc molecules tend to aggregate because of their nature of π-π interactions between aromatic rings. This fact, along with the appropriate preference of substitution both in the central metal atom and in the periphery, can be used to achieve ordered supramolecular structures, which give Pcs their applicability as molecular materials. The most well known Pc organization types are the following [78b]:

Crystals

Pcs generally have two types of polymorphic crystals. These are the α and β forms, which are thermodynamically more stable. The angle formed by the molecules is the main difference between these two sturctures. (Figure 2.11).
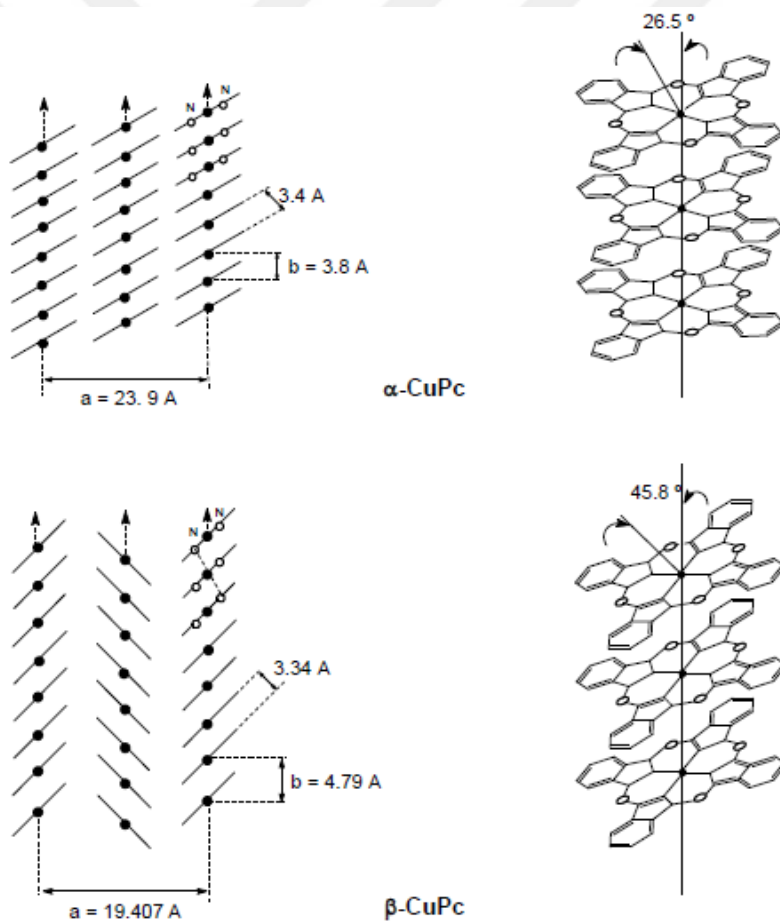
Figure 2.11. Crystal packing of Pcs

Liquid crystals

In these systems, Pcs are normally substituted on the periphery by lipophilic chains. These structures interact and create a fluid medium and encircle the flat aromatic Pc nuclei. Thes Pc nuclei are stacked together to give rise to mesophases columnar discotics [79] (Figure 2. 12), which can be arranged in different geometries. The first Pc with mesogenic properties was obtained by *J. Simon et al* in 1982 [80]. After that they have described a large number of phthalocyanines with liquid crystal behavior [81].
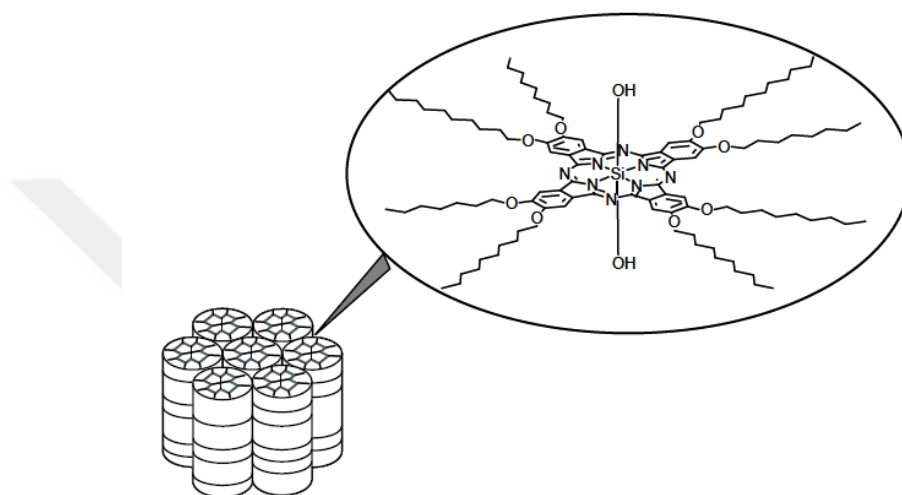
Figure 2.12. Hexagonal columnar discotic mesophase of a phthalocyanine.

Thin films

Deposition in thin films is the most direct way to use Pcs in molecular devices. This can be prepared by vacuum sublimation [82], dispersion in a polymer matrix [83] or "spin-coating" [84]. Highly ordered Pc films have been prepared using the Langmuir-Blodgett technique [84a,84b,85] and by self-organization of macrocycles with thiol substituents on a gold surface [84a,84b,86].

"Shish-Kebab" polymers

The central metal atom of the Pcs and connecting bridges have a significant role in this type of organization. The bridge ligands connect the Pc molecules through their central atoms (Figure 2. 13) [87,88].

M = Transition metals (II), (III), (IV)
(Fe, Ru, Os, Co, Mn, Cr, Si, Ge, Se)
L= pyz, tz, bpy, dib, me2dib, me4dib, CN⁻, SCN⁻, O²⁻
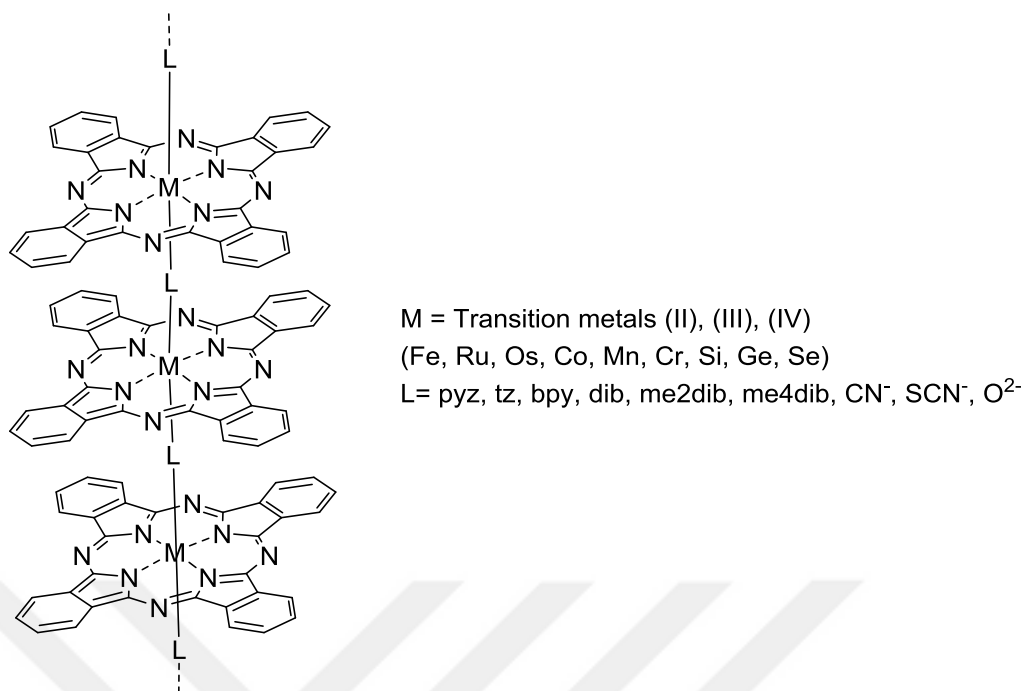
Figure 2.13. Organization of metal phthalocyanines through bridge ligands

Phthalocyanines substituted with crown ethers

Crown ether substituents help form cofacial aggregates of Pcs in the presence of alkali and alkaline earth metal salts (Figure 2. 14) due to the cooperative complexation of the cation between adjacent units [89].
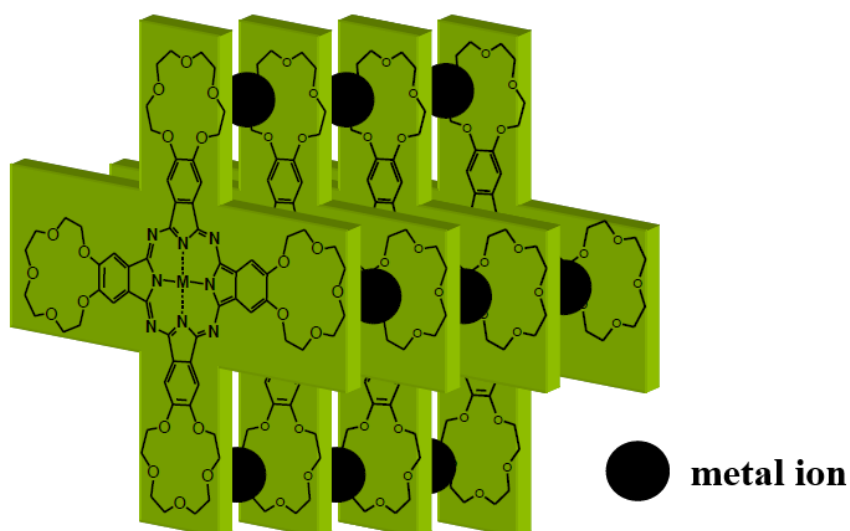
Figure 2.14. Complexes of crown ether substituted Pcs and metal salts.

Formation of nanostructures on surfaces

It is important to understand the organization of Pcs on a nanometric scale, since their most relevant applications (photovoltaic cells, gas sensors, etc.) are obtained from thin films, whose structural arrangement is still unknown.

Recently it has been observed how Pcs can self-organize to form nanometric-sized tapes, the nature of which depends on the type of substrate on which they are deposited, and on the deposition conditions [90].

2.7. Applications of phthalocyanines

2.7.1. As a colorant

CuPc and its derivatives are important colorants [91-94]. This is due to their absorption range (650 to 750 nm, i.e. blue, green with partly reddish or yellowish color components), their color depth (high extinction coefficients) and their chemical and photochemical stability against environmental influences. Insoluble copper Pc (CuPc) is used as the most important blue pigments. They have wide application in different forms. Among the dyes, the water-soluble sulfonic acids of CuPc are first of all to mention. They are obtained by electrophilic substitution on CuPc and carry statistically two to four sulfonic acid groups. These Pcs have application as textile colorants. Broadly used are the sulfochlorides of CuPc, where further modifications are carried out with a wide variety of functionalized amines [95, 96] and most of the substituents are saponified to sulfonic acids. If the partial amination with diamines is carried out, amphoteric dyes are formed which are soluble in the alkaline and acidic aqueous medium but insoluble in the neutral. The dyes which are also readily soluble in organic solvents are used for dyeing various materials such as paper, textile fibers, but also as inks. Second group being direct dyes and are used in particular for dyeing cotton. A third important group is, CuPcs carrying a chloro-methylated $ClCH_2$ group. Follow-up reactions with amines, alcohols, and phenols are used to prepare further substituted CuPcs [97, 98].

2.7.2. Recordable compact discs

Figure 2.15-A shows the construction of a blank recordable compact with the order; polycarbonate → dye → silver → paint protection layer. The irradiation is carried out at a wavelength of 780 nm. In the "writing process", the dye is converted into an excited state by absorption of photons in the rotating disk with an intense laser beam along the pregroove, follows deactivation as heat. Heated dye decomposes and forms bubbles. As a result, deformation of the polycarbonate layer takes place in the affected regions. Thus, at the burned areas, there forms information in the form of pits (Figure 2.15-B), which is perceived as a weakening of the reflection when read out. The non-affected

and affected areas of the pregroove result in the binary code 0 or 1 as one bit, which conduct to form data set.
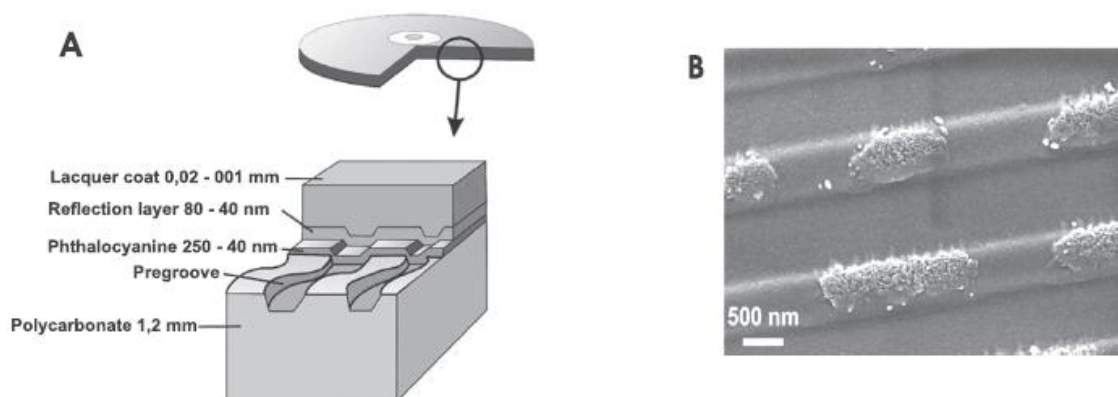
Figure 2.15. A) Structure, B) Microscobic view of a data track

The requirements placed on the dye for use in CD/Rs are very complex. In addition to Pcs, especially polymethine imines and azo metal complexes have gained importance. Only by the complex interaction in Pcs by selecting suitable substituents on the ligand and a suitable metal ion in the ligand, a solution for suitability in CD/Rs could be found. This is illustrated by the example of Palladium (II) Pc (PdPc) substituted with alkoxy groups (Figure 2.16). These groups have electron-donating effect. Therefore, its main absorption at 725 nm with a decrease in absorbance to over 760 nm. Thus, during the reading process, detection of a pit is possible by the weaker reflection. A large proportion of the dye destroyed irreversibly in a short time of burning. Decisive is also the balancing of the temperature. Polycarbonate softens around 150 °C and melts around 265°C. The ideal temperature should be between the two. It should deform the layer of the polymer but not to flow away. Furthermore, the dye must have a very good solubility. Solvent is evaporated after application on the film. The dye must not aggregate in the film. Because, in the aggregate, the excitation energy would be distributed from an excited to unexcited molecules. The alkoxy groups on the Pc ring yield to very good solubilities of the PdPc and prevent aggregation of the macrocycles in the solid thin film. Furthermore, photophysical characteristics also play a very important role. Large absorption coefficient ε is a significant requirement. It needed for

excitation with light and thermal decomposition of the dye. This is about 2×10^5 L mol^{-1} cm^{-1} for PdPc at 725 nm. The excited state should be thermally deactivated as efficiently as possible and not deactivated by luminescence, i.e. light emission. For PdPc, the fluorescence and phosphorescence quantum yield is around less than one percent, and the thermal deactivation is in the foreground [93].
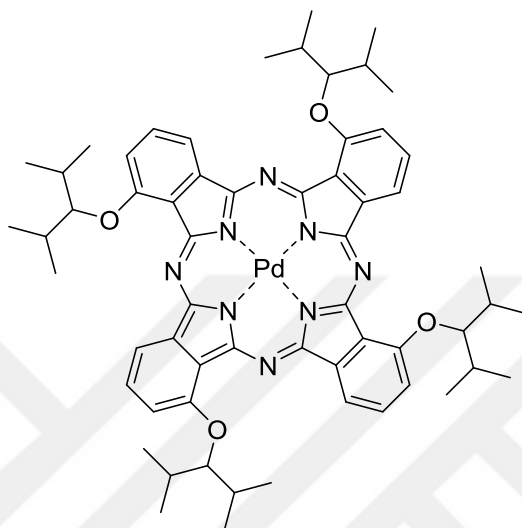
Figure 2.16. Structure of Palladium (II) phthalocyanine substituted with alkoxy groups

2.7.3. Active matrix liquid crystal displays

The development of improved liquid crystal displays (LCD), for the automotive industry, laptop computers or television sets, is an interdisciplinary challenge for the 1990s. In colored liquid crystal displays, the Pcs represent two of the three color components. Figure 2.17 shows the structure of an LCD display [99,100]. Electric field vectors orient in opposite directions. Because of that liquid crystals are twisted. When a voltage of about 2-3 V is applied to the component, the liquid crystals lose their twisting and orient themselves parallel to the electric field. As a result, light does not pass and the display is black. By controlling the individual areas in switching times of less than 20 ms, you get a black and white display.

For the color representation the display has a color filter segment. The filter converts white backlight into colored lights through its absorptive color surfaces in the three

basic colors. These are blue, green and red. (Figure 2. 17). Each pixel now made up of subpixels for each of the three basic colours. For large-screen HD LCDs, there must be as many individually addressable transistors for 25 million addressable points.
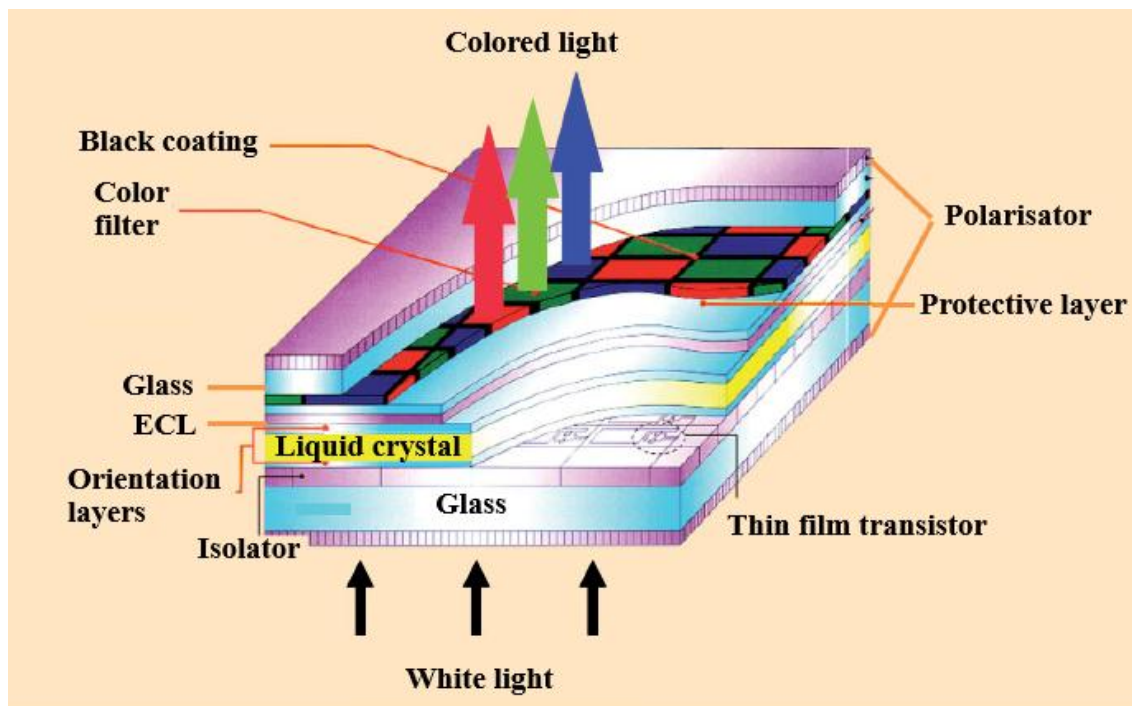
Figure 2.17. Structure of a LCD display

The three basic colors of the color filter are subject to special requirements. These are homogeneity, fastness, stability and the intensity of the colors. Light scattering must be avoided. For this reason, dyes should not aggregate. Different modifications of CuPcs are suitable for the primary blue color and halogenated CuPcs are available for the primary green color. Diketopyrrolopyrrole pigments are generally applied as primary red color among others [27a].

2.7.4. Photovoltaic devices

Due to their high absorption coefficients in the visible light and high quantum emission yields, Pcs have been incorporated into donor-acceptor systems along with other electro- and / or photo-active species. In this way, it is possible to achieve rapid

processes of photoinduced charge separation, and therefore the manufacture of organic photovoltaic devices [101]. There are two types of organic solar cells in which Pcs can play an important role, namely: dye-sensitized solar cells, and fully organic solar cells. In the former, commonly called Grätzel cells, an organic dye (ruthenium-bipyridine complexes, Pcs, etc.) is anchored to a film of a mesoporous inorganic semiconductor (TiO_2, ZnO, CdSe, etc.) [102]. This type of cell has the advantage that after photoexcitation, the charge transporters generated in the dye are close to the union with the oxide, thus producing electronic transfer to the conduction band of the latter and therefore increasing the efficiency in the process of charge separation. Usually these cells combine donor-acceptor mixtures, in which the Pcs act as chromophores [103]. On the other hand, fully organic solar cells have the advantage of including in their structure exclusively organic materials, cheaper and easier to process. They are flexible cells, capable of adapting to virtually any surface, and totally inorganic cells, such as mono- and polycrystalline silicon, cannot compete with them in this regard. Examples of this class of cells are those formed by interpenetrated polymer networks [104] or mixtures of polymers and fullerene [105], as well as those containing Pcs [106].

In organic solid-state solar cells, Pcs are among the active components for converting the energy of visible light into electrical energy. For this application, it must be an organic p-conductor, absorbing in the visible region with high extinction coefficient, and having very good photostability. Figure 2.18 shows schematically the structure and energy flow of the electrons and holes in a stacked p-i-n cell ("I" stands for the intrinsic absorber layer for visible light, "p" for p-conductor and "n" for n-conductor). Zinc (II) Pc is used as p-conductor. It has an absorption at 550 to 750 nm. C60 fullerene used as n-conductor and it has an absorption at 400 to 550 nm. Photon absorption causes electrons to migrate from HOMO to LUMO with exciton formation. From there, the electrons travel in the direction of their lower energy to the aluminum electrode (cathode). The holes in the HOMO travel in the direction of their lower energy to the anode [108]. So that not a part of the electrons moves towards the anode, there is still a p-layer as a doped hole transporting layer (HTL), which consists of tertiary aromatic amines such as MeOTPD [107,109]. On the other hand, on the electrode side, an electron transport layer such as doped C60, which blocks against holes, is used. The efficiency of the cells is> 3.4%. To increase the efficiency, a second is built directly on

the first p-i-n cell. In this tandem arrangement, Heliatek GmbH (Dresden, Germany) measured a certified efficiency of 9.8%. These cells are about to be launched on the market [93].
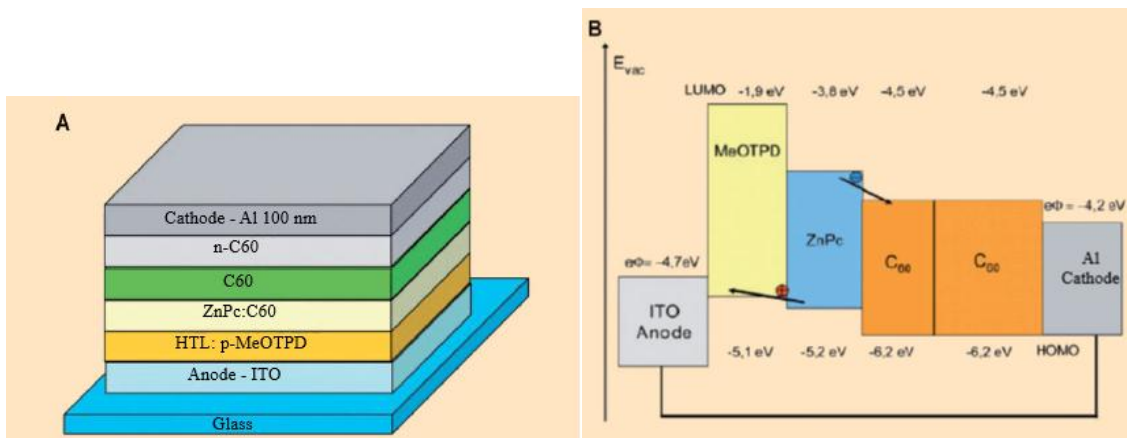
Figure 2.18. The p-i-n cell. A) Structure, B) Energy scheme; ITO, indium tin oxide; HTL, hole transport layer; from p-MeOTPD, tertiary aromatic amine; ZnPc, zinc (II) Pcs; C60, C60 fullerene; eF, electron emission work.

2.7.5. Photodynamic Therapy

Today, Photodynamic therapy (PDT) is a widely used and recognized method for the treatment of numerous tumor diseases and for controlling bacterial infestation [110-112]. As early as 1,400 years before Christ, the Indians in their sacred book Atharava-veda described the positive effect of light in connection with the seeds of the plant *Psoralea corylifolia* in the treatment of white spot disease. The psoralen contained therein, which has a coumarin-like basic structure, served as a photoactive agent. The ancient egyptians also used extracts of the plant *Ammi majus* to treat vitiligo [112]. However, the concept of the phototherapeutic treatment of diseases has long been forgotten and was taken up again by Tappeneier at the beginning of the 20th century [113]. He investigated the effects of dyes such as eosin or fluorescein in the treatment of tumors or skin diseases such as *Lupus erythematosus* (butterfly lichen) and *Condylomata acuminata* (genital warts) [114, 115].

The basic principle of PDT is based on the interaction of the three factors; light, photoactive substance and oxygen. For this purpose, the phototherapeutic agent, also called photosensitizer (PS), irradiated with light after accumulation in the tumor tissue. This irradiation leads to the excitation of the enriched PS, which then reacts with the oxygen present in the cell. In this case, a spin-permissible energy transfer from the excited photosensitizer to the triplet oxygen of the cell takes place in the ground state. The resulting highly reactive singlet oxygen can now react with the damaged tissue and induce necrosis of the tumor [116].

For a closer look at the mechanism of action of PDT at the cellular level as well as in the tissue, the work of Moan [117], Josefsen and Boyle [111] can be used. Despite the successes of 1st generation photosensitizers such as Photofrin®, Photosan® and some hematoporphyrine derivatives, scientists are searching for new compounds that meet the demands of modern medicine. Important aspects are absorption in the long-wave range, high absorption coefficients and stability during irradiation. In addition, a second-generation PS should have the features of rapid tumor accumulation, low dark toxicity, and a broad spectrum of activity [116,118,119]. One class of compounds that fulfills these properties in many ways are the Pcs. Since the early 1980s, these macrocycles have been considered potential sensitizers for PDT and are the subject of intense research [120]. Known representatives are Photosens®, BAM-SiPc and Pc4® (Figure 2.19).
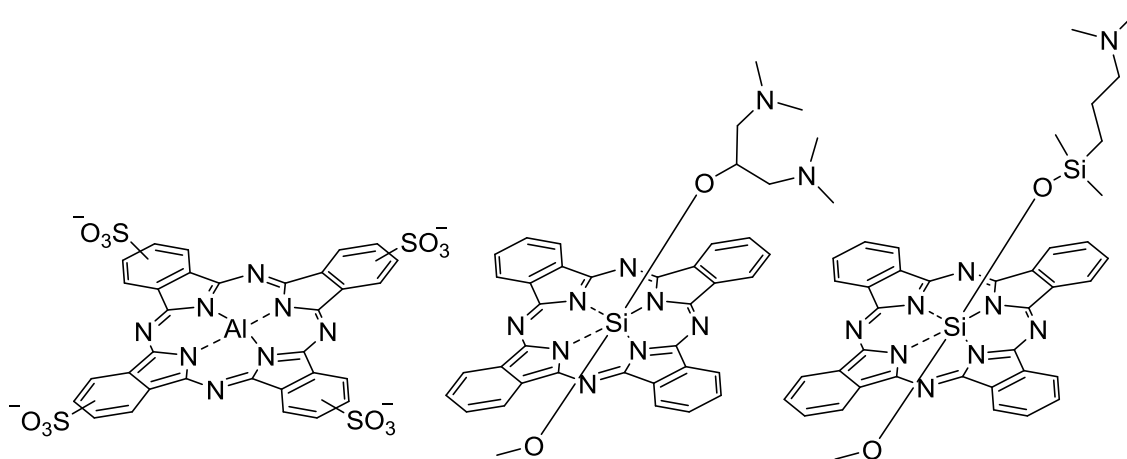
Figure 2.19. Structures of Photosens® (left), BAM-SiPc (middle) and Pc4® (right)

2.7.5.1. Photodynamic process

Pcs have special photochemical properties due to the location of the HOMO and LUMO energy levels and their energy difference (ΔE). Since the molecular orbitals are quantized in terms of their energy, Pcs absorb the photons of a certain intensity (hν). This intensity corresponds to the energy difference between the ground state and the excited state (ΔE=hν). Since the HOMO / LUMO energy difference of the Pcs is ~ 170 kJ / mol (~ 700 nm), Pcs can be excited by visible light. The Jablonski diagram describes the processes (Figure 2.20) [120-126].

Due to the light absorption, the molecule changes from the ground state S0 to excited electronic states S1, S2, ... and their vibration-excited sublevels without changing the overall spin. There are only transitions between singlet states (A). The excited states have various options for deactivation: vibration relaxation (SR), internal conversion (IC), fluorescence (F) and intersystem crossing (ISC) [127].

The fluorescence (F) is light emission from excited singlet states (S1) to the singlet ground state (S0). The radiation-free transitions between electron states of the same spin multiplicity (e.g. S2 → S1) form the basis of the internal conversion (IC). The deactivation by means of vibration relaxation (SR) is due to radiationless transitions between core vibration levels of the respective excited state. Radiation-free spin reversal

processes, such as intersystem crossing (ISC), lead to triplet states (T1, T2) which, contrary to the prohibition of spin, can return to ground state (S0) through phosphorescence (P). In addition to the monomolecular deactivation by the processes described above, bimolecular processes can also occur from the singlet or triplet states [128-130]. There are two main types. Intermolecular deactivation can either be by energy transfer to appropriate acceptors, e.g. Oxygen or electron transfer to a substrate molecule. Chemical processes such as fragmentation reactions, rearrangements or bimolecular addition reactions can also take place on the excited phthalocyanine [131,132].
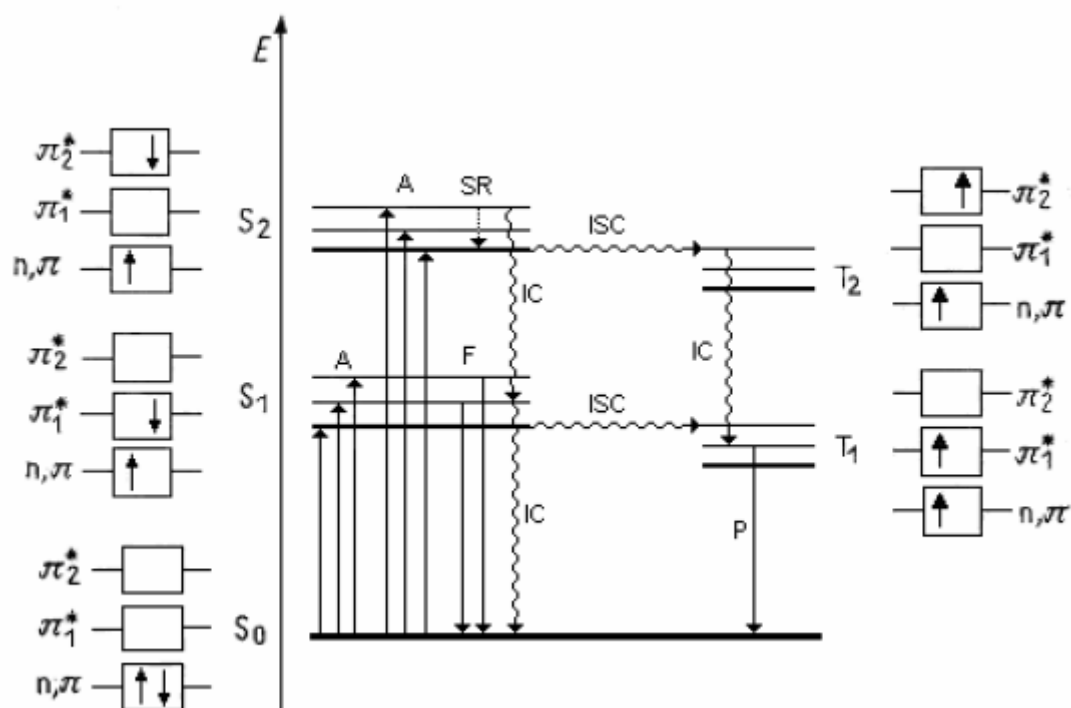
Figure 2.20. Jablonski diagram

2.7.5.2. Generation of singlet oxygen

The energy of the excited molecule can be transferred to a suitable acceptor. Ideally, the excited state of the acceptor has a lower energy than the energy of the excited donor molecule. The acceptor molecule is excited and the donor molecule changes to the

ground state. According to the spin conservation law, three different types of energy transfer can be distinguished [133]:

Singlet-singlet energy transfer $\qquad {}^{1}D^{*} + {}^{1}A_{0} \rightarrow {}^{1}D_{0} + {}^{1}A^{*}$

Triplet-triplet energy transfer $\qquad {}^{3}D^{*} + {}^{1}A_{0} \rightarrow {}^{1}D_{0} + {}^{3}A^{*}$

Triplet-singlet energy transfer $\qquad {}^{3}D^{*} + {}^{3}A_{0} \rightarrow {}^{1}D_{0} + {}^{1}A^{*}$
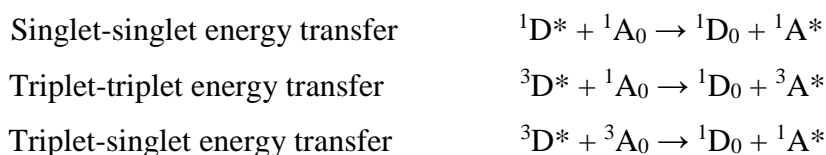
The photochemical generation of singlet oxygen with the help of photosensitizers such as phthalocyanines, porphyrins, rose bengal, methylene blue or chlorophyll takes place after the triplet singlet energy transfer [134].

The triplet energy for the porphyrins and phthalocyanines is approx. 108-150 kJ / mol. The energies of the first excited state ($^{1}\Delta_{g}$) and the second excited state ($^{1}\Sigma_{g}^{+}$) of oxygen are 94.7 kJ / mol and 157.8 kJ / mol, respectively. The energy of the excited state of oxygen is therefore below the energy of the triplet state of the photosensitizer. This is one of the most important conditions for energy transfer [135].

2.7.5.3. Singlet oxygen quantum yield (Φ_{Δ})

In order to calculate the singlet oxygen produced by the photosensitizer, singlet oxygen quenchers such as 1,3-diphenylisobenzofuran (DPBF) are used. Decomposition of DPBF by singlet oxygen has shown below (Scheme 2.7).

1,3-diphenylisobenzofuran $\qquad\qquad$ endoperoxide
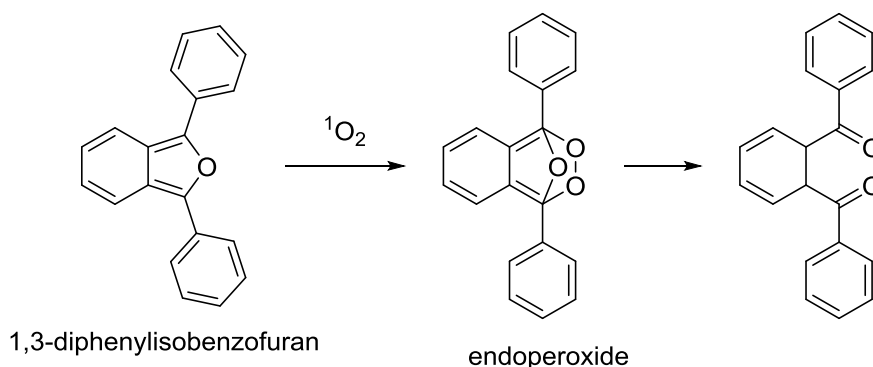
Scheme 2.7. Decomposition reaction of DPBF

The quantum yield for the reaction between DPBF and singlet oxygen (ΦDPBF) can be determined experimentally from the decrease in DPBF after each irradiation interval. It

is defined as the number of converted DPBF molecules (nDPBF) in relation to the number of light quanta absorbed by the photosensitizer.

The experimental setup of the group of ZIMČÍK and NOVÁKOVÁ was used to determine Φ_Δ. Figure 2.21 illustrates the experimental setup. ZnPc was used as reference. The filter transmits the desired wavelength of light and prevents excessive heating of the sample.
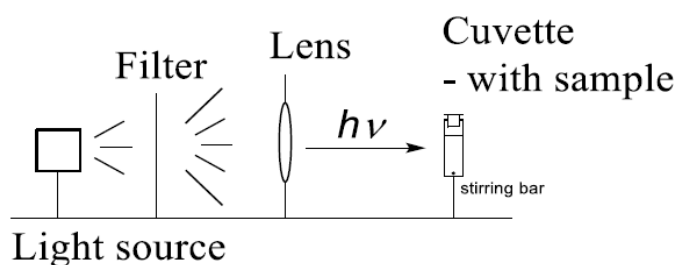
Figure 2.21. Illustration of experimental setup for measurement of singlet oxygen production.

We can define singlet oxygen quantum yield (Φ_Δ) of the sample by the following formula.

$$\Phi_\Delta = \Phi_\Delta^{Std} \frac{R.I_{abs}^{Std}}{R^{Std}.I_{abs}}$$

Φ_Δ: Singlet oxygen quantum yield of the sample

Φ_Δ^{Std}: Singlet oxygen quantum yield of the standard (0.67 for our ZnPc in DMF).

 R: Absorbance change of the quencher (DPBF) in the presence of the sample.

R$_{Std}$: Absorbance change of the quencher (DPBF) in the presence of the standard.

I$_{abs}$: Light absorbed by the sample.

I$_{abs}^{Std}$: Light absorbed by the standard.

2.7.5.4. Stability of Pcs

Phthalocyanines as solids are thermodynamically and chemically very stable substances. They are stable in a vacuum at temperatures up to 800 °C and can thus be purified by sublimation [136]. In contrast, the stability of some phthalocyanines in solution is lower compared to the solid state. A distinction is made between dark stability and photooxidative stability. Dark stability is the stability of the phthalocyanines in the solution with the exclusion of light. The photooxidative stability shows how stable the phthalocyanines are under radiation. Most phthalocyanines have high dark stability. In contrast, many phthalocyanines differ in their photooxidative stability. This property is very important for the use of phthalocyanines. As photocatalysts, the phthalocyanines must have high dark stability and also high photooxidative stability [137]. In the case of PDT, however, substances are required that have rather low photooxidative stability and also dark stability. In this way, a photosensitizer can be broken down in the body more quickly after irradiation. The stability of the phthalocyanines is determined by many factors. On the one hand, these are the parameters that are determined by the structure of the macrocycles: the size of the conjugated system [138] (enlargement of the conjugated system leads to increasing destabilization of the HOMO and consequently increasing oxidizability of the macrocyclic system), the electron configuration of the central metal (destabilization by open shell metals) and the nature of the substituents (electron-donating substituents have a destabilizing effect and electron-withdrawing substituents have a stabilizing effect). On the other hand, external factors such as the presence of oxygen (higher stability in the presence of inert gases) and the solvent (lower stability due to chlorinated solvents) influence the stability of the phthalocyanines [127].

Photodegradation quantum yield (Φ_d) calculations help us to interpret PS's stability when they exposed to light. Photodegradation quantum yields of stable ZnPcs are around 10^{-6} and it is around 10^{-3} for unstable ones [125]. We can calculate the photodegradation quantum yield (Φ_d) by the following formula:

$$\Phi_d = \frac{\Delta A}{\Delta t} \; x \; \frac{V}{\varepsilon} \; x \; \frac{1}{I_{abs}}$$

In this formula;

Φ_d: Photodegradation quantum yield

$\dfrac{\Delta A}{\Delta t}$ **:** Slope of absorbance – time graph

V: Volume of the solution

ε: Slope of absorbance – concentration graph

I_{abs}: Absorbed photon intensity

Ideal photosensitizers should show some fluorescence behavior in order to be able to follow them in the body. Therefore, it is important to investigate their fluorescence quantum yield (**Φ_f**) characteristics for PDT studies. We can calculate the fluorescence quantum yield (**Φ_f**) by the following formula:

$$\Phi_f = \Phi_f^{Std} \frac{F x A_{abs}^{Std} \, x \, \eta^2}{F_{Std} \, x \, A \, x \, \eta_{Std}^2}$$

In this formula;

Φ_f, Φ_f^{Std}**:** Fluorescence quantum yields of the sample and the standard

F, F_{Std}**:** The area under the fluorescence emission slope of the sample and the standard

η^2, η_{Std}^2**:** Refractive index of the solvent that used with the sample and the standard

A, A_{abs}^{Std}**:** Absorbances of the sample and the standard at the wavelength of excitation.

CHAPTER 3. EXPERIMENTAL SECTION

Materials and Methods

Melting Point

The Melting Point BUCHI M-565 device was used for determination of melting point of synthesized compounds.

UV/*vis* spectroscopy

The UV/*vis* spectra were carried out with the SHIMADZU UV-2450. The following abbreviations are used in the evaluation of the absorption bands: sh = shoulder and max = maximum.

Fluorescence spectra

Fluorescence spectra were recorded using the VARIAN CARY ECLIPSE FLUORESCENCE SPECTROPHOTOMETER.

IR spectroscopy

The infrared spectra were recorded with the PERKIN ELMER SPECTRUM 100 FT-IR SPECTROMETER.

NMR spectroscopy

The nuclear magnetic resonance spectra were recorded using the BRUKER AVANCE III 500 MHz NMR SPECTROMETER. $CDCl_3$ (residual proton signal in ^{1}H-NMR: 7.25 ppm; solvent signal in ^{13}C-NMR: 77.0 ppm) and DMSO-d_6 (residual proton signal in ^{1}H-NMR: 2.49 ppm; solvent signal in ^{13}C-NMR: 39.7 ppm) were used as solvents. The multiplicity of the signals is represented by the following abbreviations: s = singlet, d = doublet, t = triplet, m = multiplet, b = (broad) broadened signal.

Mass spectrometry

MALDI-TOF measurements were carried out with BRUKER MICROFLEX LT MALDI-TOF.

3. 1. Synthesis of phthalonitrile starting compounds

All of the synthesized phthalocyanines were prepared starting from phthalonitrile derivatives. The synthetic route for obtaining phthalonitriles is a widely used method based on commercially available chemicals. Starting with phthalic acid (**I**) derivatives, phthalic anhydride (**II**), imide (**III**) and amide (**IV**) gave phthalonitrile derivatives (**V**). This synthetic sequence has been known since 1993 [124a]. Individual steps were modified in this work on the basis of similar synthetic protocols.

a) $R^1=R^2=Cl$
b) $R^1=NO_2$, $R^2=H$
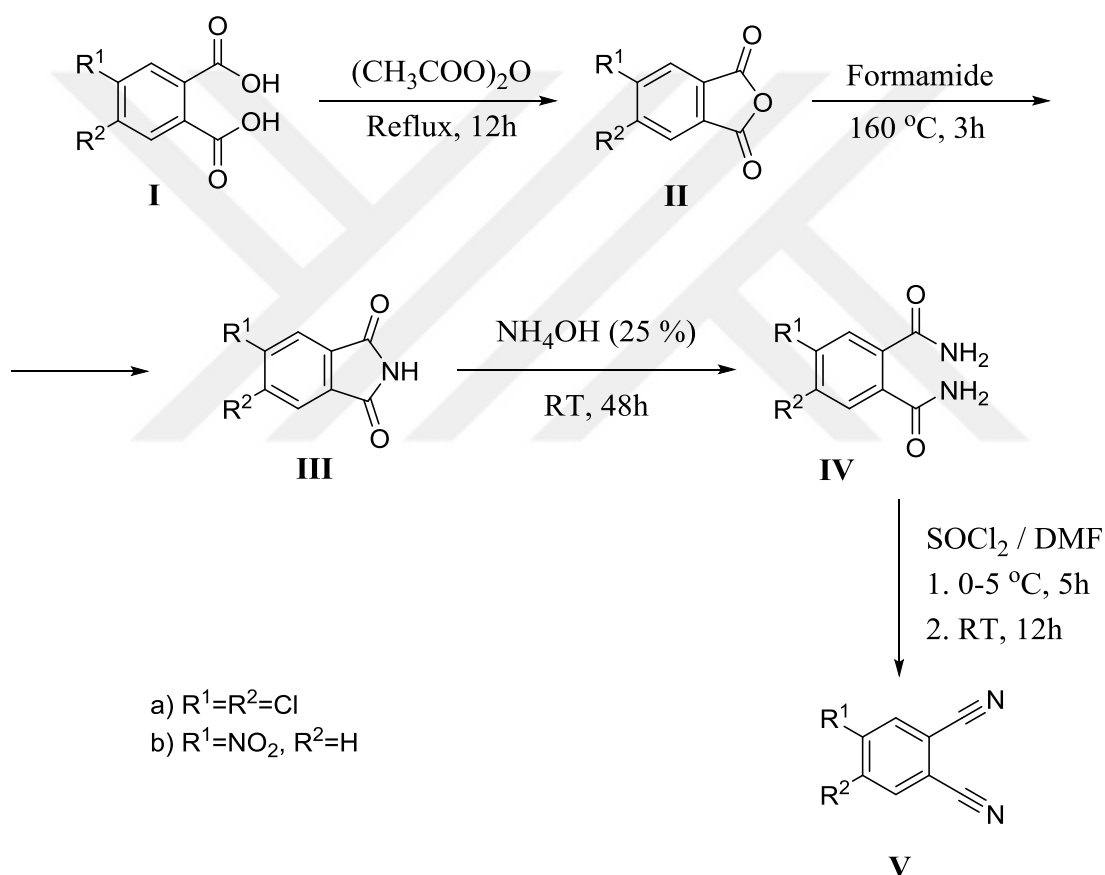
Scheme 3.1. Synthetic procedure for starting phthalonitrile compounds

30 g (0.127 mol) 4,5- dichlorophthalic acid (**Ia**) was converted into 4,5-dichlorophthalic anhydride (**IIa**) by heating under reflux in acetyl anhydride for 12
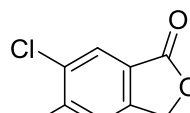
hours. The educt must be dry and the acetyl anhydride should be distilled. The beige product was washed with petroleum ether and diethyl ether.

Molecular weight: 217.00 g/mol

Yield: % 93

Mp: 185 °C

22 g (0.102 mol) of previously obtained 4,5- dichlorophthalic anhydride (**IIa**) was dissolved in 30 mL of formamide and stirred under condenser at 160 °C for 3 hours. Obtained precipitate was cooled at room temperature, filtered under vacuo and washed with excess water. Drying over P_2O_5 for 12 hours yielded 22.2 g of 4,5-dichlorophthalimide (**IIIa**).

Molecular weight: 217.02 g/mol

Yield: % 97

Mp: 194 °C
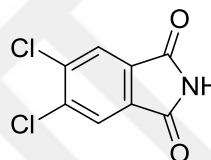
22 g (0.102 mol) 4,5-dichlorophthalimide (**IIIa**) was stirred in %25 NH_4OH for 24 hours. Then 100 mL of %33 NH_4OH was added and stirred for one more day. The precipitates filtered under vacuo and washed with distilled water until it became neutral. Drying over P_2O_5 for 12 hours yielded 18.2 g of 4,5-dichlorophthalamide (**IVa**).

Molecular weight: 233.05 g/mol

Yield: % 77

Mp: 246 °C
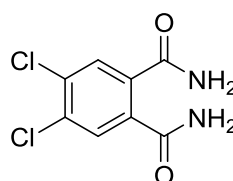
96.3 mL of dry DMF was cooled to 0 °C. Then 67.4 mL of $SOCl_2$ was added dropwise under N_2 atmosphere. Then 19.26 g (0.083 mol) 4,5-dichlorophthalamide (**IVa**) was added in portions in 2 hours. The reaction mixture was stirred 5 hours at 0-5 °C and 12 hours at room temperature. After completion of the reaction, the product was poured into 700 mL ice water and until complete precipitation. The crude product was then

filtered under vacuo and washed with distilled water until neutralization. Crystallization from methanol yielded 12 g of 4,5-dichlorophthalonitrile (**Va**).

Molecular weight: 197.02 g/mol

Yield: % 73

Mp: 178 °C
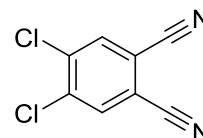
Same procedure was followed for the synthesis of 4-nitrophthalonitrile (**Vb**). But we obtained 4-aminophthalonitrile (**VIb**) from reduction reaction of 4-nitrophthalonitrile (**Vb**).
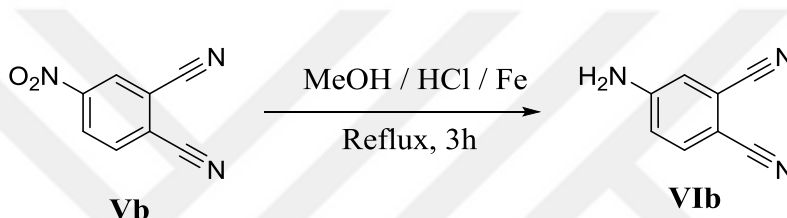
On a mixture of methanol (450 ml) and % 38 HCl (96 ml) was prepared. Then 4-nitrophthalonitrile (**Vb**) (20 g, 115.6 mmol) was added added slowly in portions while stirring. The mixture was heated to reflux temperature and kept stirring until observing the complete dissolution of the solid. After that, powdered iron (22 g, 393.9 mmol) was added in eight portions for an hour. The brown solution was heated under reflux for another hour and cooled until it reaches room temperature. Cold water (600 ml) was added, the yellow-green precipitate was filtered, washed with water and dried under vacuum. The recrystallization of toluene yields 12.6 g of ocher solid compound 4-aminophthalonitrile (**VIb**).

Molecular weight: 143.15 g/mol

Yield: % 76

Mp: 173 °C

3. 2. Synthesis of starting materials from the reactions between thymol and phthalonitrile compounds

3. 2. 1. Synthesis of 4-chloro-5-(2-isopropyl-5-methylphenoxy) phthalonitrile (1)
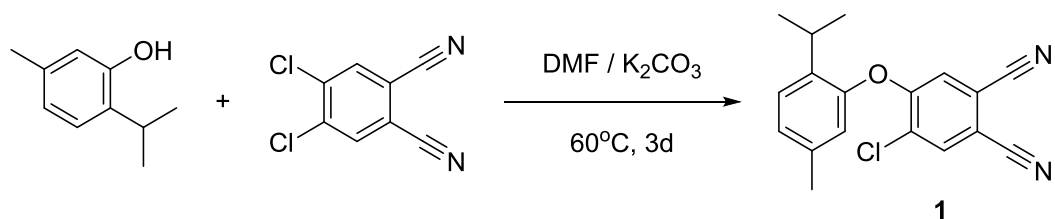
Solution of thymol (2-isopropyl-5-methylphenol) (1.5 g, 10 mmol) in 20 mL dry DMF was added slowly while stirring to the solution of 4,5-dichlorophthalonitrile (1.97 g, 10 mmol) in 30 mL dry DMF and the solution stirred further for 15 min. Afterwards finely powdered K_2CO_3 (2.76 g, 20 mmol) was added. The reaction solution was stirred at 60°C for 3 days under vacuo. The reaction solution was followed by TLC and it was stopped after the disappearance of spots on TLC plate belongs to the reactants. The reaction solution was cooled and followed by filtering of K_2CO_3. The solution was then poured into ice-water. After the complete precipitation, obtained solids were filtered with sand funnel. The product washed with water several times. Purification of the compound **1** was achieved by column chromatography (silica gel). $CHCl_3$ was used as an eluent. The collected fraction was dried to obtain the compound **1** in a good yield.

Chemical formula: $C_{18}H_{15}ClN_2O$

Molecular weight: 310.78 g/mol

Yield: % 71.

Mp: 125 °C

Solubility: DCM, $CHCl_3$, THF, Acetonitrile, Acetone, Toluene, DMF and DMSO.

FT-IR γ max (cm^{-1}): 523, 610, 826, 959, 1020, 1069, 1094, 1179, 1246, 1364, 1420, 1486, 1514, 1588, 1607, 2233, 2848, 2965, 3046, 3080.

^{1}H-NMR (500 MHz, CDCl$_3$) δ, ppm: 8.55 (s, 1H), 7.45 (s, 1H), 7.35 (d, $J = 7.8$ Hz, 1H), 7.13 (d, $J = 7.8$ Hz, 1H), 6.89 (s, 1H), 2.96 (septet, $J = 6.9$ Hz, 1H), 2.29 (s, 3H), 1.16 (d, $J = 6.9$ Hz, 6H).

¹³C-NMR (500 MHz, CDCl₃) δ, ppm: 158.5 (1C), 151.0 (1C), 139.0 (1C), 136.9 (1C), 135.5 (1C), 128.9 (1C), 128.0 (1C), 128.0 (1C), 120.9 (1C),119.6 (1C), 116.0 (1C), 114.7 (1C), 114.6 (1C), 110.9 (1C), 27.3 (1C), 22.9 (1C), 22.8 (2C).
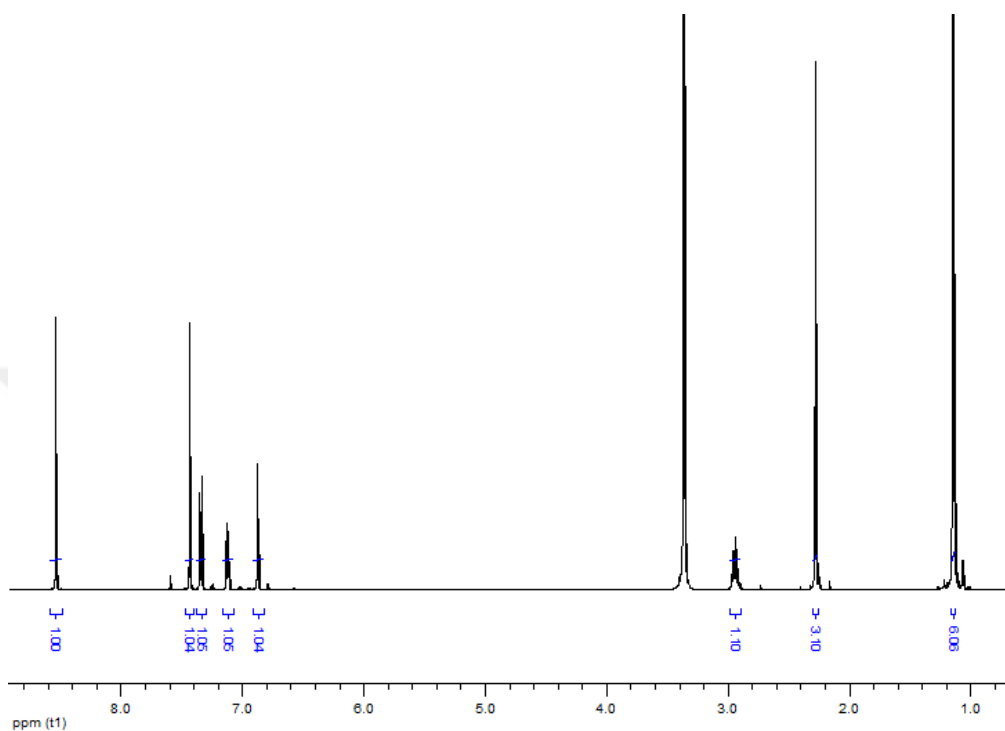
Figure 3.1. ¹H-NMR spectrum of 4-chloro-5-(2-isopropyl-5-methylphenoxy) phthalonitrile (**1**) in CDCl₃.
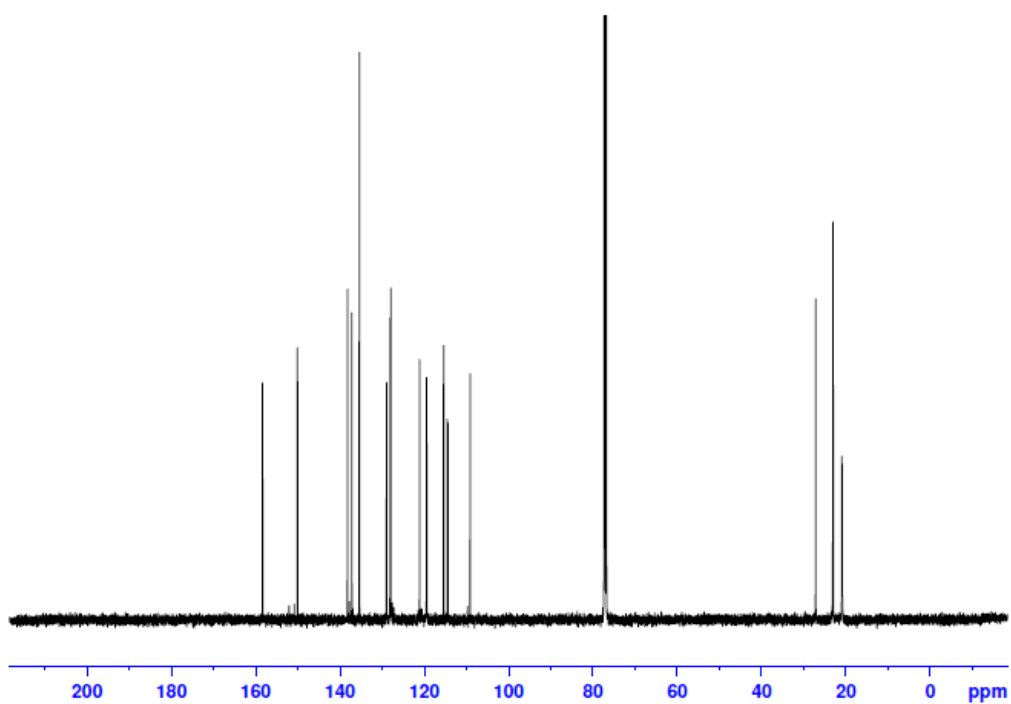
Figure 3.2. ^{13}C-NMR spectrum of 4-chloro-5-(2-isopropyl-5-methylphenoxy) phthalonitrile (**1**) in CDCl[3].
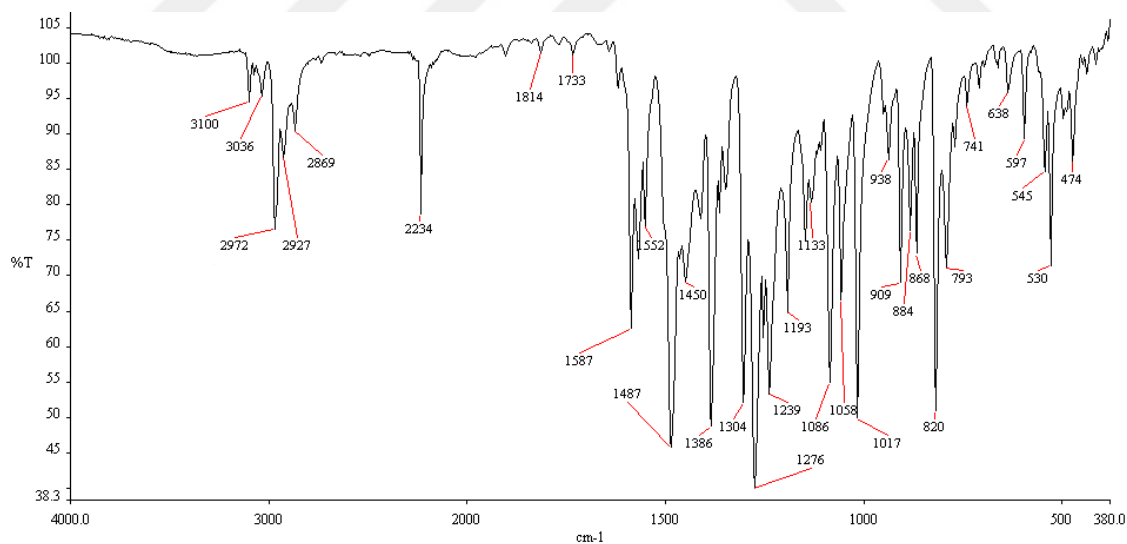
Figure 3.3. FT-IR spectrum of 4-chloro-5-(2-isopropyl-5-methylphenoxy) phthalonitrile (**1**)
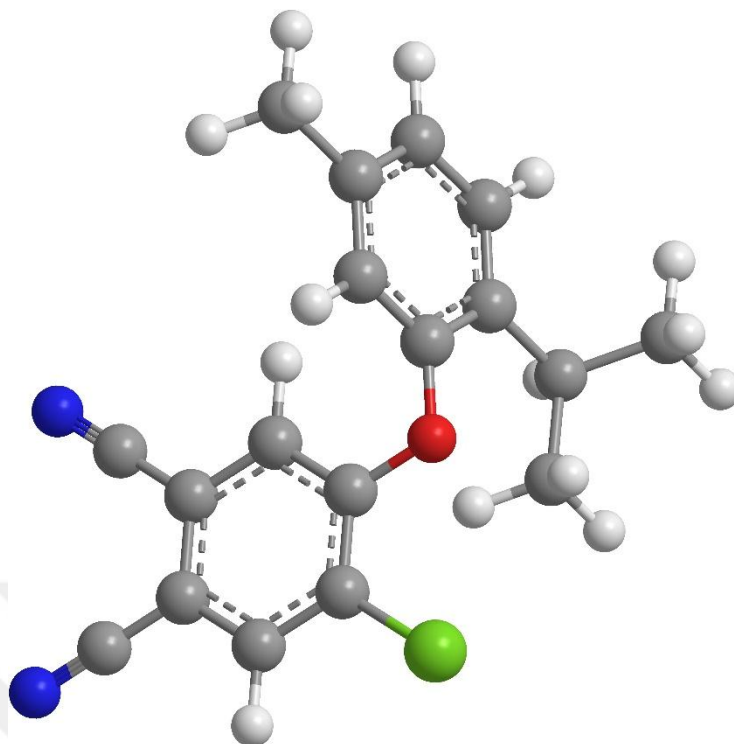
Figure 3.4. 3D structure of 4-chloro-5-(2-isopropyl-5-methylphenoxy)phthalonitrile (**1**)

3. 2. 2. Synthesis of 4,5-bis(2-isopropyl-5-methylphenoxy)phthalonitrile (**2**)
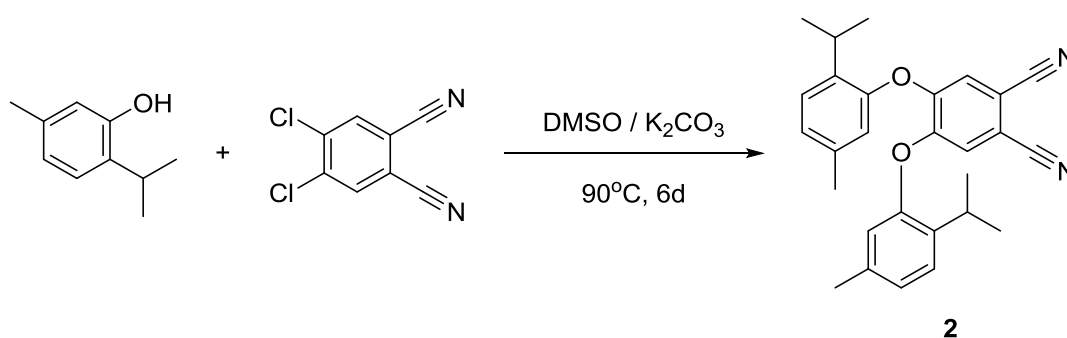
We have followed the literature of *Şehriman Atalay et al.* (124b) for the synthesis of the following phthalonitrile compound.

Solution of thymol (2-isopropyl-5-methylphenol) (1.5 g, 10 mmol) in 20 mL dry DMSO was added slowly while stirring to the solution of 4,5-dichlorophthalonitrile (1 g, 5 mmol) in 30 mL dry DMSO and then the solution stirred further for 15 min. Afterwards finely powdered K_2CO_3 (2.76 g, 20 mmol) was added in portions in one hour. The

reaction solution was stirred at 90 °C for 6 days under argon atmosphere. The reaction solution followed by TLC until the disappearance of spots belong to 4,5-dichlorophthalonitrile and 4-chloro-5-(2-isopropyl-5-methylphenoxy)phthalonitrile (**1**). The reaction terminated and cooled to room temperature, followed by filtering of K_2CO_3. The solution was poured into ice cold water. After the complete precipitation, obtained solids were filtered with sand funnel and washed with water. Purification of the raw product **2** was achieved by column chromatography (silica gel). $CHCl_3$ was used as an eluent. The collected fraction was dried to obtain the 4,5-bis(2-isopropyl-5-methylphenoxy)phthalonitrile (**2**) in a considerably good yield (70%).

Yield: % 70

Mp: 139 °C

Chemical formula: $C_{28}H_{28}N_2O_2$

Molecular weight: 424.54 g/mol

Solubility: DCM, $CHCl_3$, THF, Acetonitrile, Acetone, Toluene, DMF and DMSO.

FT-IR γ max (cm^{-1}): 771, 823, 866, 911, 947, 1006, 1058, 1086, 1176, 1201, 1246, 1292, 1396, 1452, 1494, 1556, 1595, 1616, 1678, 1728, 1775, 1820, 1908, 1982, 2223, 2961, 3041, 3108.
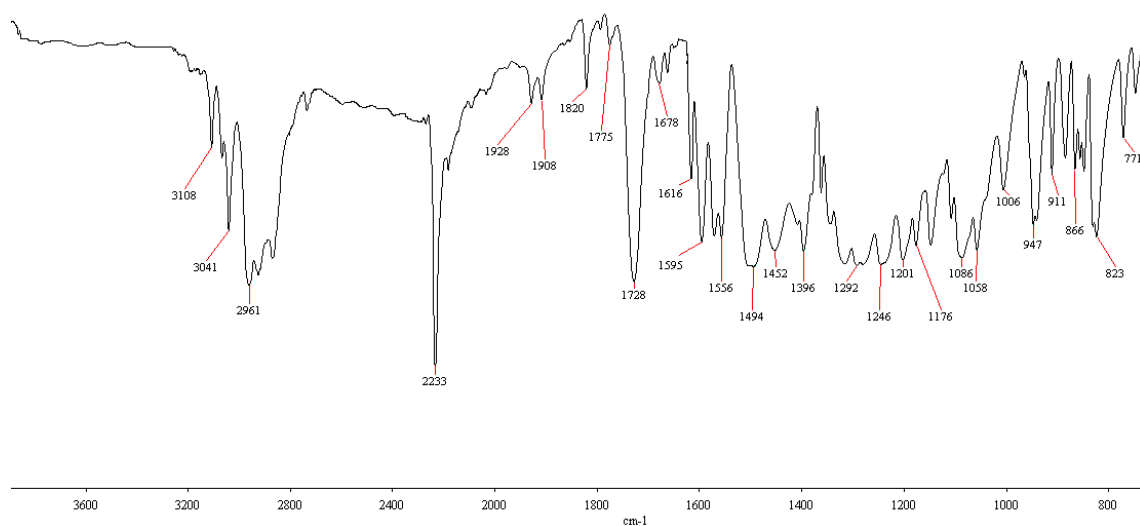
Figure 3.5. FT-IR spectrum of 4,5-bis(2-isopropyl-5-methylphenoxy)phthalonitrile (**2**)
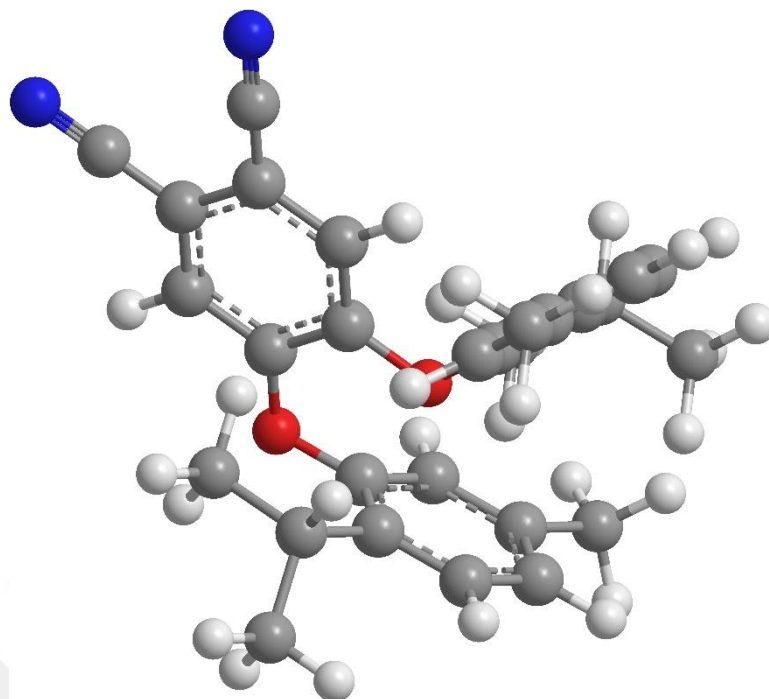
Figure 3.6. 3D structure of 4,5-bis(2-isopropyl-5-methylphenoxy)phthalonitrile (**2**)

3. 2. 3. Synthesis of (E)-4-((4-hydroxy-5-isopropyl-2-methyl phenyl) diazenyl)phthalonitrile (3)
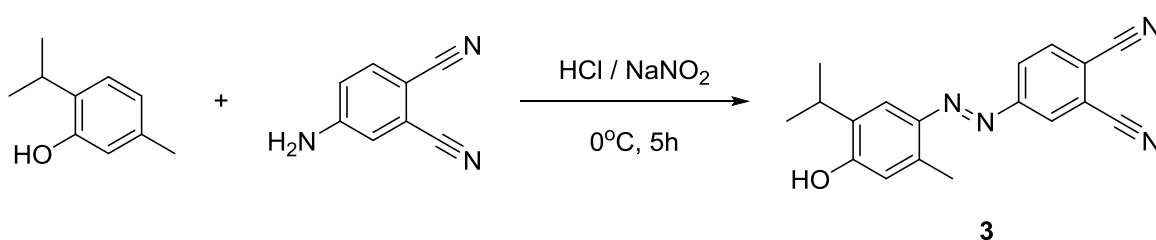
4-aminophthalonitrile (5 mmol, 0.715 g) was dissolved in 16 mL %13 HCl at 0°C and stirred for 10 min. While stirring, solution of $NaNO_2$ (8 mmol, 0.55 g) in 10 mL of distilled water was added dropwise in 20 min. The solution was stirred until it turned completely clear and further stirred for 1 h. Unreacted solids was then filtered of and the reaction solution was added dropwise to a stirring solution of thymol (2-isopropyl-5-methylphenol) (5 mmol, 0.75 g) in 10 mL of glacial acetic acid while cooling in the ice bath. The solution was controlled continuously and pH value kept between 4~5 with

saturated CH₃COONa solution. Dark amaranth solution was precipitated and the mixture stirred one more hour at room temperature. The reaction mixture poured into cold water. The precipitates were isolated by filtration. The crude product recrystallized in MeOH to yield (E)-4-((4-hydroxy-5-isopropyl-2-methyl phenyl)diazenyl) phthalonitrile **3** in %95

Yield: % 95

Mp: 139 °C

Chemical formula: $C_{18}H_{16}N_4O$

Molecular weight: 304.13 g/mol

Solubility: DCM, CHCl₃, THF, Acetonitrile, Toluene, DMF and DMSO.

FT-IR γ max (cm⁻¹): 457, 519, 602, 717, 735, 850, 898, 1004, 1040, 1108, 1132, 1150, 1179, 1224, 1247, 1304, 1354, 1378, 1413, 1440, 1452, 1576, 1600, 1632, 2231, 2255, 2961, 3068, 3454, 3525.

¹H-NMR (500 MHz, d₆-DMSO) δ, ppm: 8.28 (s, 1H), 8.21 (d, *J*=7.21, 1H), 7.98 (d, *J*=7.21, 1H), 7.77 (s, 1H), 6.79 (s, 1H), 3.26 (m, 1H), 2.73 (s, 3H), 1.34 (d, *J*=5.83, 6H).

¹³C-NMR (500 MHz, d₆-DMSO) δ, ppm: 157.8 (1C), 155.4 (1C), 144.4 (1C), 136.8 (1C), 136.4 (1C), 133.4 (1C), 129.2 (1C), 128.1 (1C), 123.0 (1C), 118.2 (1C), 117.6 (1C), 116.2 (1C), 115.9 (2C), 27.2 (1C), 23.8 (2C), 18.3 (1C).
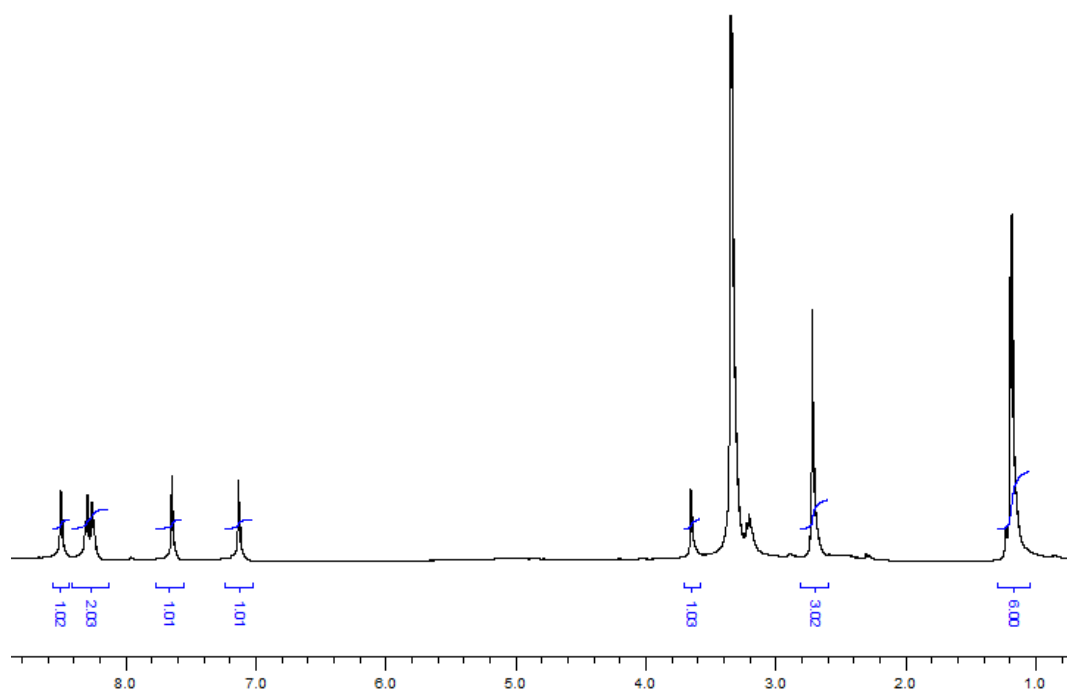
Figure 3.7. ^{1}H-NMR spectrum of (E)-4-((4-hydroxy-5-isopropyl-2-methylphenyl)di-azenyl)phthalonitrile (**3**) in d6-DMSO.
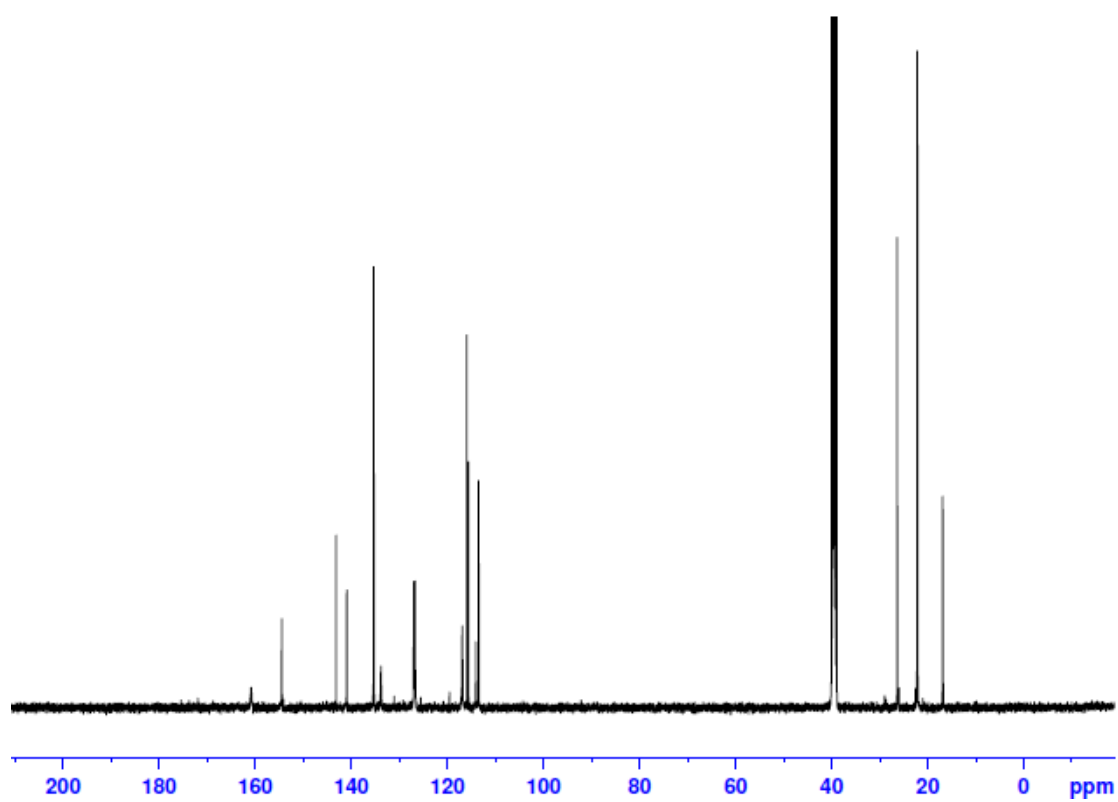
Figure 3.8. ^{13}C-NMR spectrum of (E)-4-((4-hydroxy-5-isopropyl-2-methylphenyl)di-azenyl)phthalonitrile (**3**) in d6-DMSO.
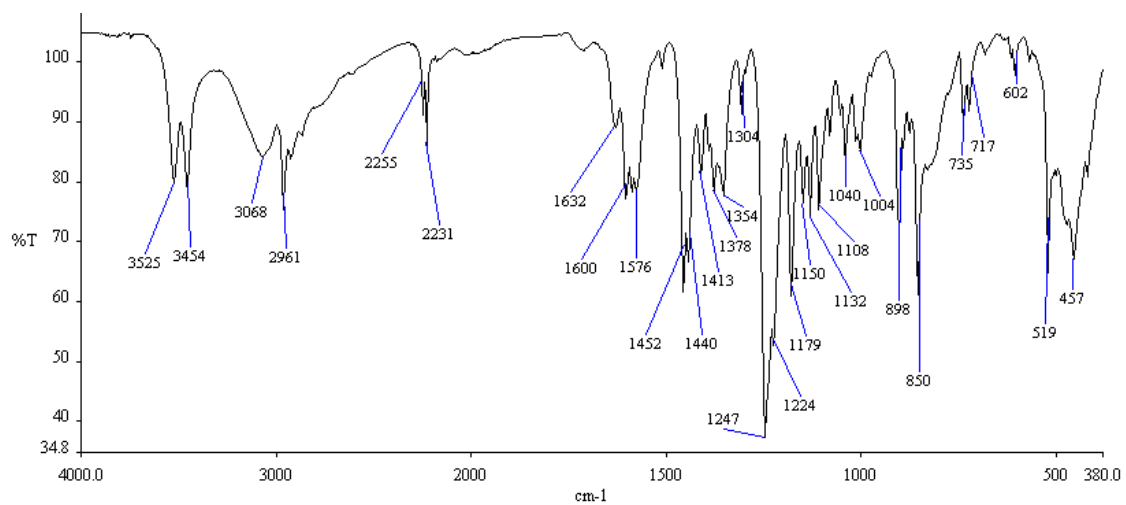
Figure 3.9. FT-IR spectrum of (E)-4-((4-hydroxy-5-isopropyl-2-methylphenyl)diazenyl)-phthalonitrile (**3**)
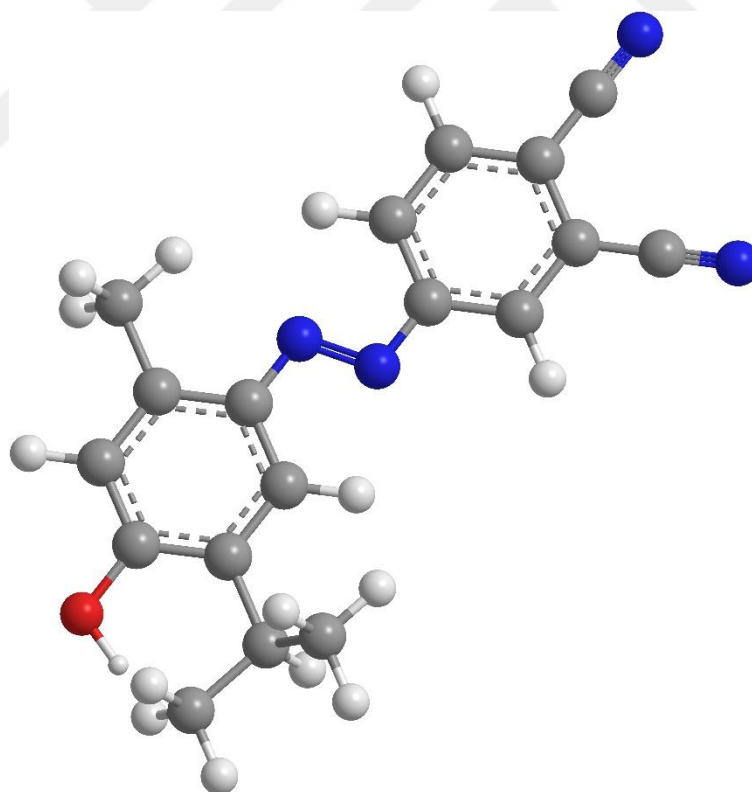
Figure 3.10. 3D structure of (E)-4-((4-hydroxy-5-isopropyl-2-methylphenyl)diazenyl) phthalonitrile (**3**)

3. 2. 4. Synthesis of (E)-4-((5-isopropyl-2-methyl-4-(pentyloxy)-phenyl)diazenyl)phthalonitrile (4)
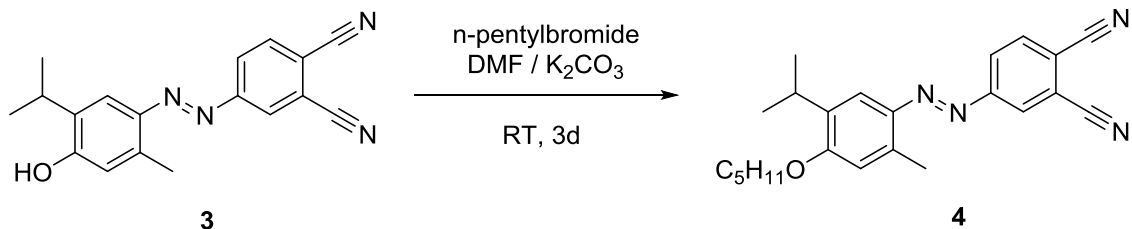
(E)-4-((5-isopropyl-2-methyl-4-(pentyloxy)phenyl)diazenyl)phthalonitrile **3** (5 mmol, 1.71 g) was dissolved in 25 mL dry DMF. The solution was stirred at room temperature for 10 min. Then n-pentylbromide (7 mmol, 1 g) was added dropwise to the solution in 5 min and further stirred for 30 min. Afterwards, anhydrous K_2CO_3 powder (1.38 g, 10 mmol) was added in portions by stirring over 5 h. After 3 days of stirring, the reaction solution was poured into cold water and solid product was isolated by filtration. Recrystallization in MeOH gave product (E)-4-((5-isopropyl-2-methyl-4-(pentyloxy)phenyl)diazenyl)-phthalonitrile **4** in a good yield.

Yield: % 78

Mp: 130 °C

Chemical formula: $C_{23}H_{26}N_4O$

Molecular weight: 374.5 g/mol

Solubility: DCM, CHCl₃, THF, Toluene, DMF and DMSO.

FT-IR γ max (cm⁻¹): 523, 580, 618, 643, 724, 775, 837, 853, 906, 964, 1006, 1057, 1112, 1133, 1186, 1246, 1320, 1246, 1320, 1355, 1387, 1452, 1498, 1571, 1605, 1678, 2230, 2852, 2973, 2967, 3033, 3073, 3093.

¹H-NMR (500 MHz, CDCl₃) δ, ppm: 8.24 (s, 1H), 8.18 (d, *J*=7.25, 1H), 7.88 (d, *J*=7.25, 1H), 7.63 (s, 1H), 7.20 (s, 1H), 4.02 (s, 2H), 3.24 (m, 1H), 2.75 (s, 3H), 1.80 (m, 2H), 1.49 (m, 4H), 1.29 (d, *J*=5.86, 6H), 0.88 (m, 3H).

¹³C-NMR (500 MHz, CDCl₃) δ, ppm: 157.8 (1C), 155.4 (1C), 144.4 (1C), 136.8 (1C), 136.4 (1C), 133.4 (1C), 129.2 (1C), 128.1 (1C), 123.0 (1C), 118.2 (1C), 117.6 (1C), 116.2 (1C), 115.9 (2C), 69.2 (1C), 29.4 (1C), 28.3 (1C), 27.2 (1C), 23.8 (2C), 22.9 (1C), 18.3 (1C), 14.2 (1C).
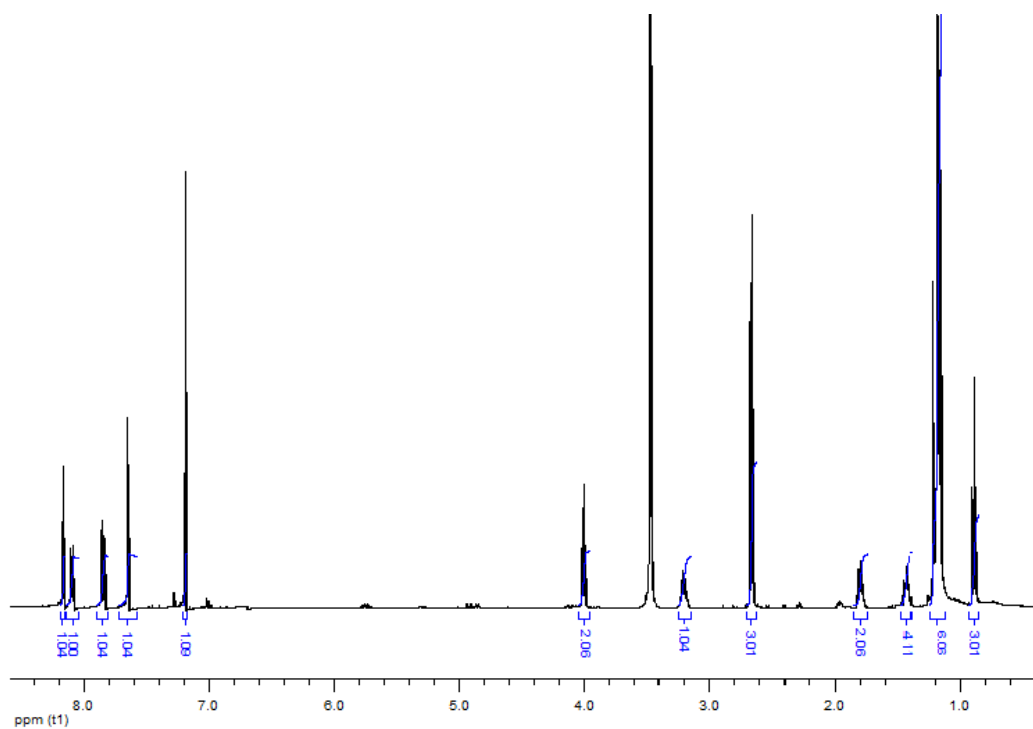
Figure 3.11. ^{1}H-NMR spectrum of (E)-4-((5-isopropyl-2-methyl-4-(pentyloxy)phenyl) diazenyl)phthalonitrile (**4**) in CDCl$_3$.
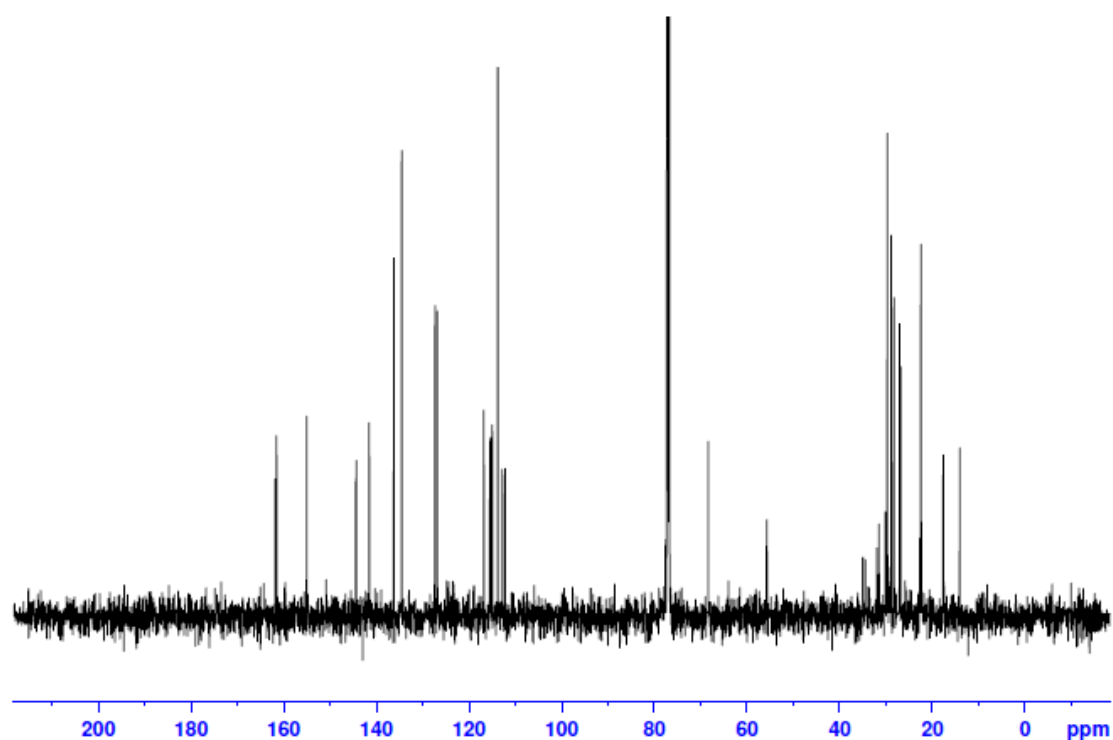
Figure 3.12. ^{13}C-NMR spectrum of (E)-4-((5-isopropyl-2-methyl-4-(pentyloxy)phenyl) diazenyl)phthalonitrile (**4**) in CDCl$_3$.
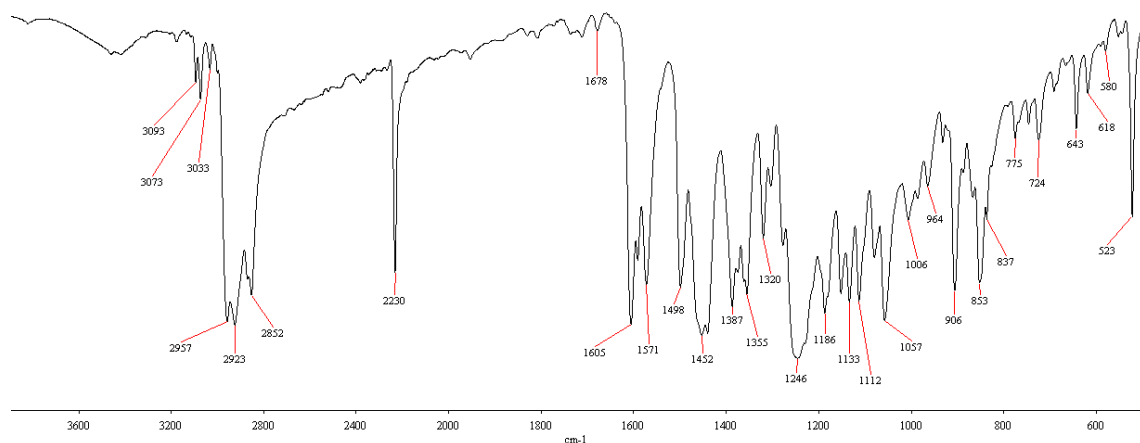
Figure 3.13. FT-IR spectrum of (E)-4-((5-isopropyl-2-methyl-4-(pentyloxy)phenyl) diazenyl)phthalonitrile (**4**)
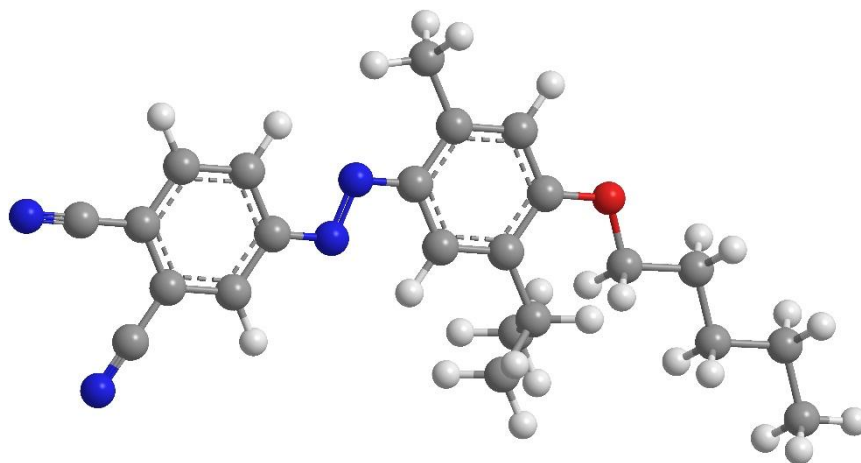
Figure 3.14. 3D structure of (E)-4-((5-isopropyl-2-methyl-4-(pentyloxy)phenyl)-diazenyl)phthalonitrile (**4**)

3. 2. 5. Synthesis of (E)-4-((5-isopropyl-2-methyl-4-(prop-2-yn-1-yloxy)phenyl)diazenyl)phthalonitrile (5)
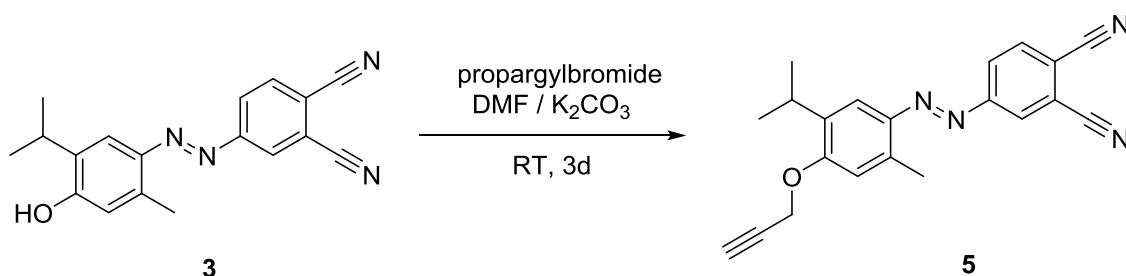
(E)-4-((5-isopropyl-2-methyl-4-(pentyloxy)phenyl)diazenyl)phthalonitrile **3** (5 mmol, 1.71 g) was dissolved in 25 mL dry DMF. The solution was stirred at room temperature for 10 min. Then %80 propargylbromide in toluene (7 mmol, 0.83 g) was added dropwise to the solution in 10 min and further stirred for 30 min. Afterwards, anhydrous K_2CO_3 powder (1.38 g, 10 mmol) was added in portions by stirring over 5 h. After 48

hours of stirring, the reaction solution was poured into cold water and solid product was isolated by filtration. Recrystallization in MeOH gave product (E)-4-((5-isopropyl-2-methyl-4-(prop-2-yn-1-yloxy)phenyl)diazenyl)phthalonitrile **5** in a good yield.

Yield: % 80

Mp: 145 °C

Chemical formula: $C_{21}H_{18}N_4O$

Molecular weight: 326.40 g/mol

Solubility: DCM, $CHCl_3$, THF, Toluene, DMF and DMSO.

FT-IR γ max (cm^{-1}): 390, 523, 544, 625, 664, 727, 779, 842, 902, 920, 948, 1018, 1056, 1109, 1186, 1235, 1358, 1442, 1495, 1575, 1603, 1670, 2231, 2870, 2926, 3249

^{1}H-NMR (500 MHz, d$_6$-DMSO) δ, ppm: 8.42 (s, 1H), 8.26 (d, J=7.25, 1H), 8.21 (d, J=7.25, 1H), 7.64 (s, 1H), 6.82 (s, 1H), 4.69 (s, 1H), 3.59 (s, 2H), 3.19 (m, 1H), 2.61 (s, 3H), 1.22 (d, J=5.86, 6H).

^{13}C-NMR (500 MHz, d$_6$-DMSO) δ, ppm: 157.8 (1C), 155.4 (1C), 144.4 (1C), 136.8 (1C), 136.4 (1C), 133.4 (1C), 129.2 (1C), 128.1 (1C), 123.0 (1C), 118.2 (1C), 117.6 (1C), 116.2 (1C), 115.9 (2C), 76.6 (1C), 78.9 (1C), 57.4 (1C), 27.2 (1C), 23.8 (2C), 18.3 (1C).
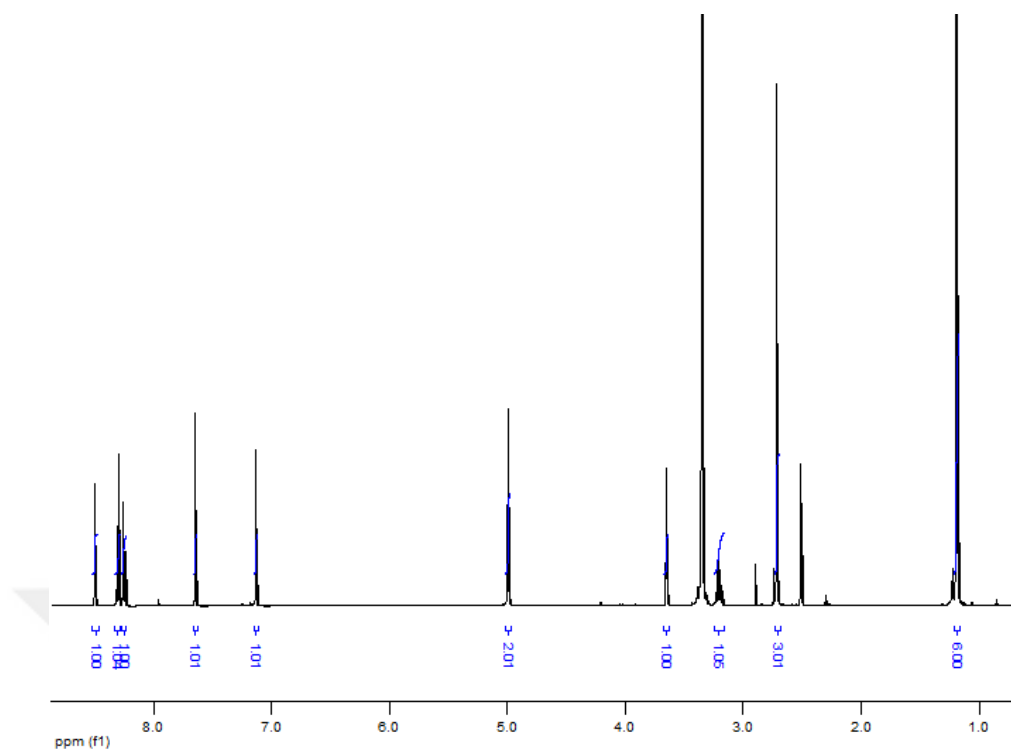
Figure 3.15. ^{1}H-NMR spectrum of (E)-4-((5-isopropyl-2-methyl-4-(prop-2-yn-1-yloxy)phenyl)diazenyl)phthalonitrile (**5**) in d$_6$-DMSO.
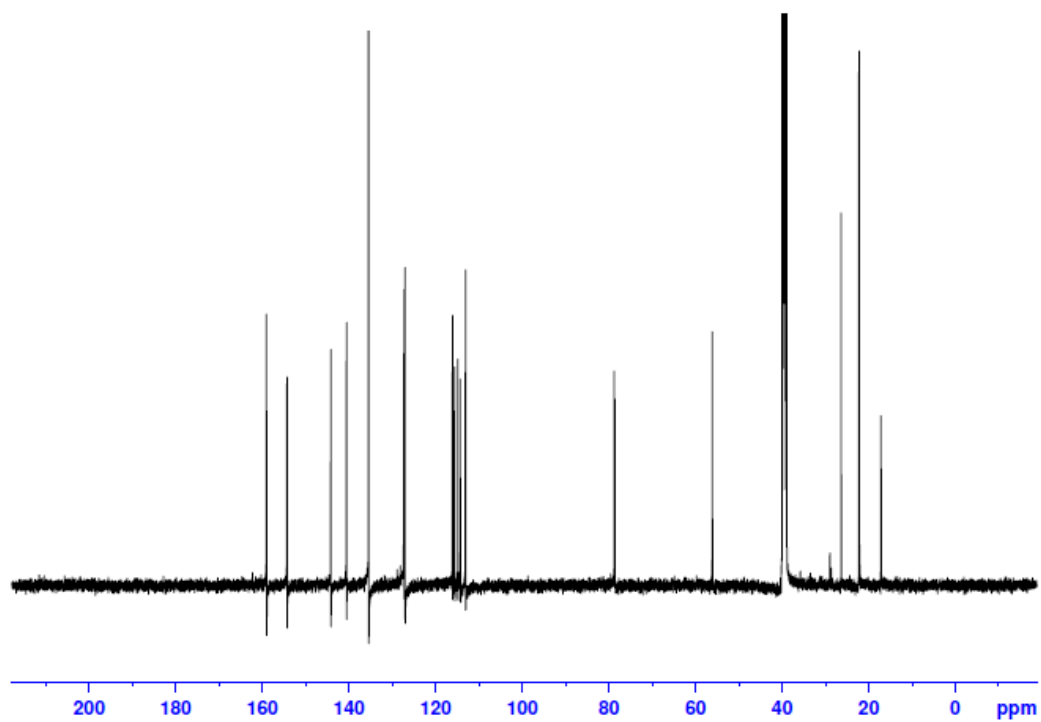
Figure 3.16. ^{13}C-NMR spectrum of (E)-4-((5-isopropyl-2-methyl-4-(prop-2-yn-1-yloxy)phenyl)diazenyl)phthalonitrile (**5**) in d$_6$-DMSO.
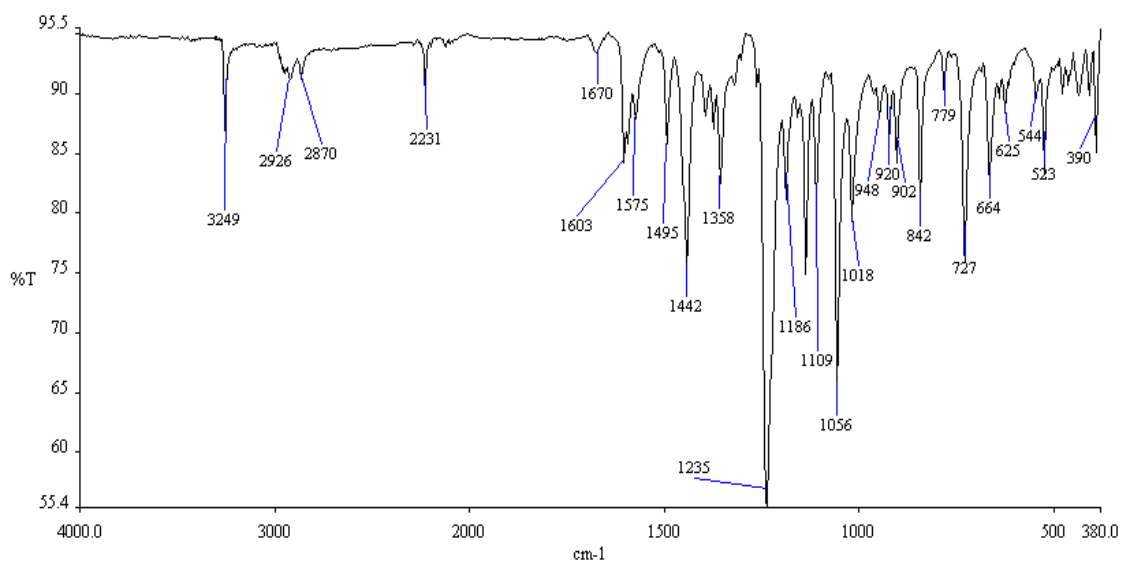
Figure 3.17. FT-IR spectrum of (E)-4-((5-isopropyl-2-methyl-4-(prop-2-yn-1-yloxy)phenyl) diazenyl)phthalonitrile (**5**)
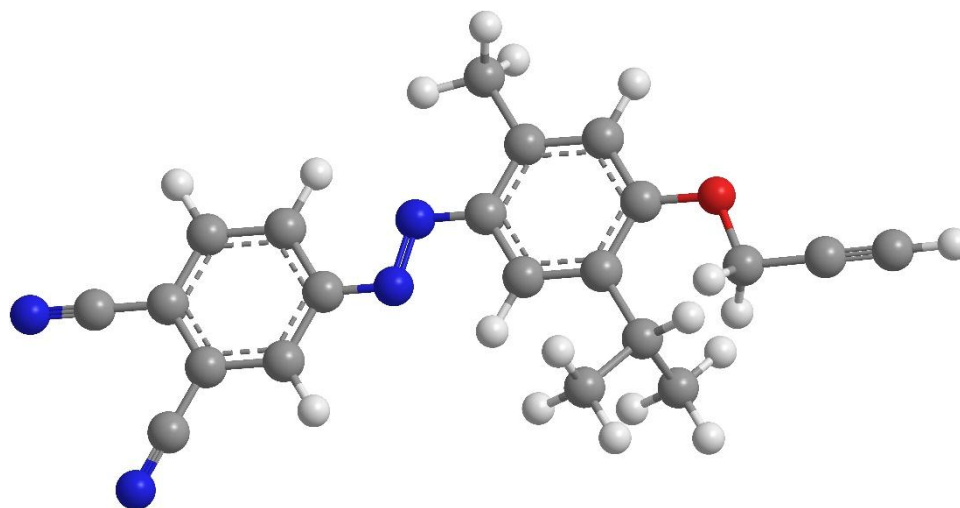
Figure 3.18. 3D structure of (E)-4-((5-isopropyl-2-methyl-4-(prop-2-yn-1-yloxy)phenyl) diazenyl)phthalonitrile (**5**)

3. 3. Synthesis of phthalocyanines

3. 3. 1. Synthesis of 2,9,16,23-tetrachloro-3,10,17,24-tetrakis(2-isopropyl-5-methylphenoxy)phthalocyanine (6)

M: 2H (**6**), Co (**7**), Cu (**8**), Fe (**9**), InOAc (**10**), LuOAc (**11**), Mg (**12**), MnCl (**13**), Zn (**14**)
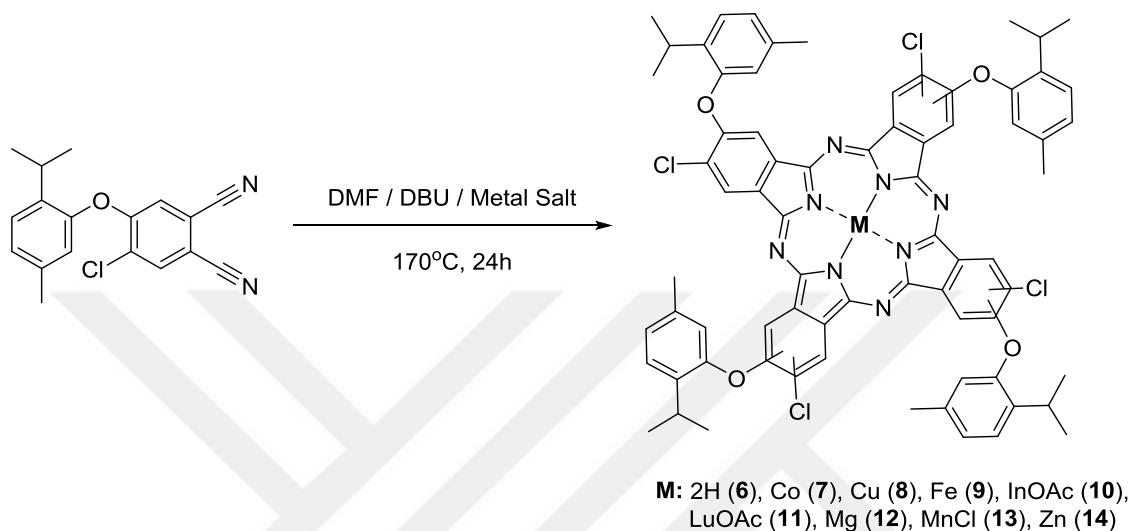
Scheme 3.2. Synthesis of 2,9,16,23-tetrachloro-3,10,17,24-tetrakis(2-isopropyl-5-methylphenoxy)phthalocyanine (**6**) and its metal derivatives.

0.31 g (1 mmol) 4-chloro-5-(2-isopropyl-5-methylphenoxy)phthalonitrile (**1**) and 0.01 g lithium (1.69 mol) in 1-pentanol (10 ml) were mixed and stirred at 170 °C for 18 hours under N_2 atmosphere. The solution was cooled. Then the solvent was evaporated under vacuo. Then CH_3COOH (30 ml) was added and the suspension was stirred for 30 minutes. The product is extracted with DCM and washed with water (3 x 30 ml). The organic phase is separated, dried with magnesium sulfate.

Yield: % 26

Mp: >300 °C

Chemical formula: $C_{72}H_{62}Cl_4N_8O_4$

Molecular weight: 1245 g/mol

Solubility: DCM, $CHCl_3$, THF, Acetonitrile, Acetone, Toluene, DMF and DMSO.

FT-IR γ max (cm⁻¹): 436, 460, 586, 688, 737, 811, 881, 937, 1011, 1084, 1147, 1246, 1417, 1502, 1575, 1603, 2014, 2161, 2554, 2867, 2924, 2959, 3028, 3286.

UV-*vis* (DCM, 1x10^{-5}M): λ$_{max}$ (nm) (log ε): 701 (5.05), 667 (5.03), 637 (4.71), 608 (4.56), 347 (4.91).

MALDI-TOF-MS: 1245.738 (M$^+$) m/z.
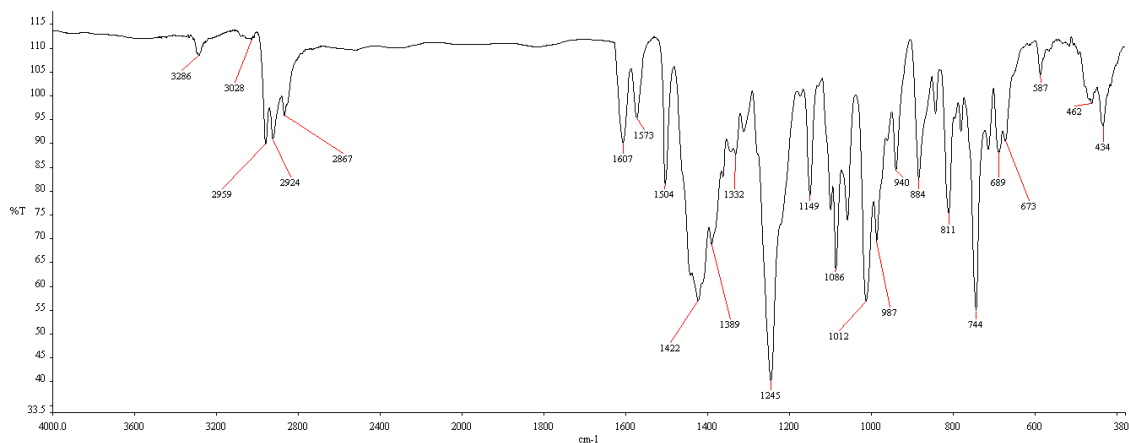
Figure 3.19. FT-IR spectrum of 2,9,16,23-tetrachloro-3,10,17,24-tetrakis(2-isopropyl-5-methylphenoxy)phthalocyanine (**6**).

Figure 3.20. UV-*vis* spectrum of 2,9,16,23-tetrachloro-3,10,17,24-tetrakis(2-isopropyl-5-methylphenoxy)phthalocyanine (**6**) in DCM at 10x10^{-5}M.

60
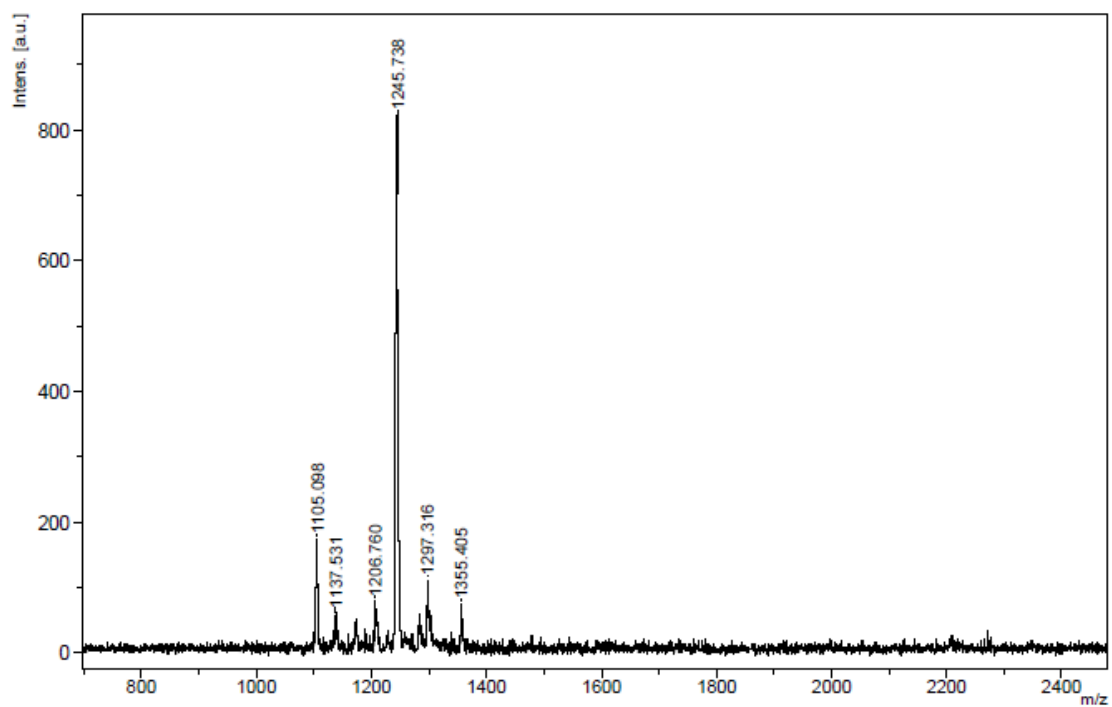
Figure 3.21. MALDI-TOF Mass spectrum of 2,9,16,23-tetrachloro-3,10,17,24-tetrakis(2-isopropyl-5-methylphenoxy)phthalocyanine (**6**).
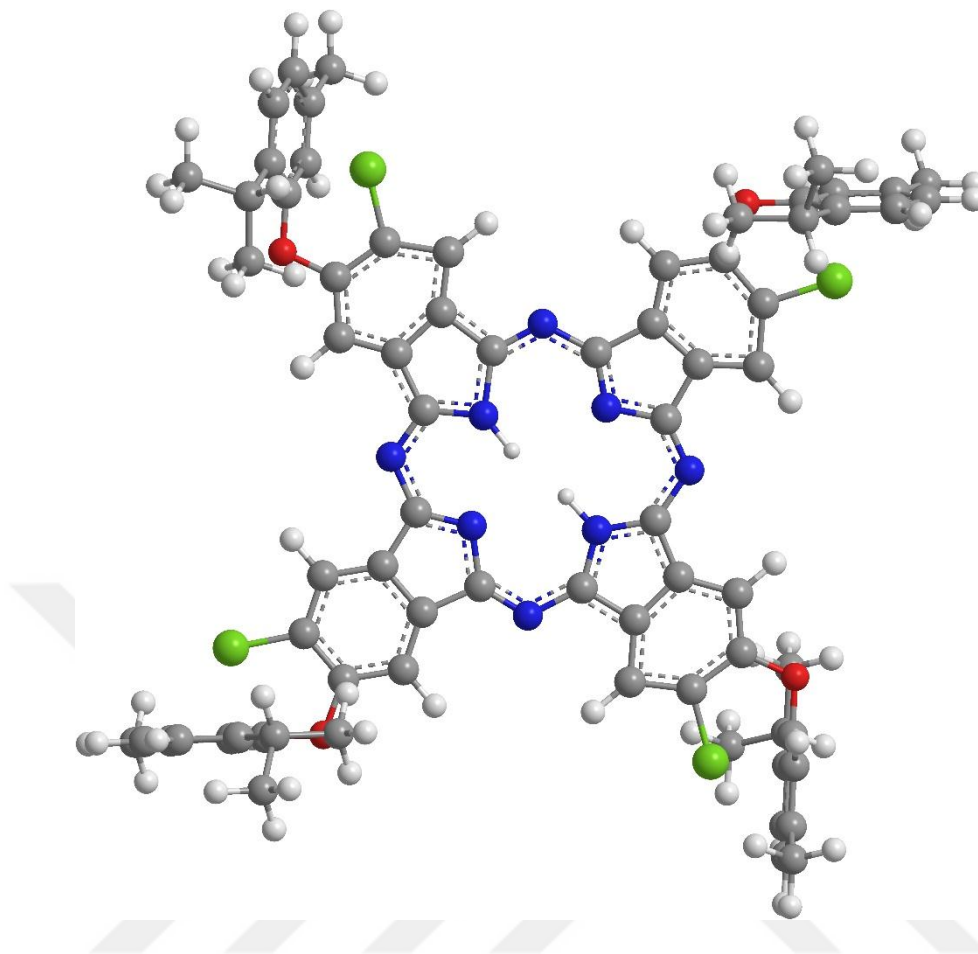
Figure 3.22. Optimized geometry of 2,9,16,23-tetrachloro-3,10,17,24-tetrakis(2-isopropyl-5-methylphenoxy)phthalocyanine (**6**).
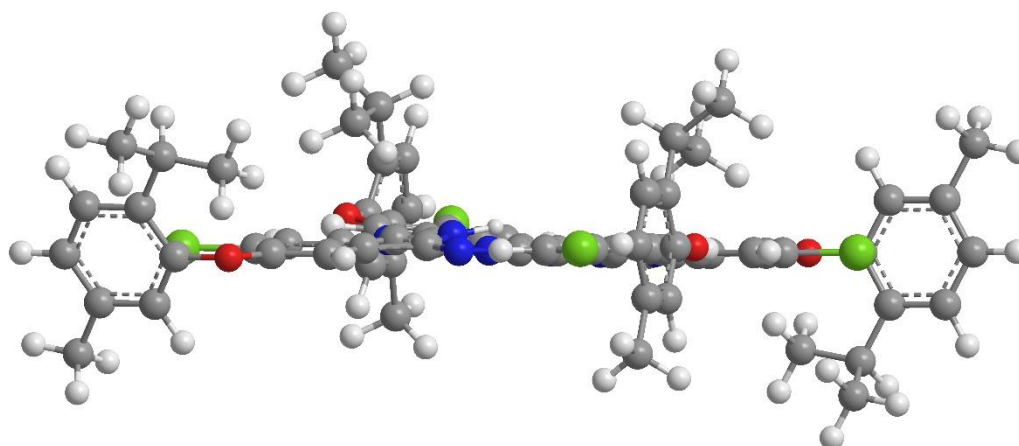
Figure 3.23. Side view of 2,9,16,23-tetrachloro-3,10,17,24-tetrakis(2-isopropyl-5-methylphenoxy)phthalocyanine (**6**).

3. 3. 2. Synthesis of 2,9,16,23-tetrachloro-3,10,17,24-tetrakis(2-isopropyl-5-methylphenoxy)phthalocyanine metal derivatives (7-14)

4-chloro-5-(2-isopropyl-5-methylphenoxy)phthalonitrile (**1**) (1 mmol, 0.31 g), 2 mmol metal salt (0.35 g cobalt(II) acetate for CoPc (**7**), 0.36 g copper(II) acetate for CuPc (**8**), 0.34 g iron(II) acetate for FePc (**9**), 0.58 g indium(III) acetate for InOAcPc (**10**), 0.73 g lutetium(III) acetate hydrate for LuOAcPc (**11**), 0.43 g magnesium acetate tetrahydrate for MgPc (**12**), 0.25 g manganese(II) chloride hydrate for MnClPc (**13**), 0.37 g Zinc acetate for ZnPc (**14**)) and 0.2 mL of DMF were evacuated into a Schlenk tube and stirred until all solids had dissolved. Then DBU (0.35 ml, 2.34 mmol) was added dropwise to a reaction tube while stirring. The reaction mixture was stirred at 170 °C under inert atmosphere overnight. After cooling to room temperature, the reaction solution poured onto 450 ml of methanol / water (8: 1). Solids were filtered. The crude product was washed overnight with water and methanol in a Soxhlet apparatus. The resulting solid was purified by column chromatography (silica gel) with $CHCl_3$/MeOH (20:1). Distillative removal of the solvents yield green crystalline solid products.

3.3.2.1. 2,9,16,23-tetrachloro-3,10,17,24-tetrakis(2-isopropyl-5-methylphenoxy)phthalocyaninato cobalt (7)

Yield: % 24
Mp: >300 °C
Chemical formula: $C_{72}H_{60}Cl_4CoN_8O_4$
Molecular weight: 1302 g/mol
Solubility: DCM, $CHCl_3$, THF, Toluene, DMF and DMSO.
FT-IR γ max (cm^{-1}): 495, 582, 662, 751, 812, 885, 943, 1009, 1060, 1104, 1148, 1251, 1344, 1402, 1440, 1504, 1522, 1574, 1607, 1654, 2868, 2924, 2959, 3051.
UV-*vis* (DCM, 1x10^{-5}M): λ_{max} (nm) (log ϵ): 674 (5.00), 611 (4.53), 330 (4.76).
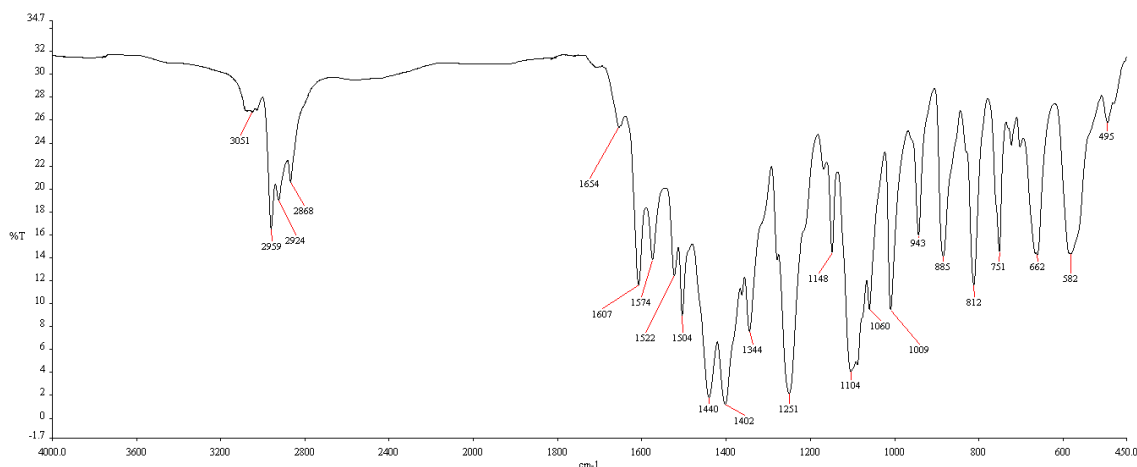
Figure 3.24. FT-IR spectrum of 2,9,16,23-tetrachloro-3,10,17,24-tetrakis(2-isopropyl-5-methylphenoxy)phthalocyaninato cobalt (**7**).

Figure 3.25. UV-*vis* spectrum of 2,9,16,23-tetrachloro-3,10,17,24-tetrakis(2-isopropyl-5-methylphenoxy)phthalocyaninato cobalt (**7**) in DCM at 1×10^{-5}M.

3.3.2.2. 2,9,16,23-tetrachloro-3,10,17,24-tetrakis(2-isopropyl-5-methylphenoxy)phthalocyaninato copper (8)

Yield: % 26

Mp: >300 °C

64

Chemical formula: $C_{72}H_{60}Cl_4CuN_8O_4$

Molecular weight: 1306 g/mol

Solubility: DCM, CHCl$_3$, THF, Toluene, DMF and DMSO.

FT-IR γ max (cm^{-1}): 492, 588, 701, 745, 811, 884, 943, 1003, 1060, 1095, 1148, 1249, 1341, 1397, 1437, 1504, 1574, 1608, 2868, 2924, 2960, 3027.

UV-*vis* (DCM, 1x10^{-5}M): λ_{max} (nm) (log ε): 681 (5.18), 619 (4.73), 343 (4.93).

Figure 3.26. FT-IR spectrum of 2,9,16,23-tetrachloro-3,10,17,24-tetrakis(2-isopropyl-5-methylphenoxy)phthalocyaninato copper (**8**).

Figure 3.27. UV-*vis* spectrum of 2,9,16,23-tetrachloro-3,10,17,24-tetrakis(2-isopropyl-5-methylphenoxy)phthalocyaninato copper (**8**) in DCM at 1x10^{-5}M.

3.3.2.3. 2,9,16,23-tetrachloro-3,10,17,24-tetrakis(2-isopropyl-5-methylphenoxy)phthalocyaninato iron (9)

Yield: % 28

Mp: >300 °C

Chemical formula: $C_{72}H_{60}Cl_4FeN_8O_4$

Molecular weight: 1299 g/mol

Solubility: DCM, CHCl$_3$, THF, Toluene, DMF and DMSO.

FT-IR γ max (cm^{-1}): 502, 701, 747, 812, 885, 943, 1007, 1090, 1149, 1252, 1328, 1395, 1439, 1504, 1575, 1605, 1632, 2863, 2961, 3047.

UV-*vis* (DCM, 1x10^{-5}M): λ_{max} (nm) (log ε): 712 (4.88), 667 (4.78), 589 (4.29), 358 (4.94).

MALDI-TOF-MS: 1299.070 (M$^+$) m/z.
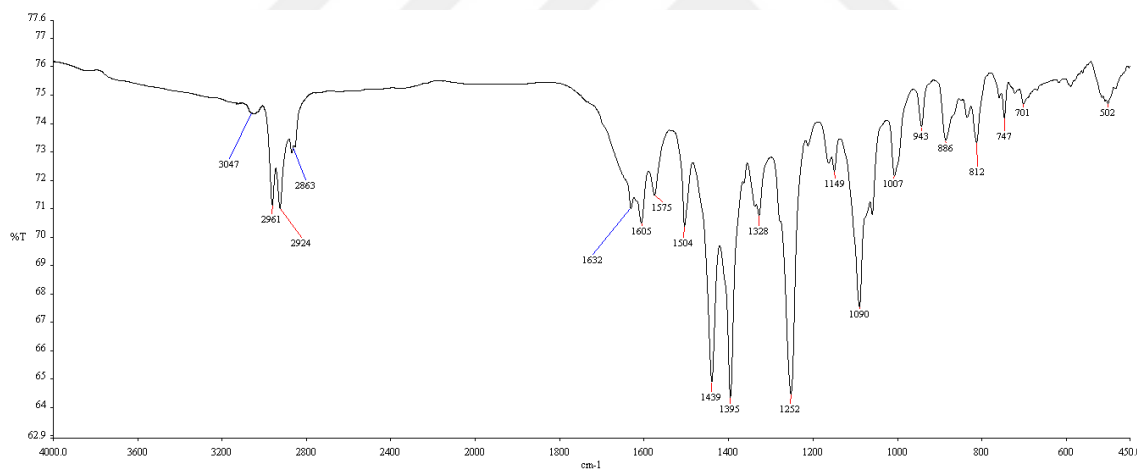
Figure 3.28. FT-IR spectrum of 2,9,16,23-tetrachloro-3,10,17,24-tetrakis(2-isopropyl-5-methylphenoxy)phthalocyaninato iron (**9**).

66
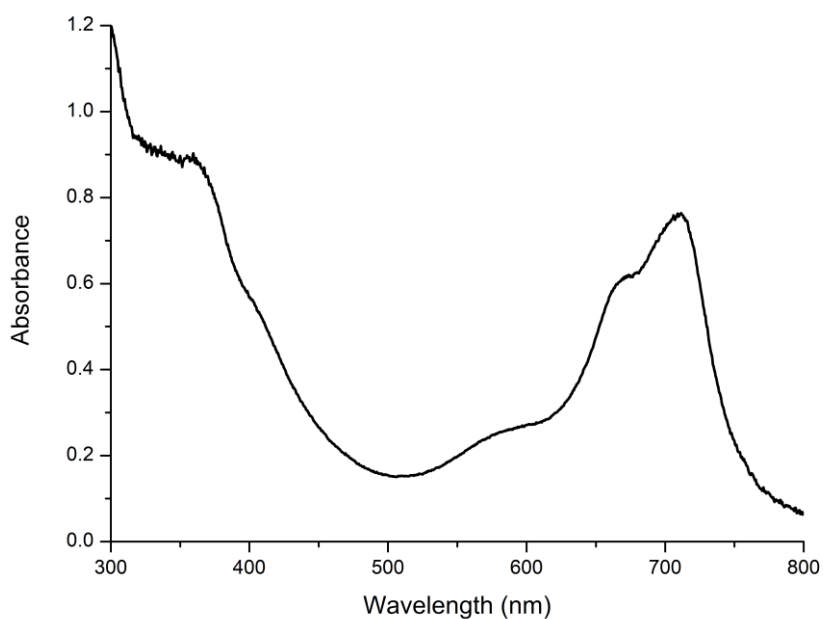
Figure 3.29. UV-*vis* spectrum of 2,9,16,23-tetrachloro-3,10,17,24-tetrakis(2-isopropyl-5-methylphenoxy)phthalocyaninato iron (**9**) in DCM at 1×10^{-5}M.
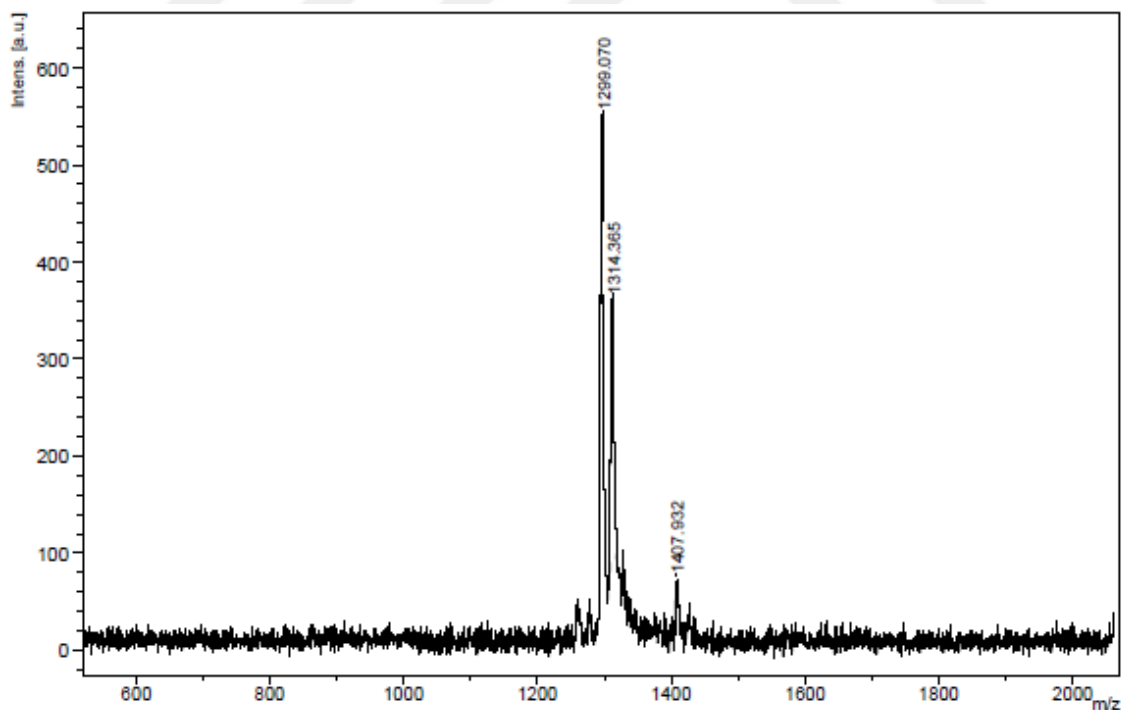
Figure 3.30. MALDI-TOF Mass spectrum of 2,9,16,23-tetrachloro-3,10,17,24-tetrakis(2-isopropyl-5-methylphenoxy)phthalocyaninato iron (**9**).

3.3.2.4. 2,9,16,23-tetrachloro-3,10,17,24-tetrakis(2-isopropyl-5-methylphenoxy)phthalocyaninato indium (III) acetate (10)

Yield: % 19

Mp: >300 °C

Chemical formula: $C_{74}H_{63}Cl_4InN_8O_6$

Molecular weight: 1417 g/mol

Solubility: DCM, CHCl$_3$, THF, Toluene, DMF and DMSO.

FT-IR γ max (cm^{-1}): 439, 555, 586, 744, 814, 944, 993, 1060, 1084, 1147, 1246, 1330, 1389, 1435, 1505, 1572, 1603, 1649, 1718, 2851, 2867, 2924, 2959, 3052.

UV-*vis* (DMSO, 1x10^{-5}M): λ$_{max}$ (nm) (log ε): 693 (4.96), 626 (4.30), 366 (4.72).
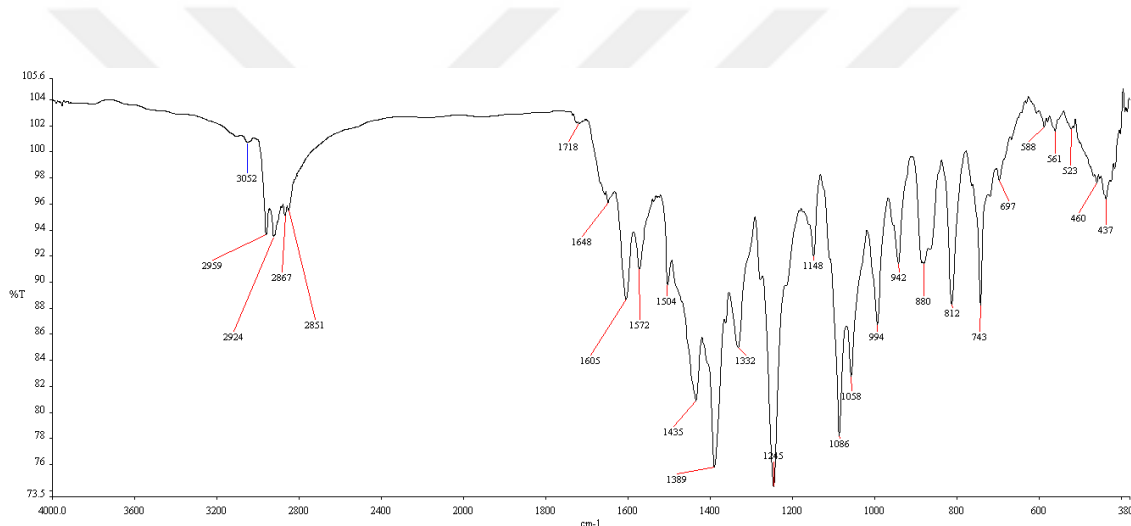
Figure 3.31. FT-IR spectrum of 2,9,16,23-tetrachloro-3,10,17,24-tetrakis(2-isopropyl-5-methylphenoxy)phthalocyaninato indium (III) acetate (**10**).
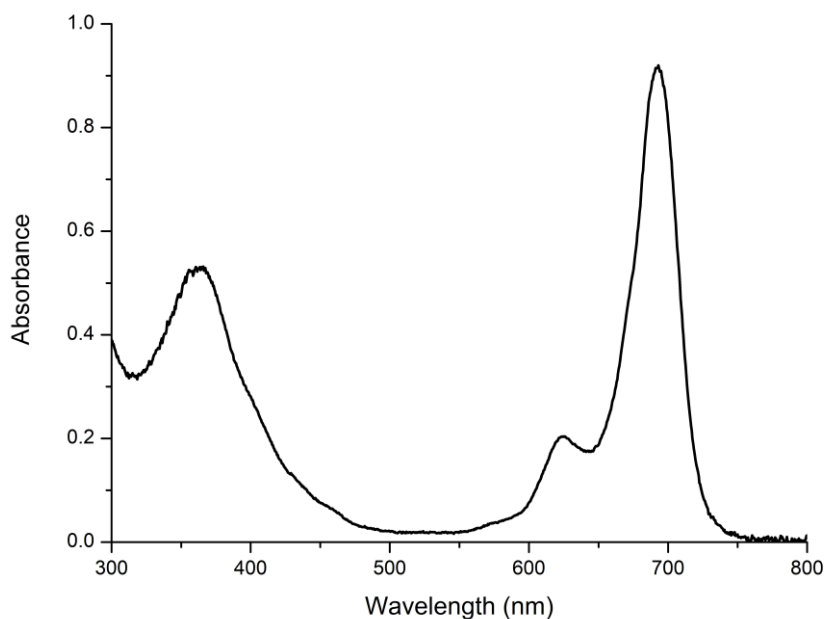
Figure 3.32. UV-*vis* spectrum of 2,9,16,23-tetrachloro-3,10,17,24-tetrakis(2-isopropyl-5-methylphenoxy)phthalocyaninato indium (III) acetate (**10**) in DMSO at 1×10^{-5}M.

3.3.2.5. 2,9,16,23-tetrachloro-3,10,17,24-tetrakis(2-isopropyl-5-methylphenoxy)phthalocyaninato lutetium (III) acetate (11)

Yield: % 21

Mp: >300 °C

Chemical formula: $C_{74}H_{63}Cl_4LuN_8O_6$

Molecular weight: 1477 g/mol

Solubility: DCM, $CHCl_3$, THF, Toluene, DMF and DMSO.

FT-IR γ max (cm^{-1}): 432, 474, 586, 678, 751, 811, 888, 944, 993, 1056, 1084, 1147, 1246, 1389, 1435, 1568, 1607, 1656, 1719, 2867, 2924, 2960, 3018.

UV-*vis* (DMSO, 1×10^{-5}M): λ_{max} (nm) (log ε): 685 (5.06), 614 (4.33), 358 (4.77).
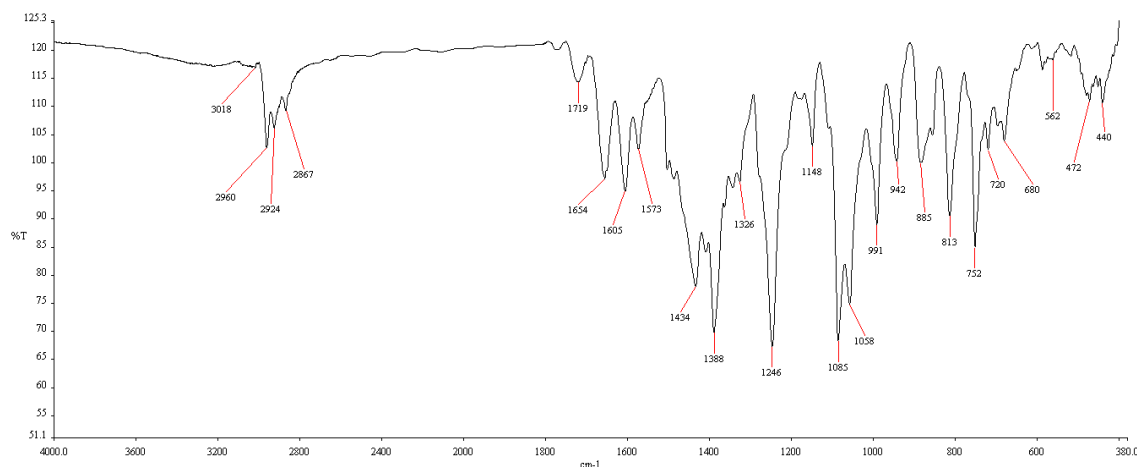
Figure 3.33. FT-IR spectrum of 2,9,16,23-tetrachloro-3,10,17,24-tetrakis(2-isopropyl-5-methylphenoxy)phthalocyaninato lutetium (III) acetate (**11**).
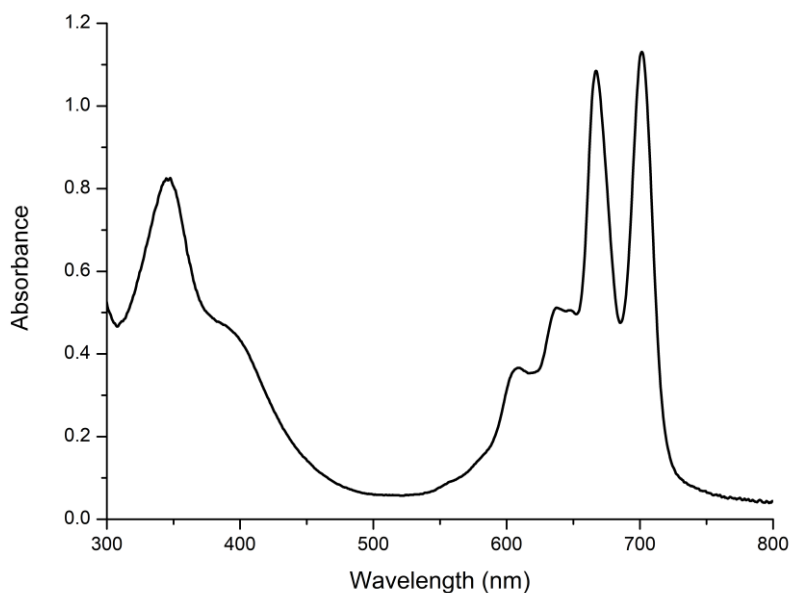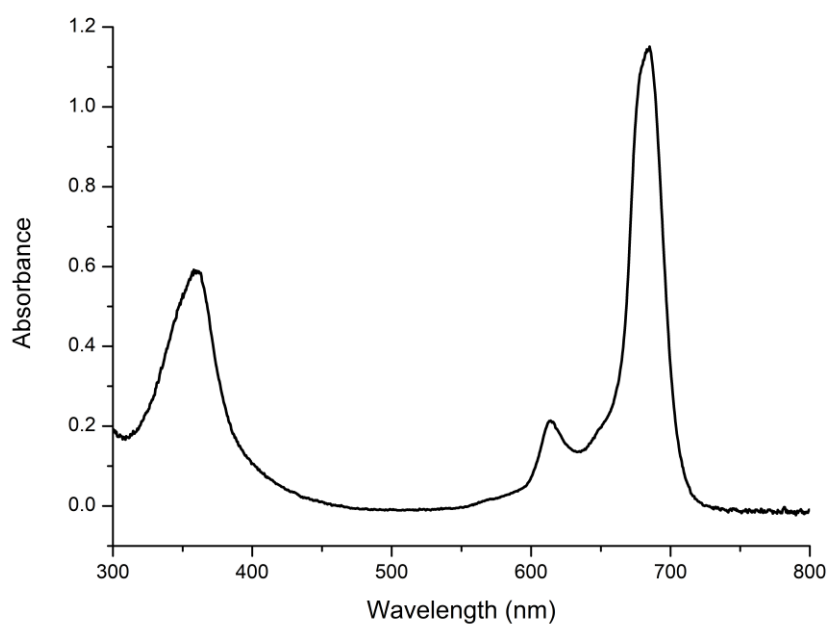

Figure 3.34. UV-*vis* spectrum of 2,9,16,23-tetrachloro-3,10,17,24-tetrakis(2-isopropyl-5-methylphenoxy)phthalocyaninato lutetium (III) acetate (**11**) in DMSO at $1x10^{-5}M$.

3.3.2.6. 2,9,16,23-tetrachloro-3,10,17,24-tetrakis(2-isopropyl-5-methylphenoxy)phthalocyaninato magnesium (12)

Yield: % 32

Mp: >300 °C

Chemical formula: $C_{72}H_{60}Cl_4MgN_8O_4$

Molecular weight: 1267 g/mol

Solubility: DCM, CHCl$_3$, THF, Toluene, DMF and DMSO.

FT-IR γ max (cm^{-1}): 432, 492, 590, 695, 748, 807, 884, 941, 986, 1053, 1088, 1151, 1242, 1333, 1389, 1424, 1498, 1572, 1603, 1663, 2856, 2919, 2954, 3024.

UV-*vis* (DMSO, 1x10^{-5}M): λ$_{max}$ (nm) (log ε): 680 (4.96), 615 (4.42), 358 (4.71).

MALDI-TOF-MS: 1266.570 (M-H)$^+$ m/z.
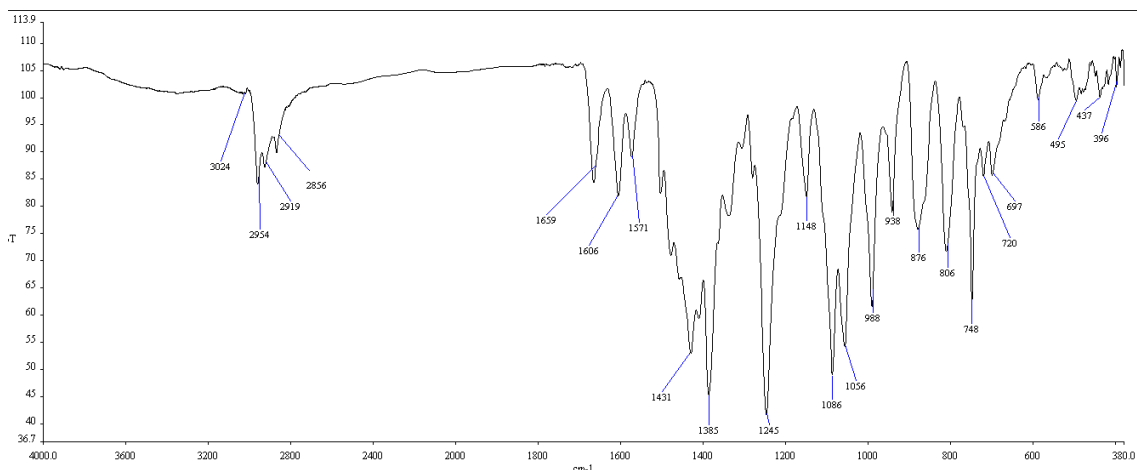
Figure 3.35. FT-IR spectrum of 2,9,16,23-tetrachloro-3,10,17,24-tetrakis(2-isopropyl-5-methylphenoxy)phthalocyaninato magnesium (**12**).
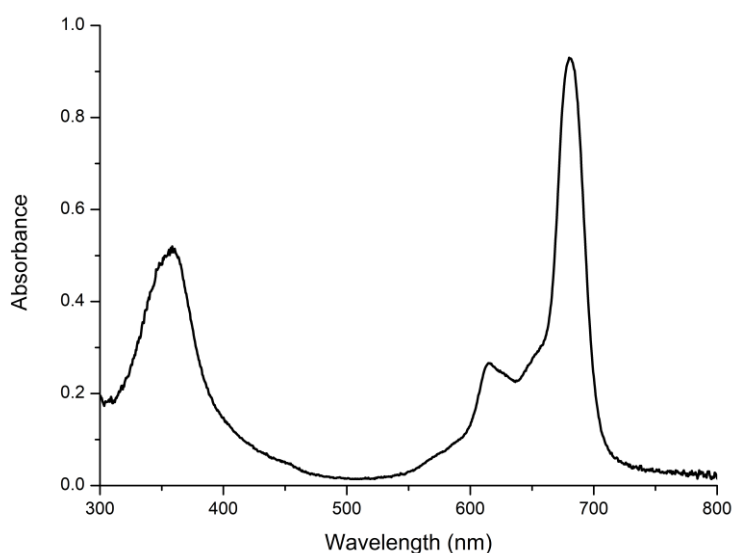
Figure 3.36. UV-*vis* spectrum of 2,9,16,23-tetrachloro-3,10,17,24-tetrakis(2-isopropyl-5-methylphenoxy)phthalocyaninato magnesium (**12**) in DMSO at 1x10^{-5}M.

71
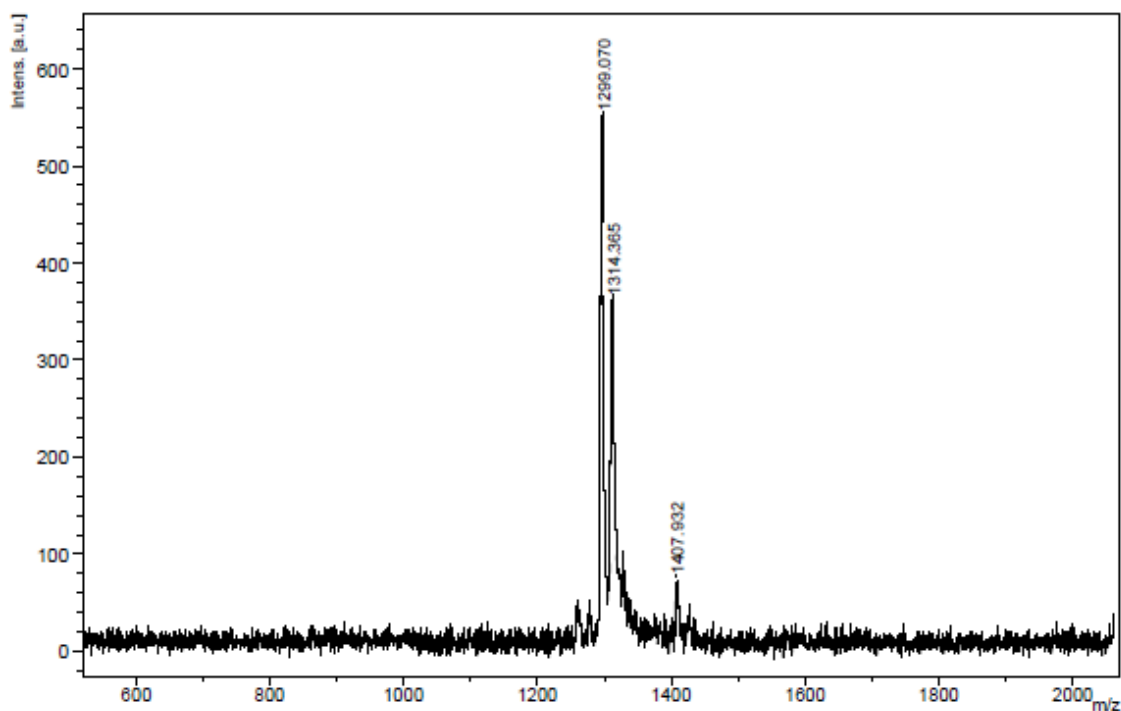
Figure 3.37. MALDI-TOF Mass spectrum of 2,9,16,23-tetrachloro-3,10,17,24-tetrakis(2-isopropyl-5-methylphenoxy)phthalocyaninato magnesium (**12**).

3.3.2.7. 2,9,16,23-tetrachloro-3,10,17,24-tetrakis(2-isopropyl-5-methylphenoxy)phthalocyaninato manganese (III) chloride (13)

Yield: % 27

Mp: >300 °C

Chemical formula: $C_{72}H_{60}Cl_5MnN_8O_4$

Molecular weight: 1333 g/mol

Solubility: DCM, $CHCl_3$, THF, Toluene, DMF and DMSO.

FT-IR γ max (cm^{-1}): 531, 632, 702, 743, 813, 885, 943, 1006, 1088, 1149, 1251, 1335, 1396, 1439, 1504, 1574, 1607, 2867, 2926, 2961, 3034.

UV-*vis* (DMSO, 1x10^{-5}M): λ$_{max}$ (nm) (log ε): 726 (5.13), 652 (4.47), 375 (4.84).
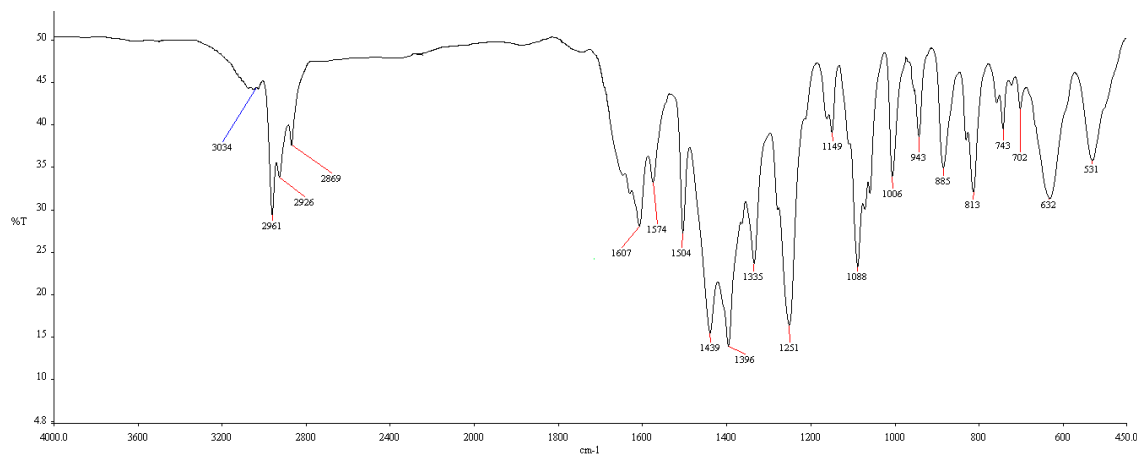
Figure 3.38. FT-IR spectrum of 2,9,16,23-tetrachloro-3,10,17,24-tetrakis(2-isopropyl-5-methylphenoxy)phthalocyaninato manganese (III) chloride (**13**).
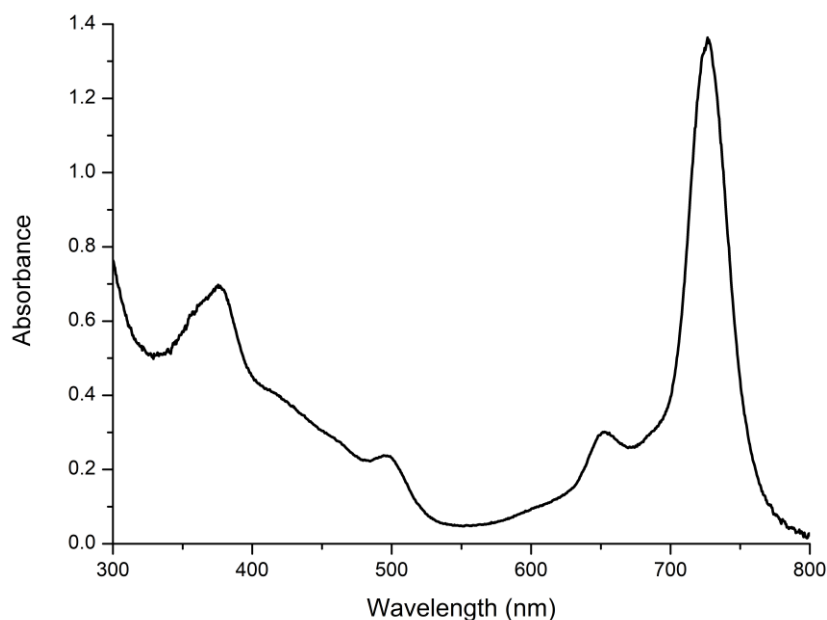
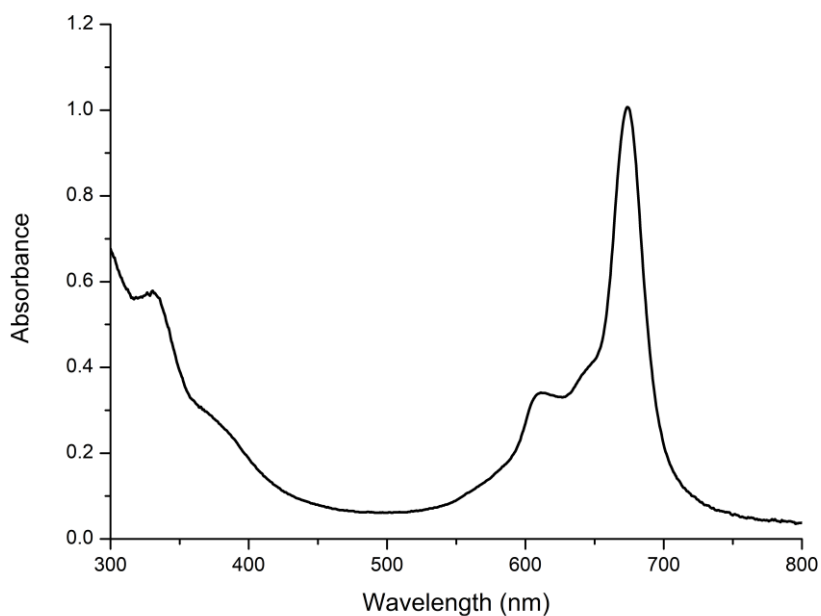**Figure 3.39.** UV-*vis* spectrum of 2,9,16,23-tetrachloro-3,10,17,24-tetrakis(2-isopropyl-5-methylphenoxy)phthalocyaninato manganese (III) chloride (**13**) in DMSO at 1×10^{-5}M.

3.3.2.8. 2,9,16,23-tetrachloro-3,10,17,24-tetrakis(2-isopropyl-5-methylphenoxy)phthalocyaninato zinc (14)

Yield: % 35

Mp: >300 °C

Chemical formula: $C_{72}H_{60}Cl_4ZnN_8O_4$

73

Molecular weight: 1308 g/mol

Solubility: DCM, CHCl$_3$, THF, Toluene, DMF and DMSO.

FT-IR γ max (cm^{-1}): 446, 692, 741, 804, 881, 941, 990, 1056, 1084, 1147, 1246, 1333, 1382, 1428, 1481, 1568, 1603, 1656, 2863, 2919, 2961, 3038.

UV-*vis* (DMSO, 1x10^{-5}M): λ$_{max}$ (nm) (log ε): 681 (5.01), 628 (4.53), 354 (4.78).
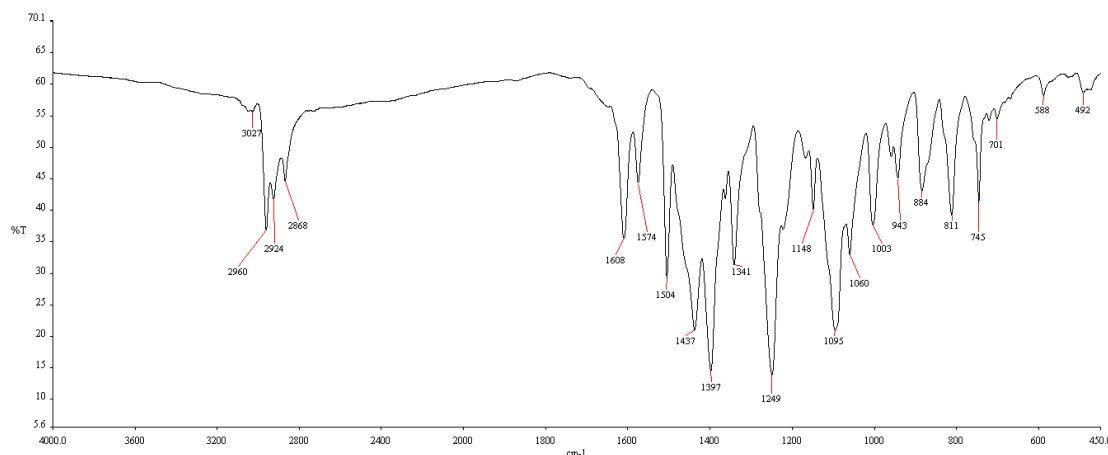
MALDI-TOF-MS: 1308.806 (M$^+$) m/z.
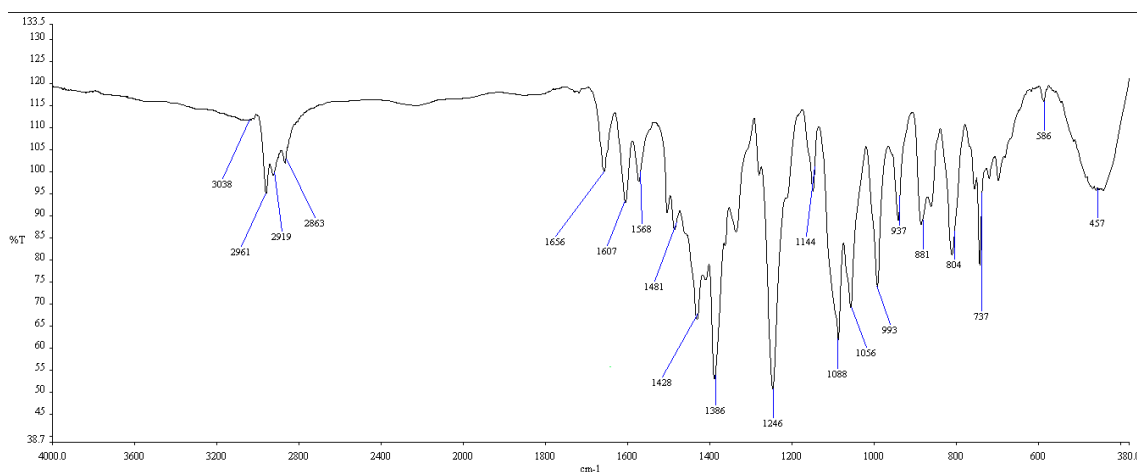
Figure 3.40. FT-IR spectrum of 2,9,16,23-tetrachloro-3,10,17,24-tetrakis(2-isopropyl-5-methylphenoxy)phthalocyaninato zinc (**14**).
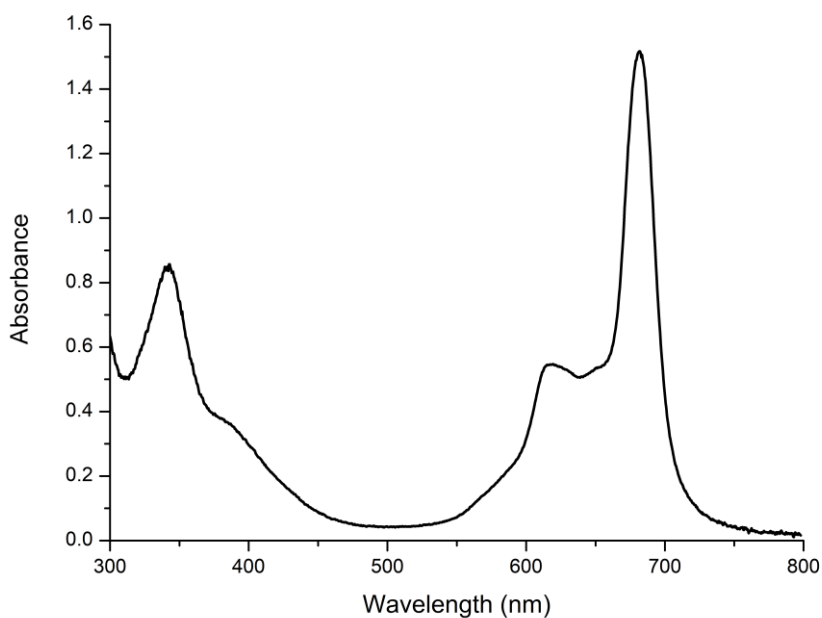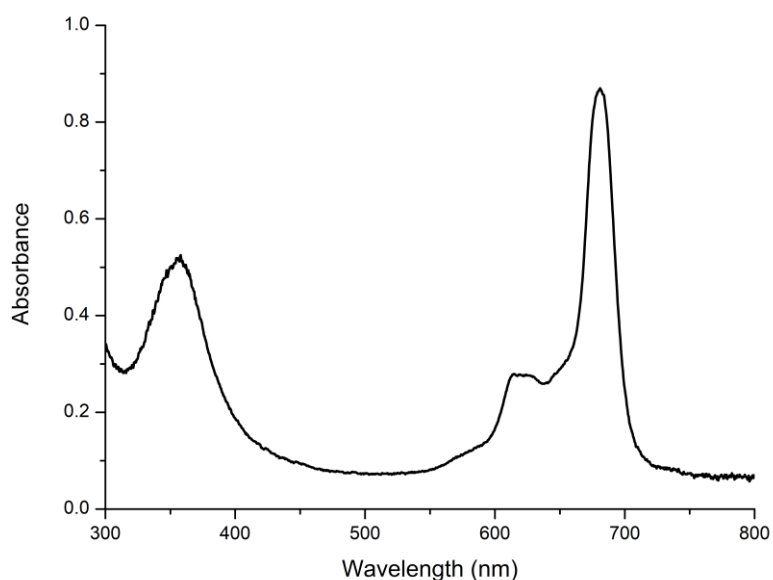

Figure 3.41. UV-*vis* spectrum of 2,9,16,23-tetrachloro-3,10,17,24-tetrakis(2-isopropyl-5-methylphenoxy)phthalocyaninato zinc (**14**) in DMSO at 1x10^{-5}M.

74
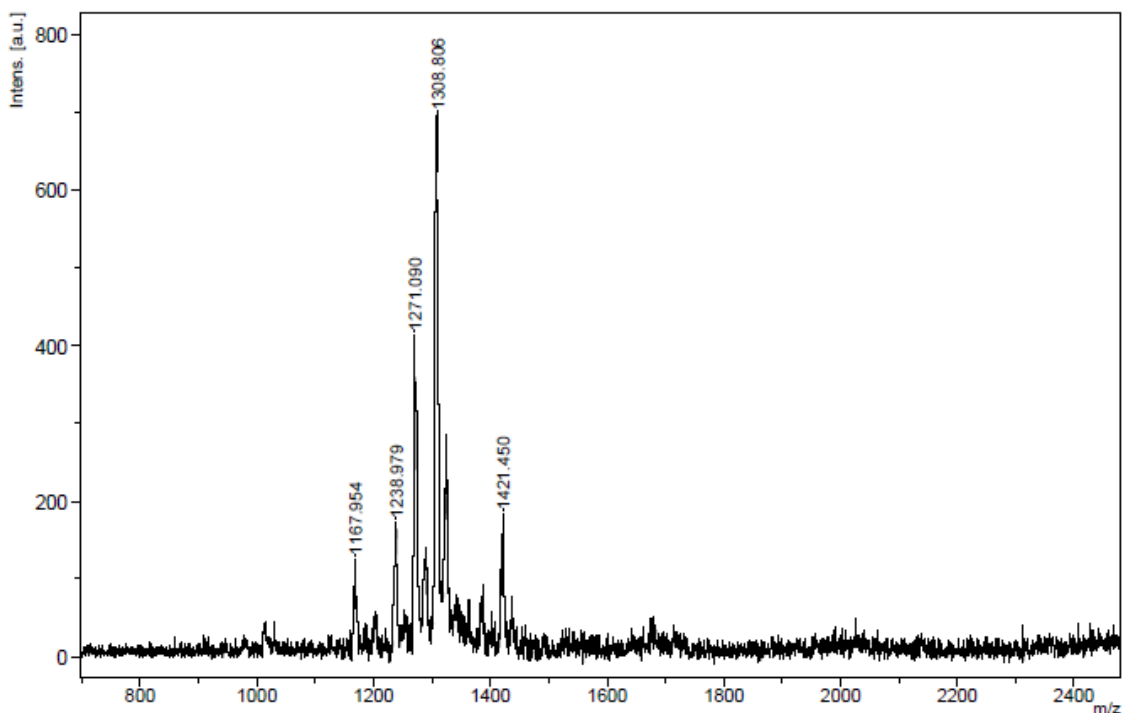
Figure 3.42. MALDI-TOF Mass spectrum of 2,9,16,23-tetrachloro-3,10,17,24-tetrakis(2-isopropyl-5-methylphenoxy)phthalocyaninato zinc (**14**).

3. 3. 3. Synthesis of 2,3,9,10,16,17,23,24-octakis(2-isopropyl-5-methylphenoxy)phthalocyanine (15)

M: 2H (**15**), Zn (**16**)
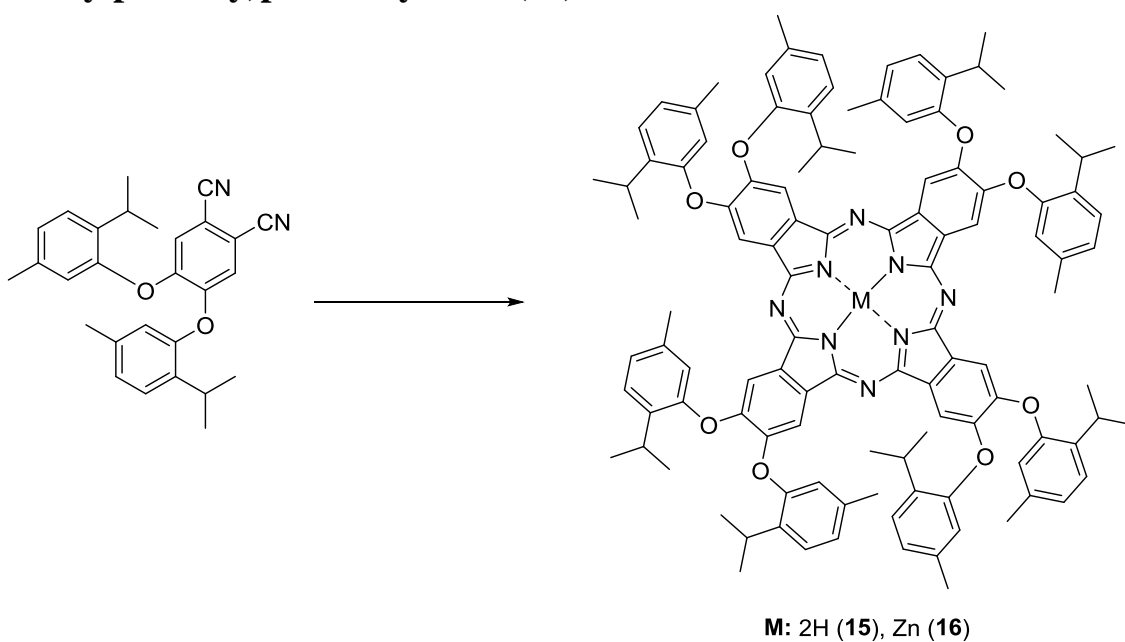
Scheme 3.3. Synthesis of 2,3,9,10,16,17,23,24-octakis(2-isopropyl-5-methylphenoxy)phthalocyanine (**15**) and its zinc derivative (**16**).

75

0.2 g (0.47 mmol) of 4,5-bis(2-isopropyl-5-methylphenoxy)phthalonitrile (**2**) was dissolved a Li/amyl alcohol solution and stirred at 180 °C for 24 h. After cooling to room temperature, the dark green crude product was diluted with methanol and protonated with acetic acid. Washing with hot acetic acid, water and methanol overnight in a Soxhlet apparatus yield 2,3,9,10,16,17,23,24-octakis(2-isopropyl-5-methylphenoxy)phthalocyanine (**15**) as a green powder.

Yield: % 35

Mp: >300 °C

Chemical formula: $C_{112}H_{114}N_8O_8$

Molecular weight: 1700.19 g/mol

Solubility: DCM, CHCl$_3$, THF, Toluene, DMF and DMSO.

FT-IR γ max (cm^{-1}): 586, 617, 695, 755, 809, 885, 948, 1013, 1089, 1180, 1245, 1270, 1344, 1401, 1441, 1504, 1575, 1613, 2868, 2924, 2960, 3026, 3296.

UV-*vis* (DCM, 1x10^{-5}M): λ$_{max}$ (nm) (log ε): 702 (5.01), 668 (4,98), 649 (4.54), 607 (4.38), 348 (4.77).

MALDI-TOF-MS: 1699.754 (M$^+$) m/z.
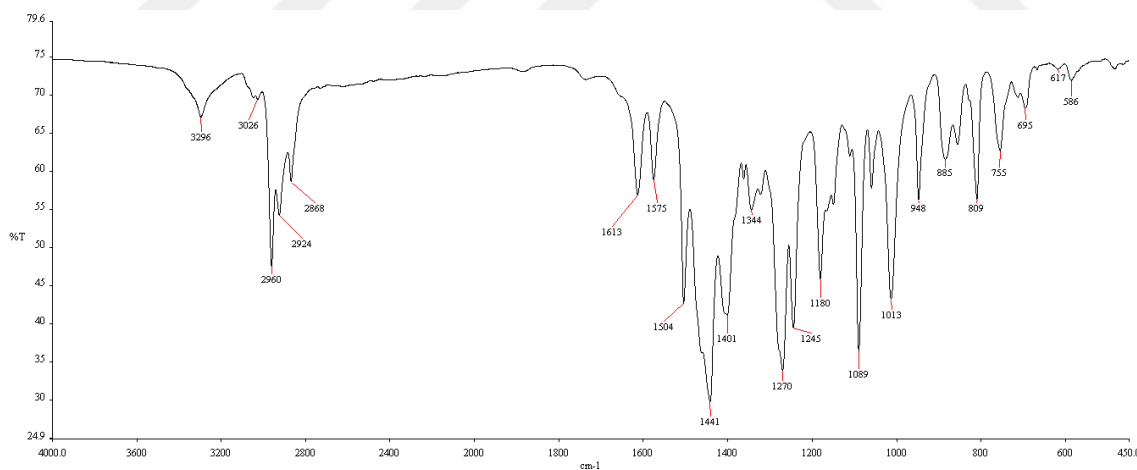
Figure 3.43. FT-IR spectrum of 2,3,9,10,16,17,23,24-octakis(2-isopropyl-5-methylphenoxy)phthalocyanine (**15**).
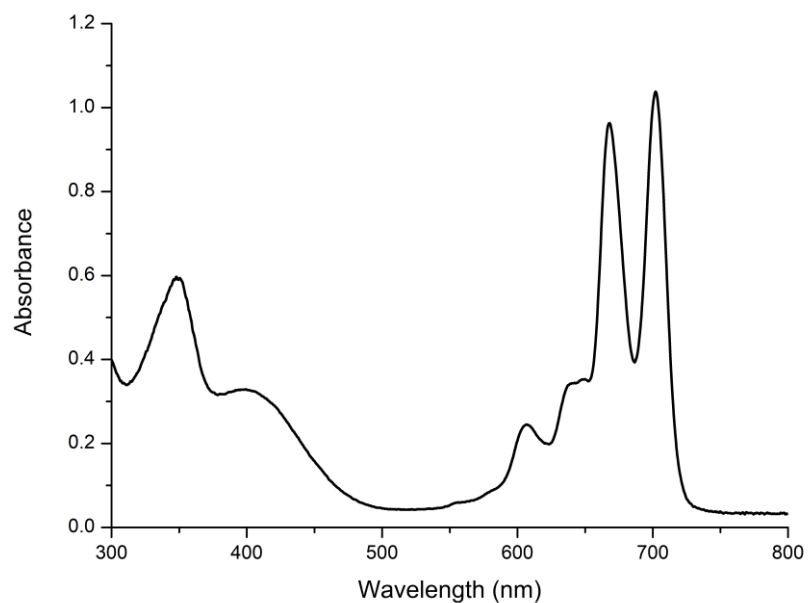
Figure 3.44. UV-*vis* spectrum of 2,3,9,10,16,17,23,24-octakis(2-isopropyl-5-methylphenoxy)phthalocyanine (**15**) in DCM at 1×10^{-5}M.
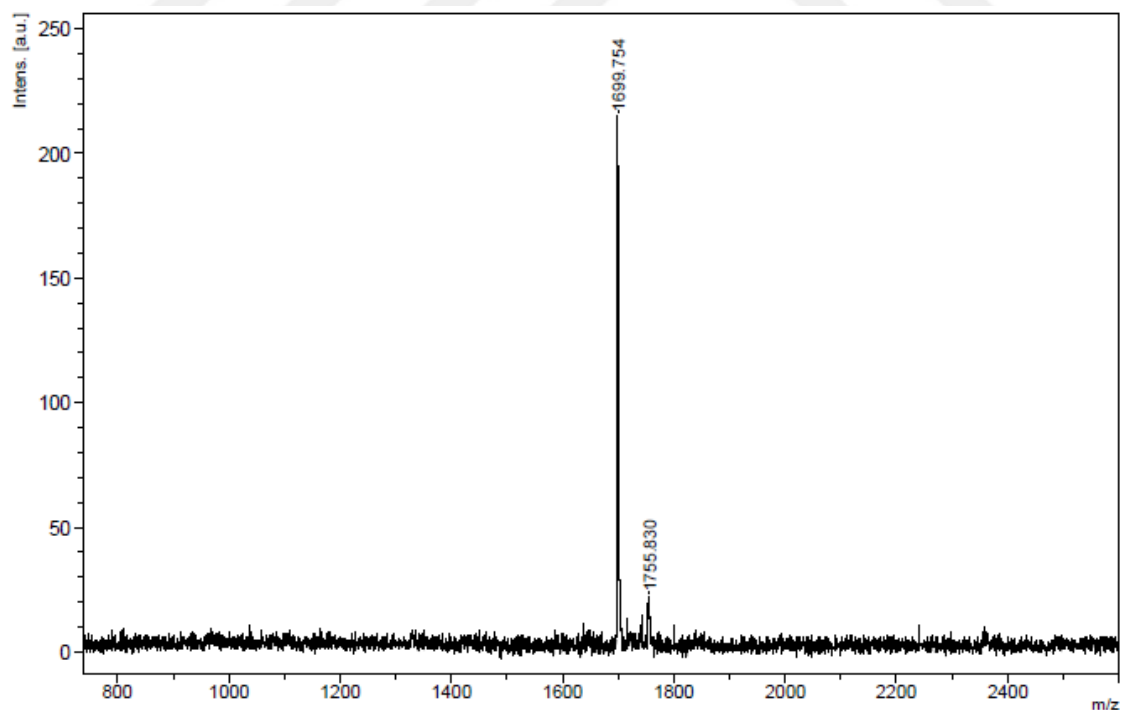
Figure 3.45. MALDI-TOF Mass spectrum of 2,3,9,10,16,17,23,24-octakis(2-isopropyl-5-methylphenoxy)phthalocyanine (**15**).
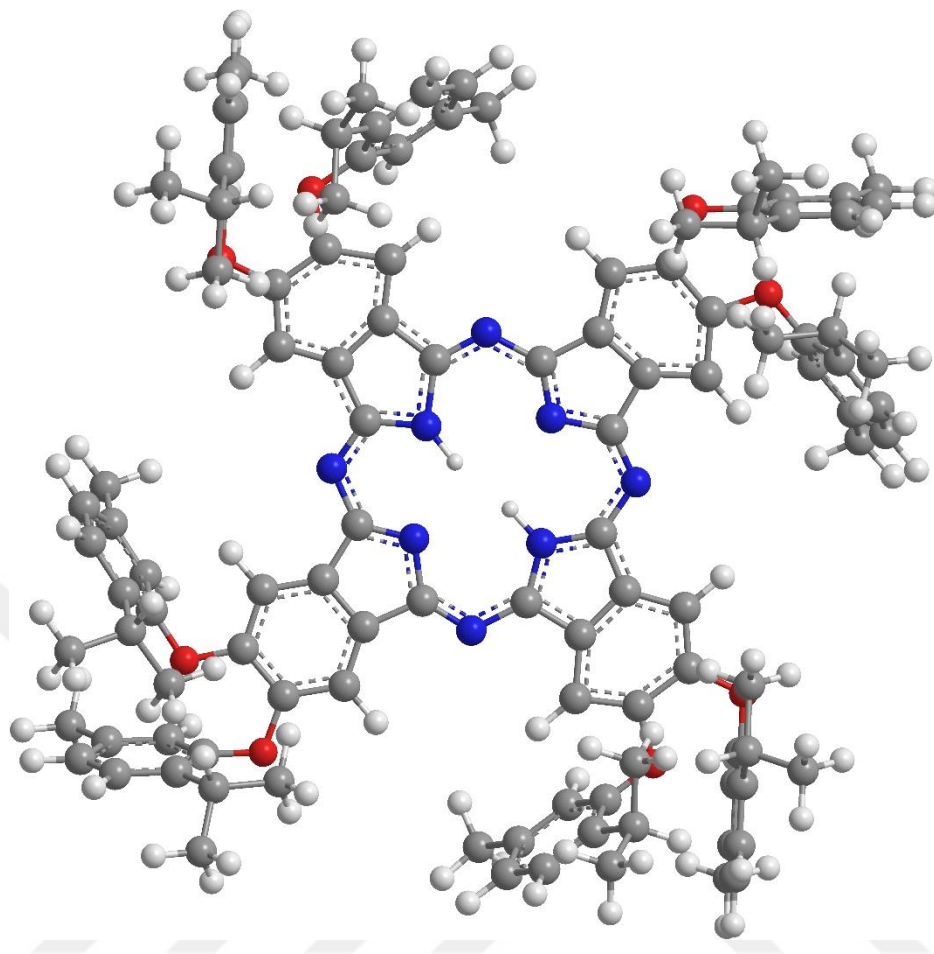
Figure 3.46. Optimized geometry of 2,3,9,10,16,17,23,24-octakis(2-isopropyl-5-methylphenoxy)phthalocyanine (**15**).
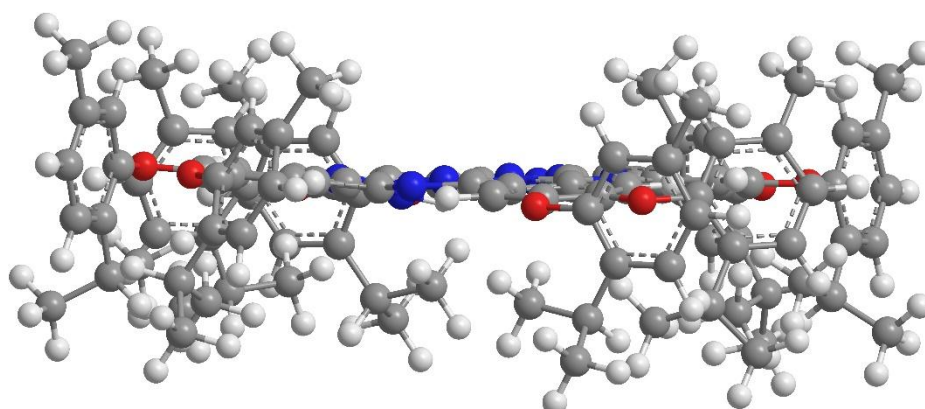
Figure 3.47. Side view of of 2,3,9,10,16,17,23,24-octakis(2-isopropyl-5-methylphenoxy)phthalocyanine (**15**).

3. 3. 4. Synthesis of 2,3,9,10,16,17,23,24-octakis(2-isopropyl-5-methylphenoxy)phthalocyaninato zinc (16)

A mixture of 4,5-bis(2-isopropyl-5-methylphenoxy)phthalonitrile (**2**) (1.0 g, 2.3 mmol), urea (0.18 g, 3.0 mmol) and three drops of DBU in 15 ml of 1-pentanol is heated under 120 °C under an N_2 atmosphere. Upon reaching that temperature, dry zinc acetate (0.27g, 1.5 mmol) was added and allowed to reflux for 7 hours at 155 °C. After cooling to room temperature, the reaction solution poured onto 450 ml of methanol / water (8: 1). The crude product was washed with hot acetic acid, water and methanol overnight in a Soxhlet apparatus. The solid is isolated by centrifugation, dried in vacuo and purified by silica gel column chromatography (toluene / chloroform). Final product obtained as a blue powder.

Yield: % 31

Mp: >300 °C

Chemical formula: $C_{112}H_{112}N_8O_8Zn$

Molecular weight: 1765.56 g/mol

Solubility: DCM, $CHCl_3$, THF, Toluene, DMF and DMSO.

FT-IR γ max (cm⁻¹): 518, 693, 745, 813, 830, 887, 948, 1030, 1088, 1180, 1244, 1272, 1350, 1400, 1451, 1504, 1575, 1719, 2868, 2926, 2960, 3047.

UV-*vis* (DCM, 1x10⁻⁵M): λ_max (nm) (log ε): 679 (4.96), 655 (4.43), 613 (4.29), 355 (4.68).

MALDI-TOF-MS: 1762.456 M-H)⁺ m/z.
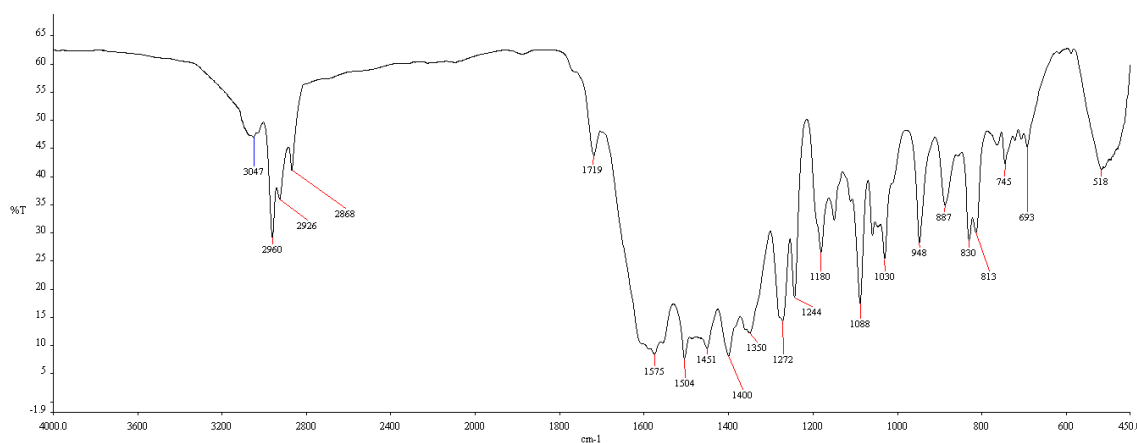
Figure 3.48. FT-IR spectrum of 2,3,9,10,16,17,23,24-octakis(2-isopropyl-5-methylphenoxy)phthalocyaninato zinc (**16**).
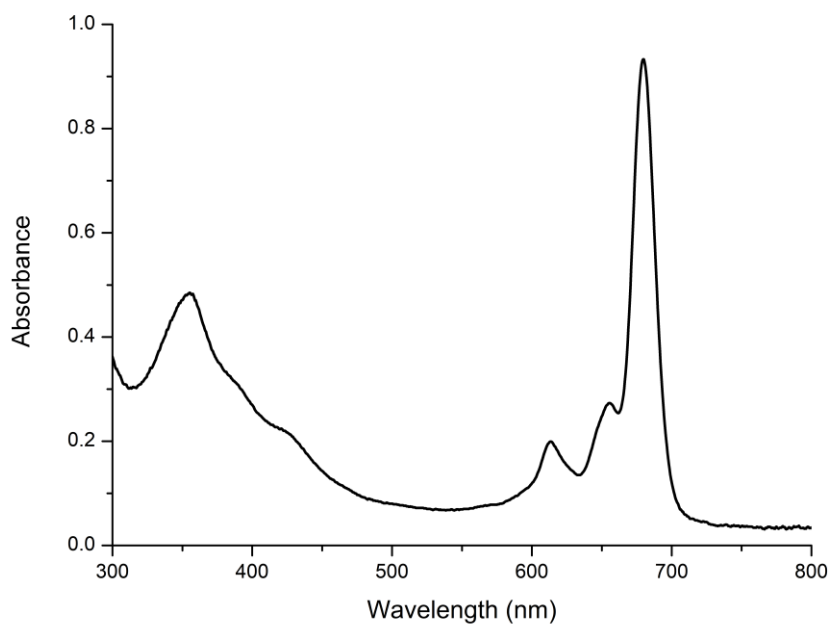
Figure 3.49. UV-*vis* spectrum of 2,3,9,10,16,17,23,24-octakis(2-isopropyl-5-methylphenoxy)phthalocyaninato zinc (**16**) in DCM at 1×10^{-5}M.
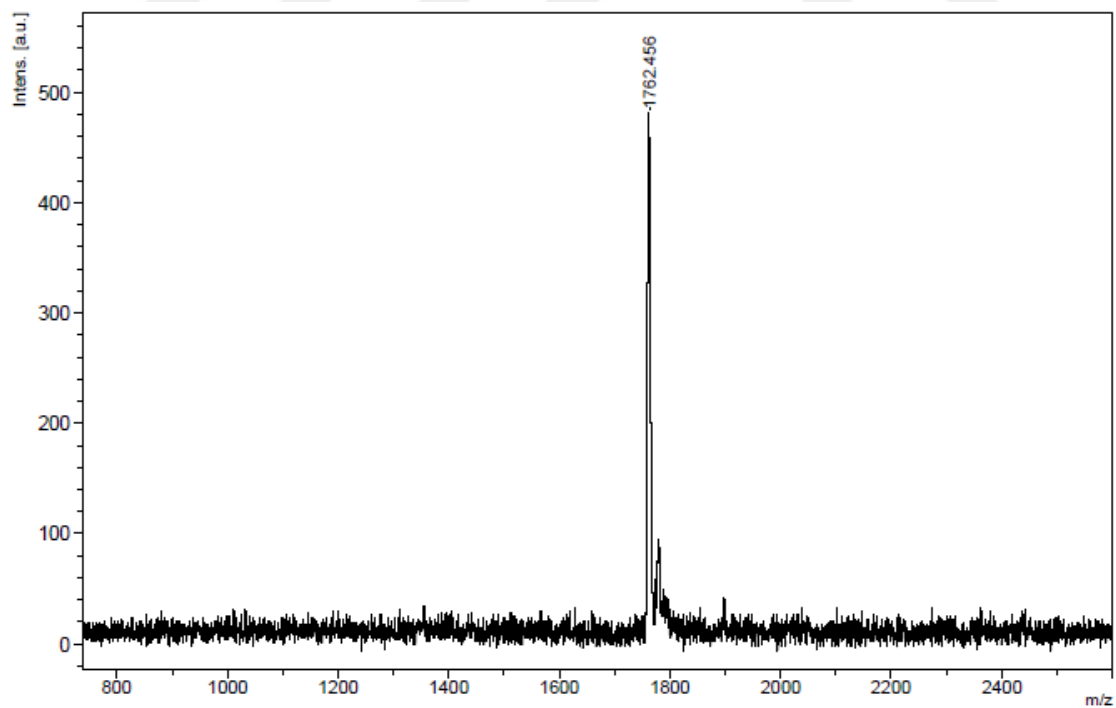
Figure 3.50. MALDI-TOF Mass spectrum of 2,3,9,10,16,17,23,24-octakis(2-isopropyl-5-methylphenoxy)phthalocyaninato zinc (**16**).

3. 3. 5. Attempted synthesis of 4,4',4'',4'''-((1E,1'E,1''E,1'''E)-phthalocyanine-2,9,16,23-tetrayltetrakis(diazene-2,1-diyl))tetrakis(2-isopropyl-5-methylphenol) and its zinc analogue.

M: 2H (**Azo-H2Pc**), Zn (**Azo-ZnPc**)
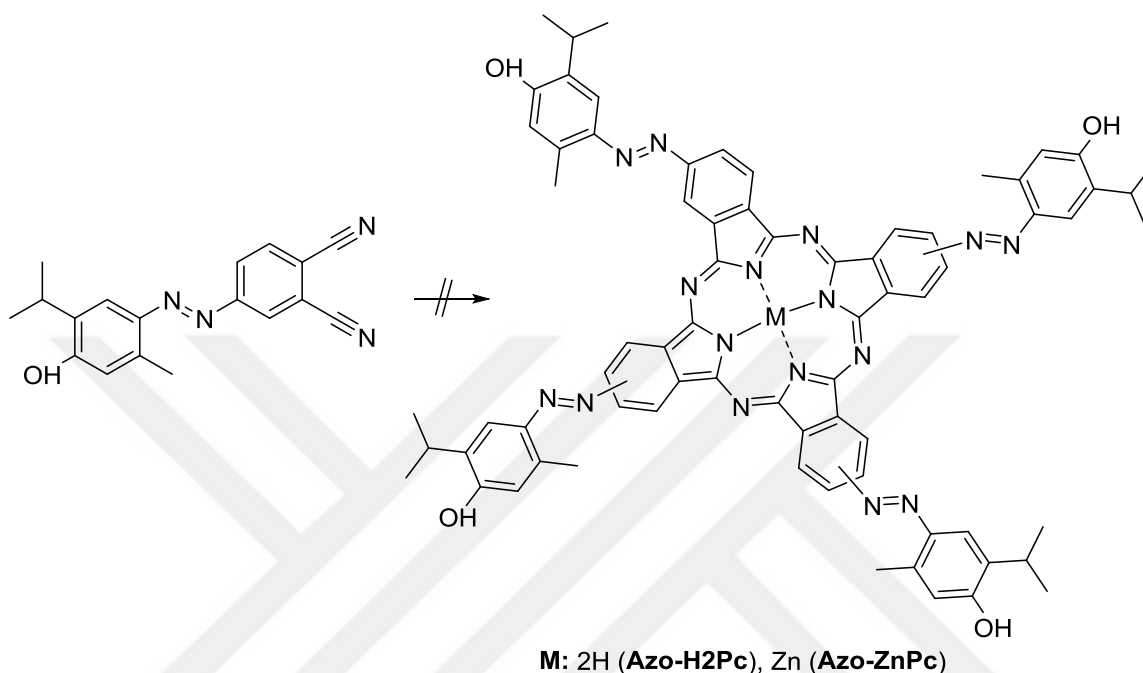
Scheme 3.4. Attempted synthesis of 4,4',4'',4'''-((1E,1'E,1''E,1'''E)-phthalocyanine-2,9,16,23-tetrayltetrakis(diazene-2,1-diyl))tetrakis(2-isopropyl-5-methylphenol) and its zinc derivative.

Different synthetic procedures including the procedures in the parts 3.3.1, 3.3.3 and 3.3.6 were tried in order to obtain metal free azo bridged Pc. The reactions did not yield the desired product. Then we have applied the procedures from the parts 3.3.2, 3.3.4 and 3.3.7 with the aim of obtaining azo bridged zinc Pc. This reaction also did not work. It seems that the free hydroxyl groups of the phthalonitrile precursor prevents the tetramerization reaction. In order to solve this problem, we have carried out a protection reaction of the free hydroxyl group of the phthalonitrile compound (**3**) with pentyl and propargyl groups as discussed in the section 3.2.4 and 3.2.5.

3. 3. 6. Synthesis of 2,9,16,23-tetrakis((E)-(5-isopropyl-2-methyl-4-(pentyloxy)phenyl)diazenyl)phthalocyanine (17)

M: 2H (**17**), Zn (**18**)
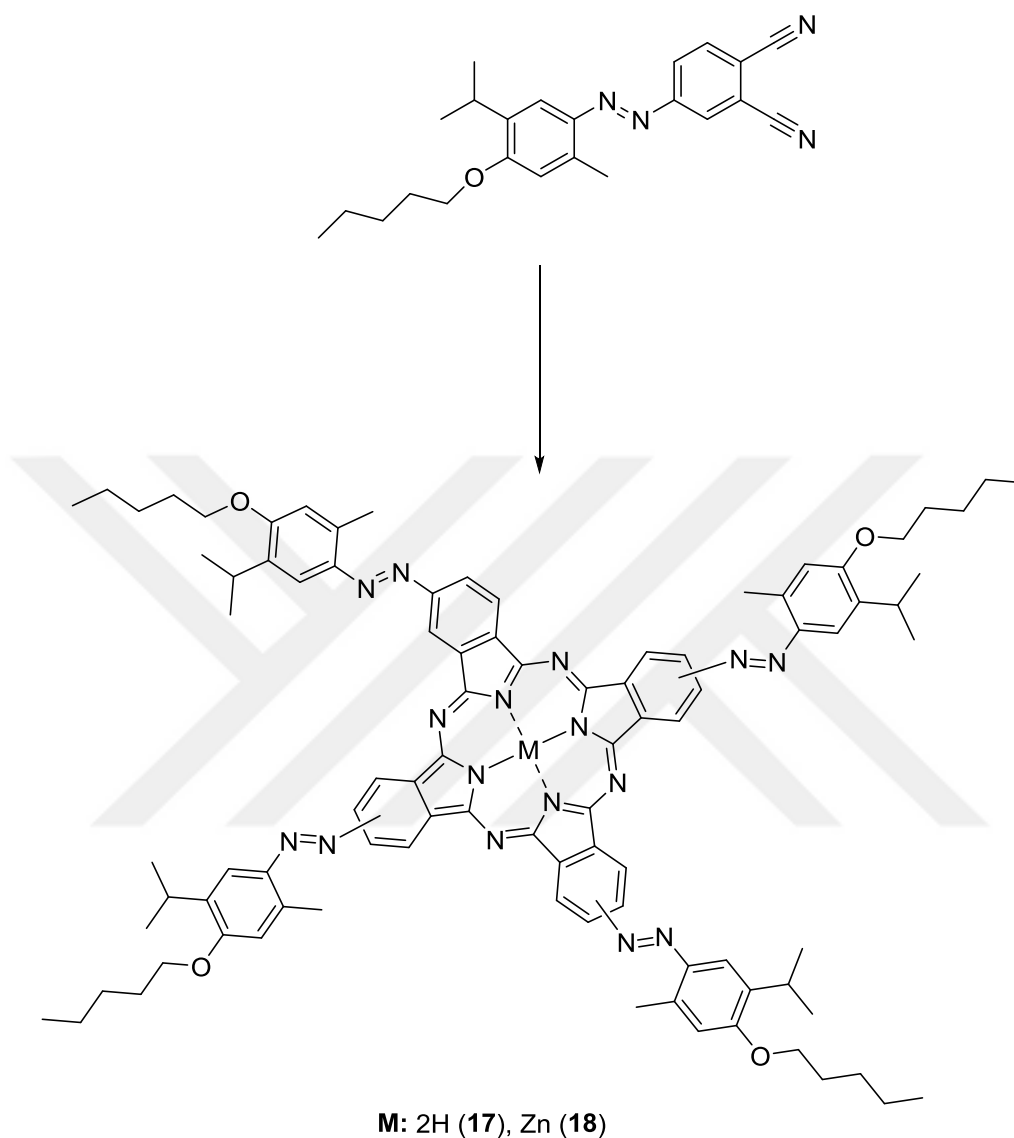
Scheme 3.5. Synthesis of 2,9,16,23-tetrakis((E)-(5-isopropyl-2-methyl-4-(pentyloxy)phenyl)diazenyl)phthalocyanine (**17**) and its zinc derivative (**18**).

176 mg of lithium (25.1 mmol, 5.0 eq) were converted into LiOPent in 10 mL of n-amyl alcohol by heating at 100 °C while stirring. Thereafter 1.87 g (5 mmol, 1.0 eq) (E)-4-((5-isopropyl-2-methyl-4-(pentyloxy)phenyl)diazenyl) phthalonitrile (**4**) was added and the mixture was heated to 130 ° C for 24 h. A few minutes after reaching the reaction temperature, the solution turned dark green and a microcrystalline solid precipitated. The product was neutralized by addition of a mixture of MeOH and glacial acetic acid

and completely precipitated. The green solid was separated and triturated three times at 50 °C with 60 mL MeOH. The product was washed in a Soxhlet apparatus with acetic acid and then with methanol overnight and dried in a fine vacuum.

Yield: % 19

Mp: >300 °C

Chemical formula: $C_{92}H_{106}N_{16}O_4$

Molecular weight: 1500 g/mol

Solubility: DCM, CHCl$_3$, THF, Toluene, DMF and DMSO.

FT-IR γ max (cm^{-1}): 501, 748, 823, 1028, 1102, 1203, 1248, 1341, 1466, 1503, 1611, 2867, 2927, 2954, 3047, 3297.

UV-*vis* (DCM, 1x10^{-5}M): λ$_{max}$ (nm) (log ε): 741 (4.93), 705 (4.94), 672 (4.76), 639 (4.59), 359 (4.93).

MALDI-TOF-MS: 1498.575 (M-H)$^+$ m/z.
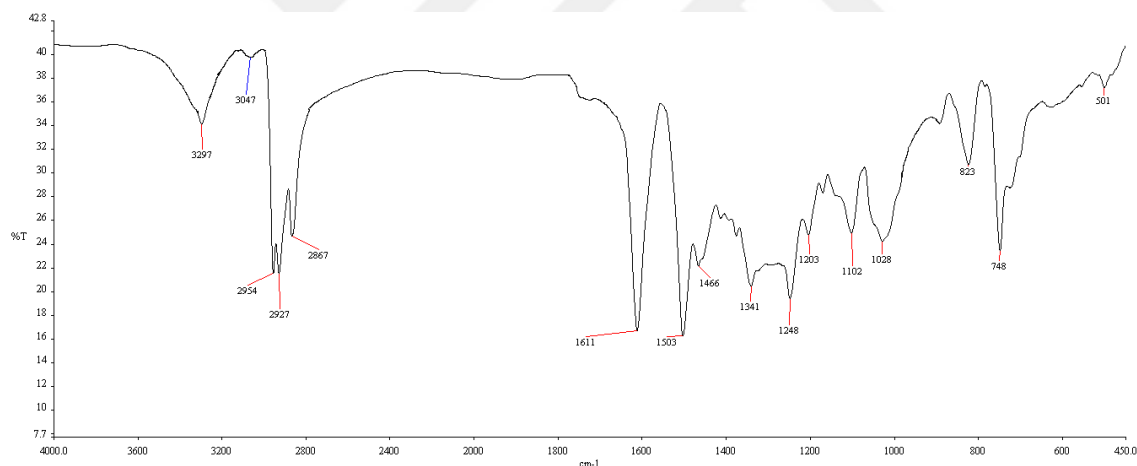
Figure 3.51. FT-IR spectrum of 2,9,16,23-tetrakis((E)-(5-isopropyl-2-methyl-4-(pentyloxy)phenyl)diazenyl)phthalocyanine (**17**)
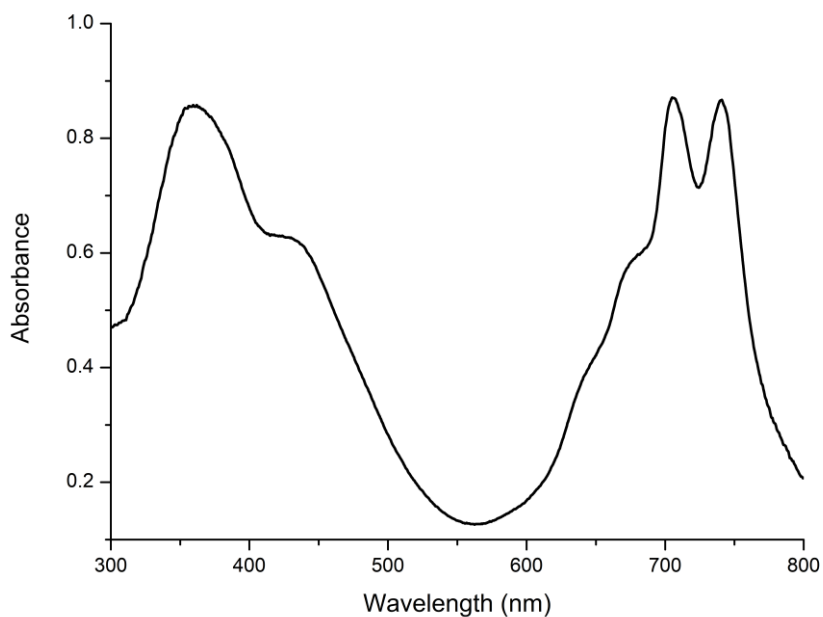
Figure 3.52. UV-*vis* spectrum of 2,9,16,23-tetrakis((E)-(5-isopropyl-2-methyl-4-(pentyloxy)phenyl)diazenyl)phthalocyanine (**17**) in DCM at 1×10^{-5}M.
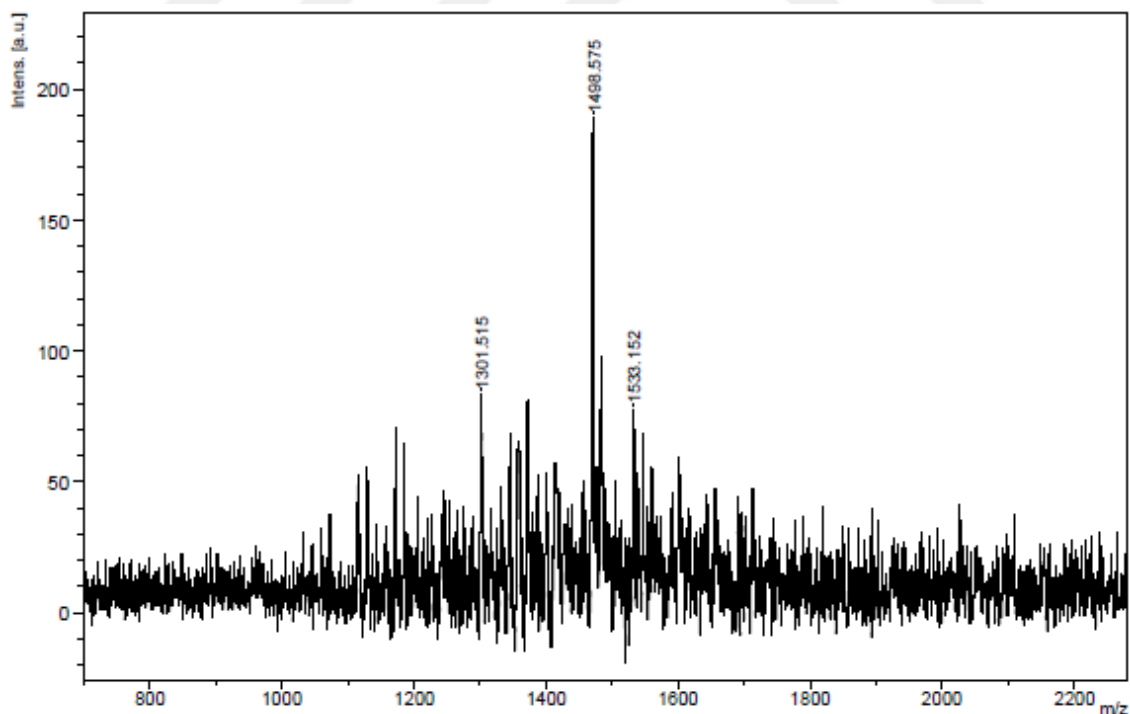
Figure 3.53. MALDI-TOF Mass spectrum of 2,9,16,23-tetrakis((E)-(5-isopropyl-2-methyl-4-(pentyloxy)phenyl)diazenyl)phthalocyanine (**17**).
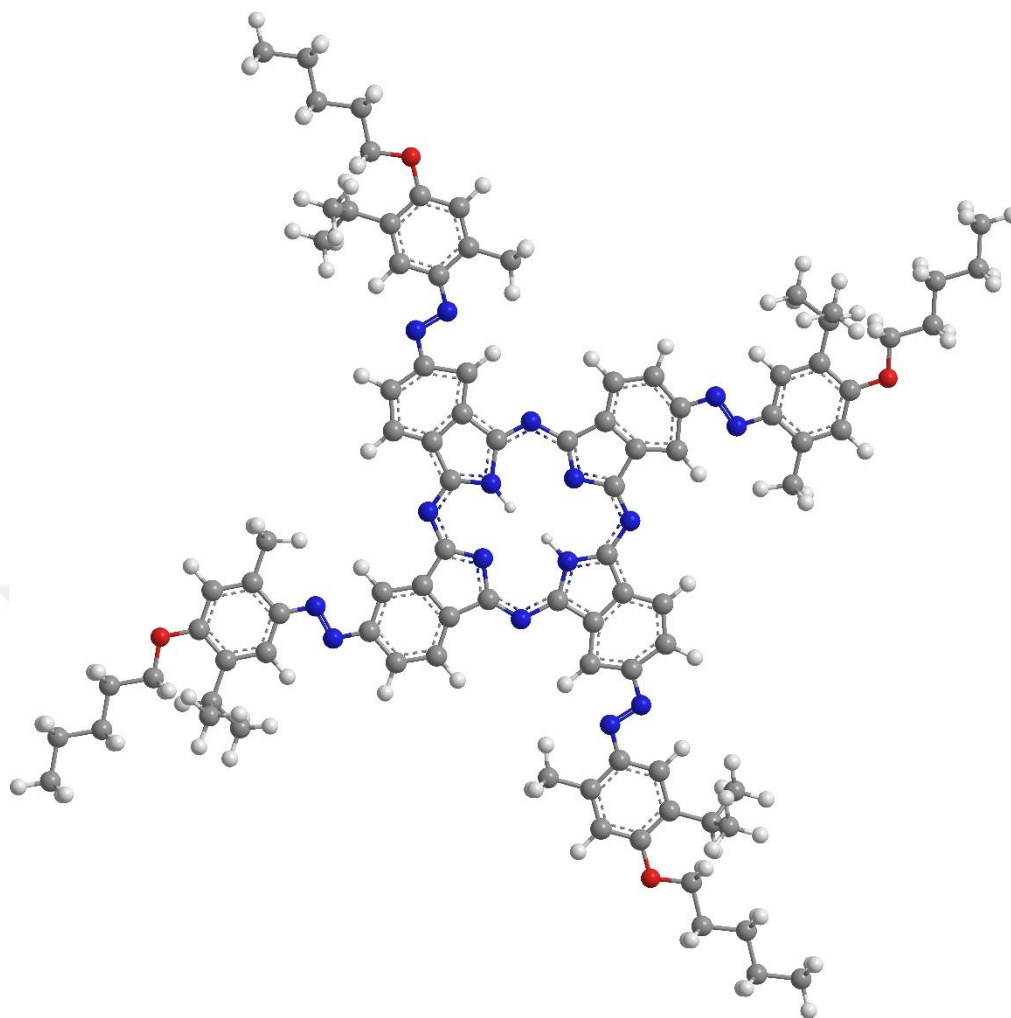
Figure 3.54. Optimized geometry of 2,9,16,23-tetrakis((E)-(5-isopropyl-2-methyl-4-(pentyloxy)phenyl)diazenyl)phthalocyanine (**17**).
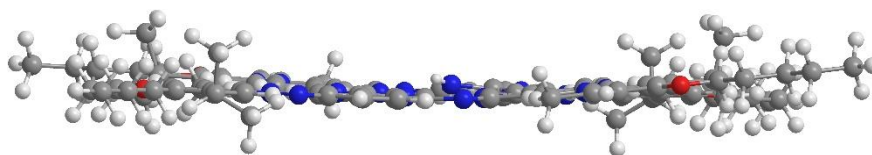
Figure 3.55. Side view of 2,9,16,23-tetrakis((E)-(5-isopropyl-2-methyl-4-(pentyloxy)phenyl)diazenyl)phthalocyanine (**17**).

3. 3. 7. Synthesis of 2,9,16,23-tetrakis((E)-(5-isopropyl-2-methyl-4-(pentyloxy)phenyl)diazenyl)phthalocyaninato zinc (18)

374 mg of (1 mmol) (E)-4-((5-isopropyl-2-methyl-4-(pentyloxy)phenyl)diazenyl) phthalonitrile (**4**) was dissolved in 10 ml of 1-pentanol. 181 mg (1 mmol) dry zinc acetate and 150 µl (1 mmol) DBU were added under N_2 atmosphere. The reaction solution was heated to boiling for about 10 minutes. After the solution was colored dark green, the reaction was stopped. The mixture was cooled to room temperature and water was added. The aqueous phase was extracted with hexane. Subsequently, hexane was removed on a rotary evaporator. The residue was chromatographed on a silica gel with hexane / ether 1: 9.

Yield: % 21

Mp: >300 °C

Chemical formula: $C_{92}H_{104}N_{16}O_4Zn$

Molecular weight: 1563.33 g/mol

Solubility: DCM, $CHCl_3$, THF, Toluene, DMF and DMSO.

FT-IR γ max (cm^{-1}): 522, 729, 832, 906, 1010, 1058, 1090, 1144, 1241, 1341, 1399, 1463, 1492, 1575, 1606, 2849, 2917, 2955, 3047.

UV-*vis* (DMSO, 1x10^{-5}M): λ$_{max}$ (nm) (log ε): 714 (4.80), 648 (4.48), 371 (4.80).

MALDI-TOF-MS: 1563.213 (M$^+$) m/z.
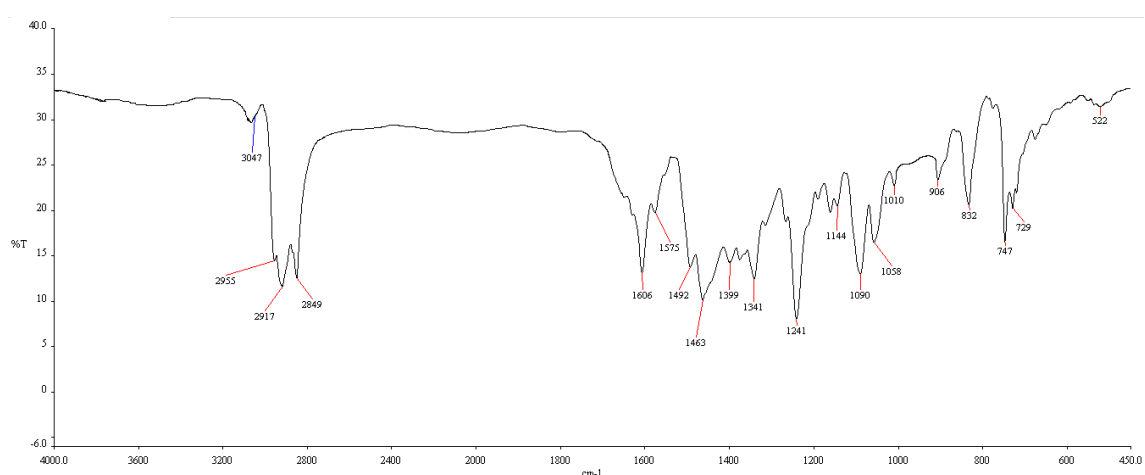
Figure 3.56. FT-IR spectrum of 2,9,16,23-tetrakis((E)-(5-isopropyl-2-methyl-4-(pentyloxy)phenyl)diazenyl)phthalocyaninato zinc (**18**)
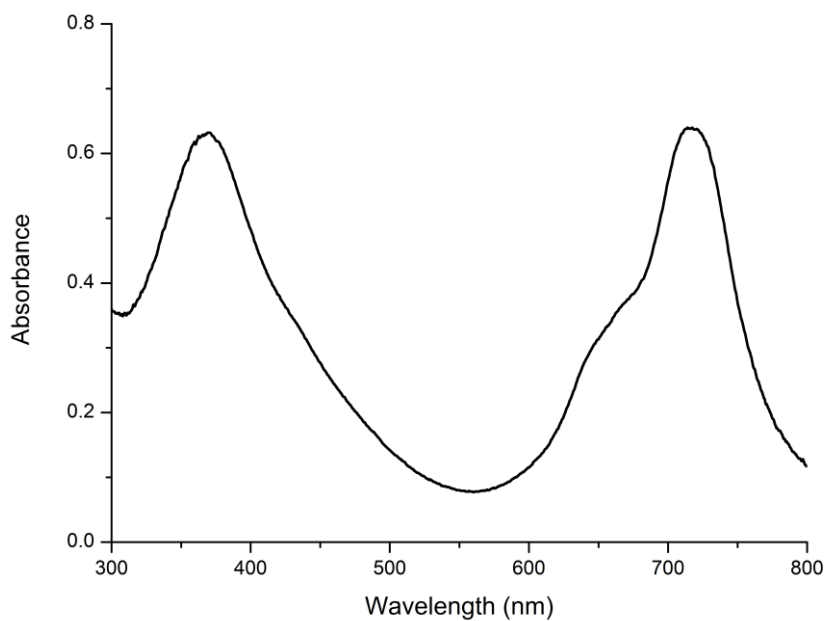
Figure 3.57. UV-*vis* spectrum of 2,9,16,23-tetrakis((E)-(5-isopropyl-2-methyl-4-(pentyloxy)phenyl)diazenyl)phthalocyaninato zinc (**18**) in DCM at 1x10^{-5}M.
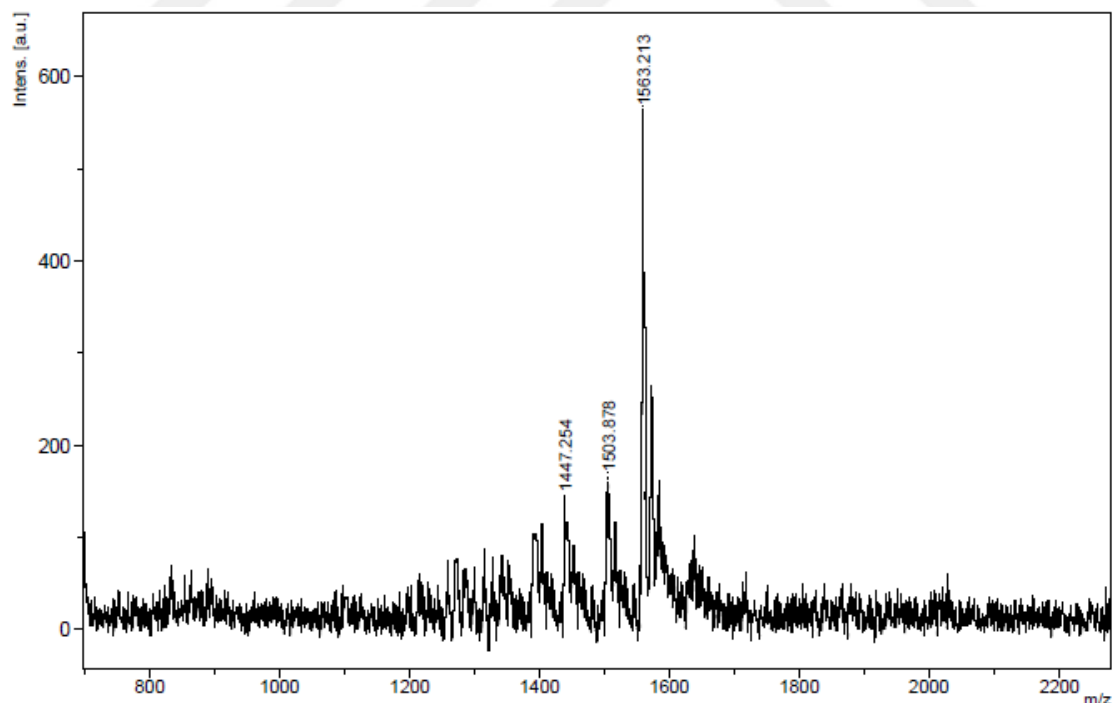
Figure 3.58. MALDI-TOF Mass spectrum of 2,9,16,23-tetrakis((E)-(5-isopropyl-2-methyl-4-(pentyloxy)phenyl)diazenyl)phthalocyaninato zinc (**18**)

3. 3. 8. Attempted synthesis of 2,9,16,23-tetrakis((E)-(5-isopropyl-2-methyl-4-(prop-2-yn-1-yloxy)phenyl)diazenyl)phthalocyanine and its zinc derivative
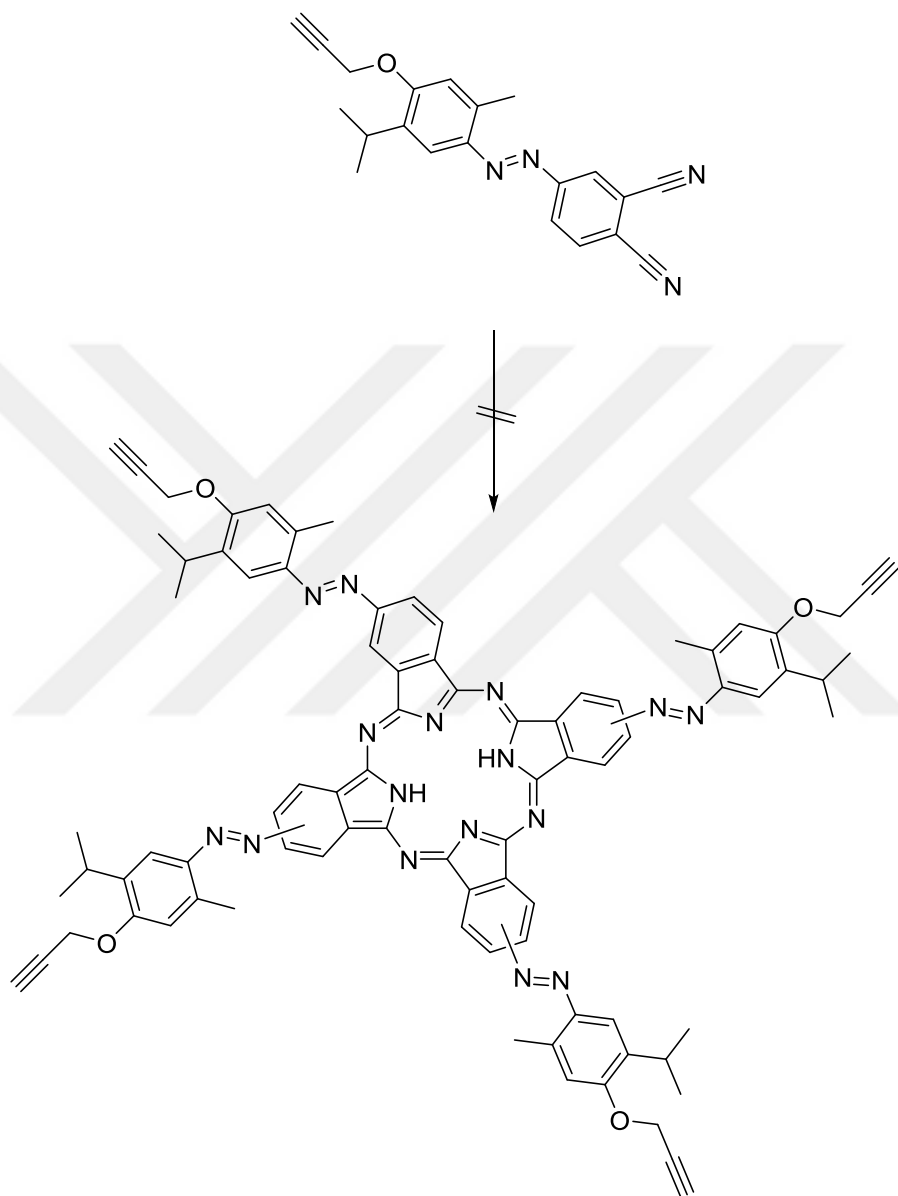
Scheme 3.6. Attempted synthesis of 2,9,16,23-tetrakis((E)-(5-isopropyl-2-methyl-4-(prop-2-yn-1-yloxy)phenyl)diazenyl)phthalocyanine and its zinc derivative

(E)-4-((5-isopropyl-2-methyl-4-(prop-2-yn-1-yloxy)phenyl)diazenyl)phthalonitrile (**5**) (0.17 g, 0.5 mmol) and lithium (0.01 g, 1.69 mol) in 1-pentanol (6 ml) were mixed and stirred at 170 °C for 18 hours under argon atmosphere. The solution was cooled and the solvent was evaporated under vacuo. Then glacial acetic acid (30 ml) was added and the suspension was stirred for 30 minutes. The product was extracted with dichloromethane and washed with water (3 x 30 ml). The organic phase was separated, dried with magnesium sulfate. The final product was not soluble and its structure couldn't identified. Different synthetic procedures including the procedures in the parts 3.3.1 and 3.3.3 were also tried. But results were not successful. It could be explained that, the tetramerization of the nitrile groups may have been intervened by the terminal alkyne groups.

In order to obtain zinc derivative of previously failed metal free phthalocyanine, we have carried out the following reaction.

0.17 g (0.5 mmol) of (E)-4-((5-isopropyl-2-methyl-4-(prop-2-yn-1-yloxy)phenyl)-diazenyl)phthalonitrile (**5**) and 90 mg (0.5 mmol) of zinc acetate were evacuated in a pressure Schlenk tube and stirred under protective gas atmosphere with 10 ml of 1-pentanol and 0.35 ml (2.34 mmol) DBU (6). The reaction mixture was stirred for 3 h in the oil bath at temperature of 170 °C, then transferred to a 30 ml of DCM in a round bottom flask and mixed with 30 ml of methanol. To remove the dichloromethane completely by distillation, the pressure was lowered continuously at 50 ° C to 400 mbar. After filtering off and washing the filter cake with 50 ml of methanol, the crude product was dried in vacuo. The final product was not soluble and its structure couldn't identified again. Different synthetic procedures including the procedures in the parts 3.3.2 and 3.3.4 were also tried. But results were not successful again. As we explained above, the terminal alkyne groups may have same effect on the tetramerization reaction for metal fee and metal Pcs.

3. 3. 7. Synthesis of Bromido[2,9,16-trichloro-3,10,17-trikis(2-isopropyl-5-methylphenoxy)phthalocyanato]boron(III) (19)
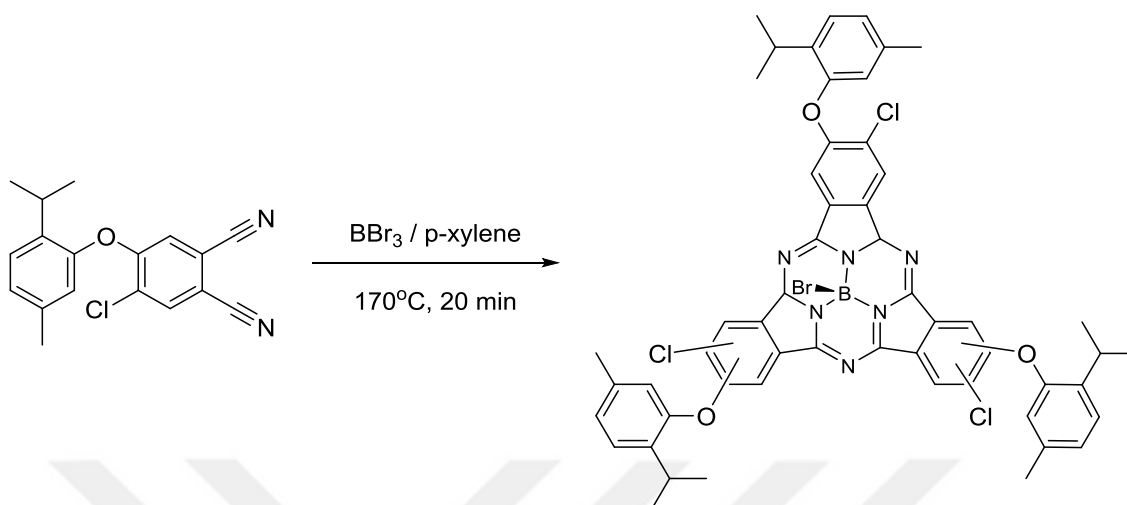
Scheme 3.7. Synthesis of bromo[2,9,16-trichloro-3,10,17-trikis(2-isopropyl-5-methylphenoxy)phthalocyaninato]boron(III) (**19**)

0.62 g (2 mmol) of 4-chloro-5-(2-isopropyl-5-methylphenoxy)phthalonitrile (**2**) was put into a heated pressure Schlenk tube and 1.90 mL of 1M boron tribromide in p-xylene was added. The reaction solution was heated to 170 ° C in an oil bath and stirred there for 20 minutes. Subsequently, excess boron trichloride and the solvent were removed by distillation in the still warm oil bath. The resulting dark purple solid was then purified by column chromatography (silica gel, n-hexane / ethyl acetate 20: 1). The product was obtained as a dark violet solid.

Yield: % 32

Mp: >300 °C

Chemical formula: $C_{54}H_{47}BBrCl_3N_6O_3$

Molecular weight: 1025.07 g/mol

Solubility: DCM, $CHCl_3$, THF, Toluene, DMF and DMSO.

FT-IR γ max (cm⁻¹): 588, 645, 720, 768, 816, 887, 977, 1012, 1060, 1086, 1157, 1256, 1347, 1408, 1454, 1504, 1541, 1575, 1611, 1726, 2850, 2930, 2959, 3075.

UV-*vis* (DCM, 1x10⁻⁵M): λ_max (nm) (log ε): 509 (4.95), 360 (5.59).

MALDI-TOF-MS: 1024.009 (M⁺) m/z.
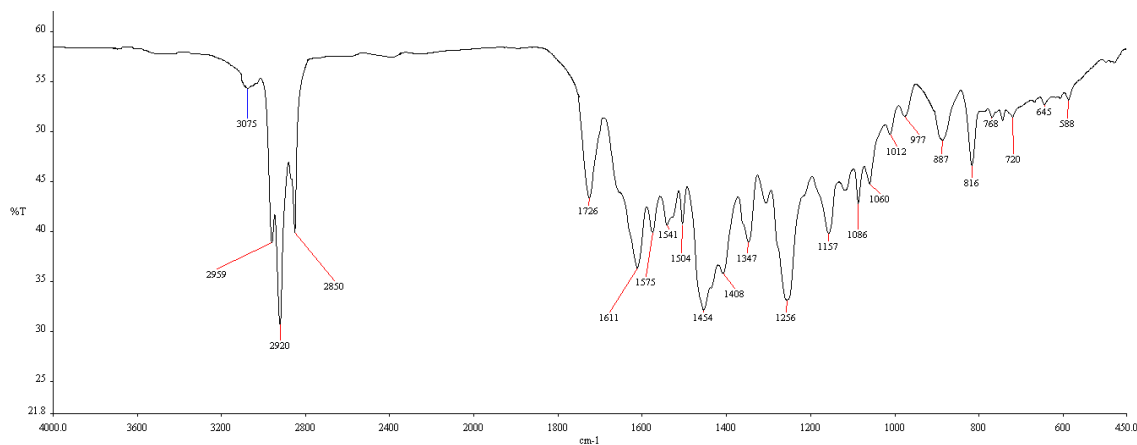
Figure 3.59. FT-IR spectrum of bromo[2,9,16-trichloro-3,10,17-trikis(2-isopropyl-5-methylphenoxy)phthalocyaninato]boron(III) (**19**).
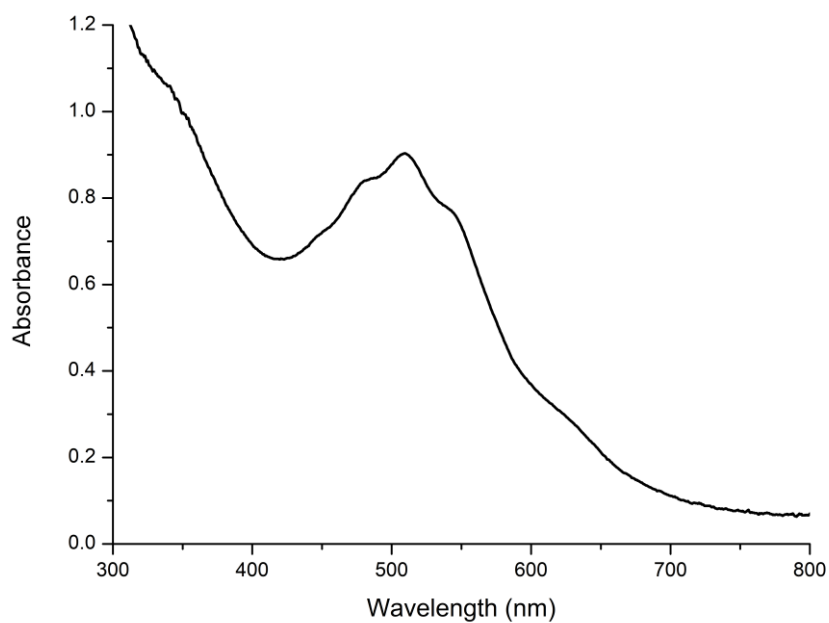
Figure 3.60. UV-*vis* spectrum of bromo[2,9,16-trichloro-3,10,17-trikis(2-isopropyl-5-methylphenoxy)phthalocyaninato]boron(III) (**19**) in DCM at 1×10^{-5}M.
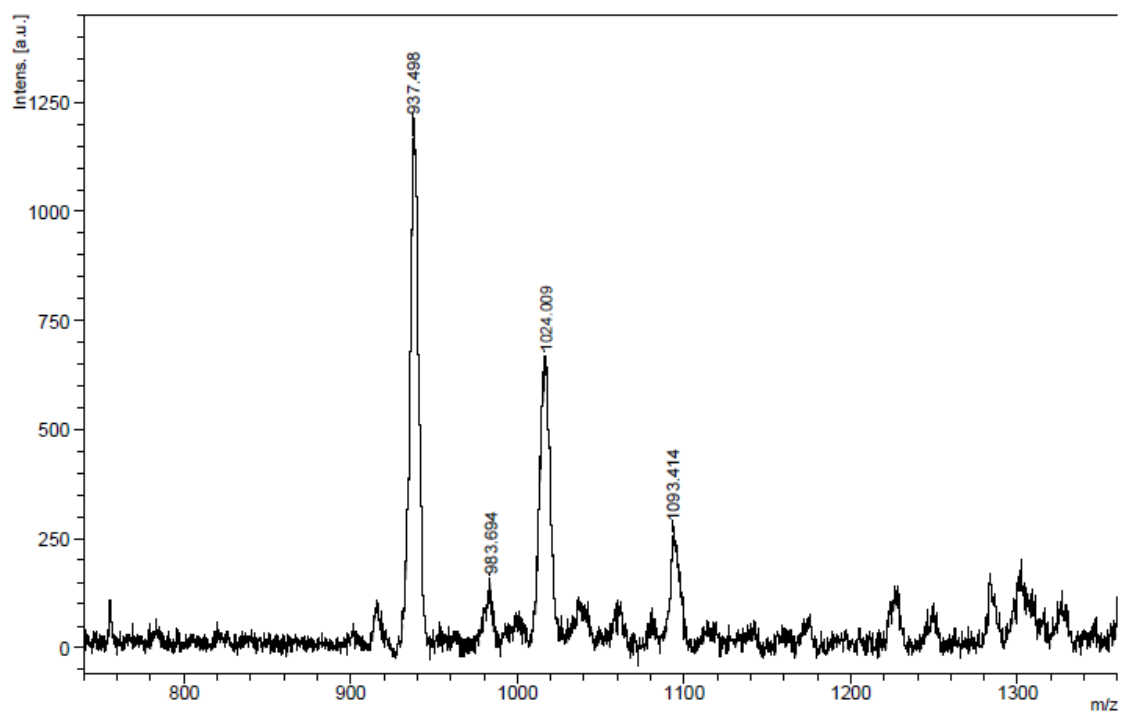
Figure 3.61. MALDI-TOF Mass spectrum of bromo[2,9,16-trichloro-3,10,17-trikis(2-isopropyl-5-methylphenoxy)phthalocyaninato]boron(III) (**19**).
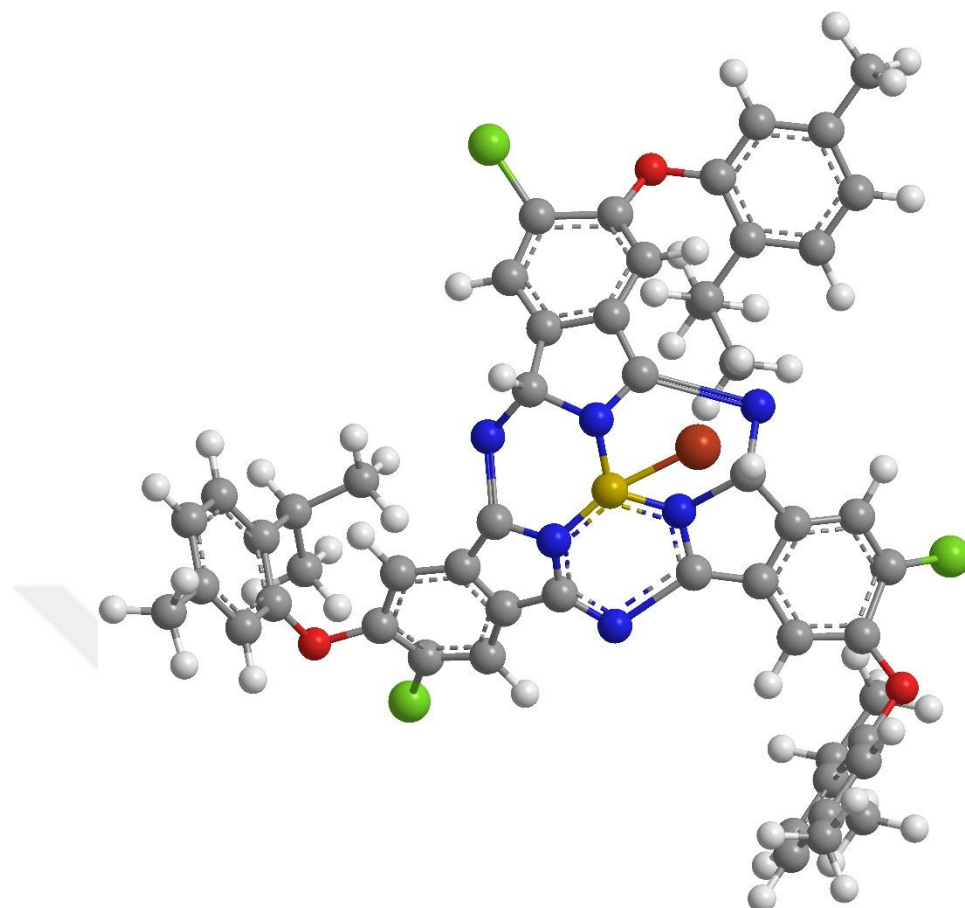
Figure 3.62. 3D structure of bromo[2,9,16-trichloro-3,10,17-trikis(2-isopropyl-5-methylphenoxy)phthalocyaninato]boron(III) (**19**)

CHAPTER 4. RESULTS AND DISCUSSION

4.1. Synthetic results and spectral characterizations

The aim of this work was the development of syntheses for new phthalocyanines and the investigation of the optical properties of these chromophores. The focus was on variations on the ligand framework and the introduction of thymol as peripheral substituents on the Pc. Phthalocyanines and related compounds are interesting materials for optoelectronic applications, such as dye sensitized solar cells (DSSCs), optical data storage or organic field effect transistors (OFETs) and also potential photosensitizers for PDT. With the introduction of thymol as tetra- or octasubstituents either with oxo- or azo bridges (Figure 4.1), some of the new compounds could be used and tested for diverse application areas including the applications mentioned above.
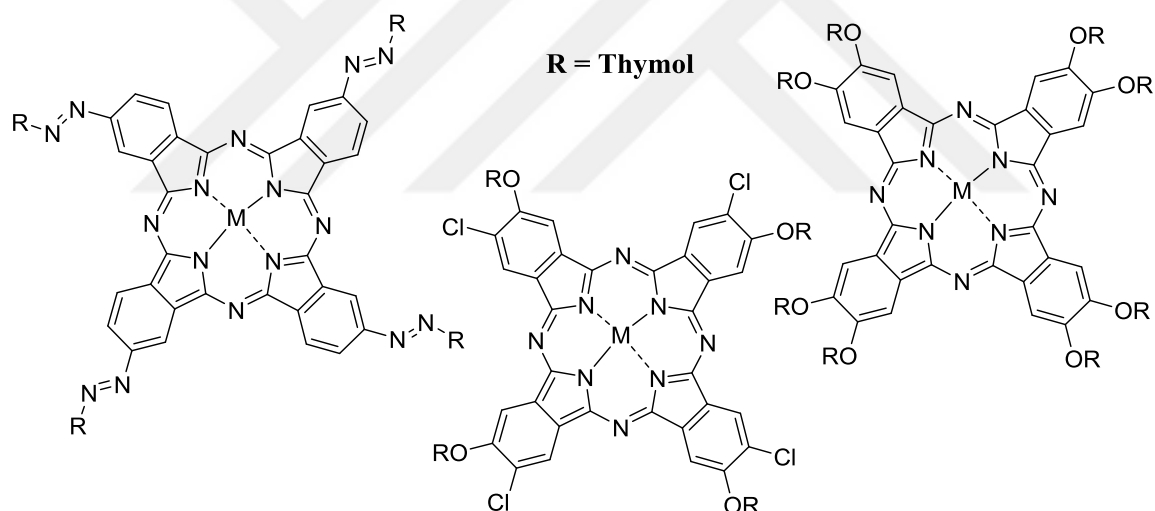
Figure 4.1. Different thymol substituted phthalocyanines

Section 3.1 describes the synthesis of phthalonitriles starting from phthalic acids, which could be used as coupling agents for phthalocyanine precursors. We carried out nucleophilic substitution reactions between thymol and 4,5-dichlorophthalonitrile in order to obtain mono or disubstituted phthalonitrile compounds (Scheme 4.1) and azo

coupling reactions between thymol and 4-aminophthalonitrile for azo bridged phthalocyanine precursors (Scheme 4.2).
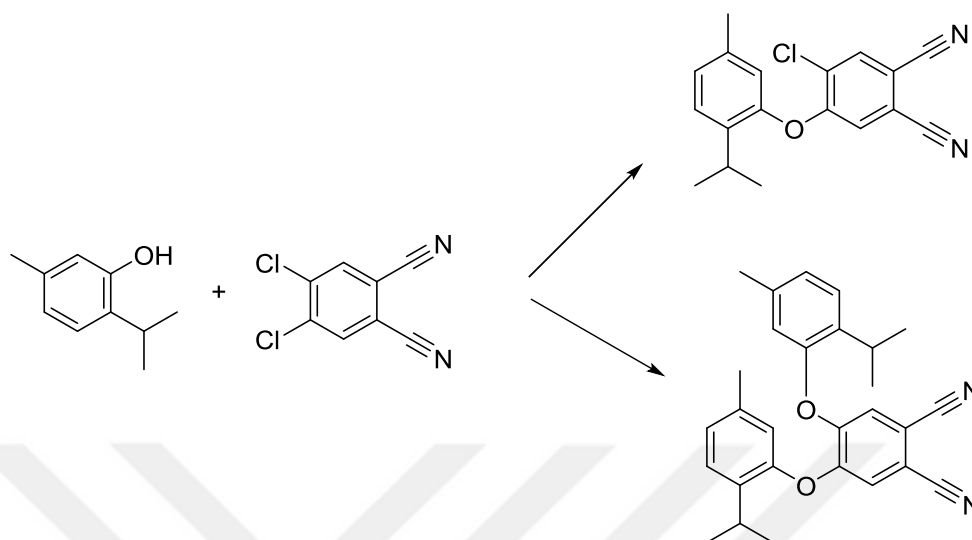
Scheme 4.1. Nucleophilic substitution reaction between thymol and 4,5-dichlorophthalonitrile.
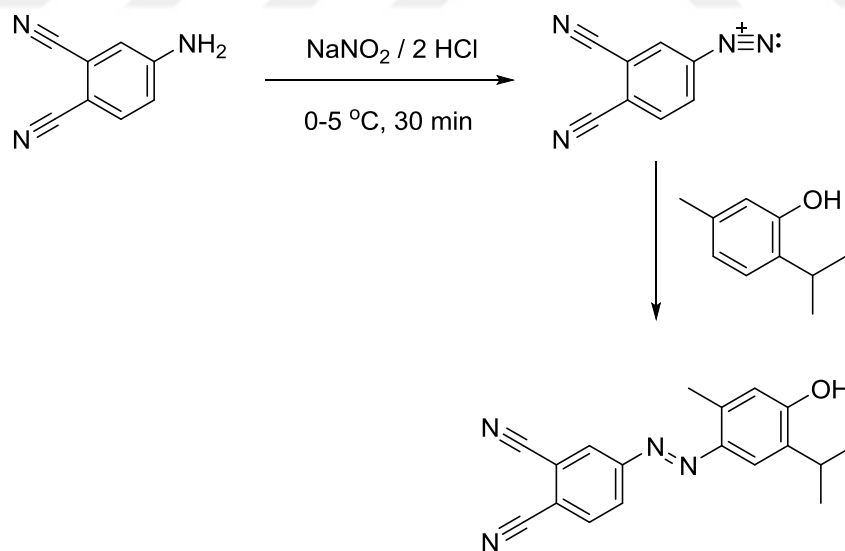
Scheme 4.2. Synthesis of the diazonium salt of 4-aminophthalonitrile and the azo coupling reaction between between thymol and the diazonium salt.

The reactions to obtain phthalocyanine molecules were carried out in pressure Schlenk tubes. It is a glass tube with screw cap and Schlenk attachment that is resistant to moderate pressures for working under inert conditions. Heating the reaction mixture in the closed system creates a slight excess pressure. It has been shown that overpressure increases the yield of phthalocyanine synthesis.

The synthesis of phthalocyanines from substituted phthalonitriles is a widely used method. Often the variant developed by *TOMODA* et al. is used with the solvent 1-pentanol and the strong, non-nucleophilic base DBU as a precatalyst for the formation of pentanolate. Phthalonitriles as starting materials give phthalocyanines with better results, purity and higher yield compared to other phthalic acid derivatives. The use of 4,5-disubstituted dinitriles leads to 2,3,9,10,16,17,23,24-identical substituted phthalocyanines but assymetric or monosubstituted phthalonitrile compounds yield isomeric mixture of phthalocyanines.

Section 3.3 describes the synthesis of various phthalocyanines from the precursors mentioned above. We synthesized metal-free phthalocyanine (**6**) and its metal analogs from 4-chloro-5-(2-isopropyl-5-methylphenoxy)phthalonitrile (**1**). We have obtained several metal analogs of Pc compound **6**, including cobalt (**7**), copper (**8**), iron (**9**) and manganese (**13**) in order to investigate their electrochemical and spectral properties. When we have compared UV-*Vis* spectra of these Pcs, Q bands of CoPc (**7**) and FePc (**9**) comes at 674 nm, CuPc (**8**) at 681 nm and the most red shifted MnClPc (**13**) comes at 730 nm (Figure 4.2). Intensely splitted Q band peaks of H_2Pc (**6**) appear at 667 nm and 701 nm respectively (Figure 4.3). We have obtained mixture of iron (II) Pc and iron (III) Pc. Q bands of these Pcs come at different wavelengths (Figure 4.4).
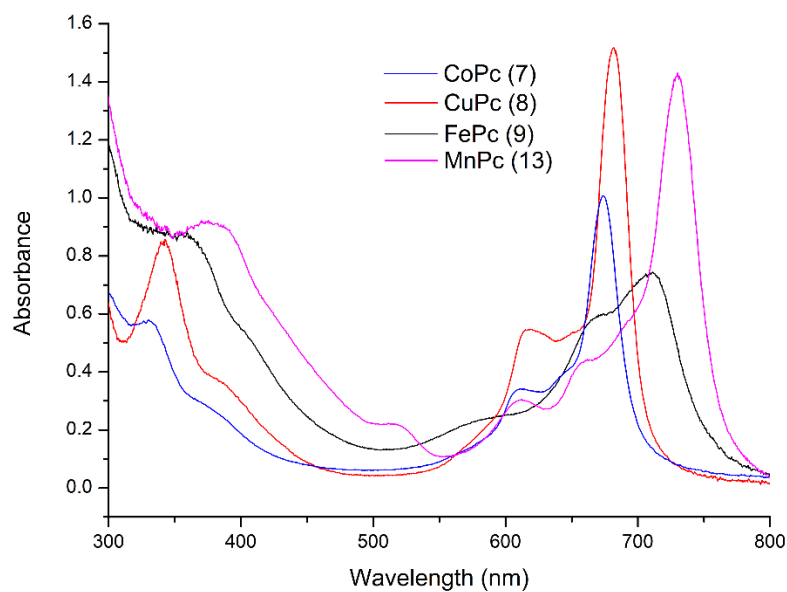
Figure 4.2. UV-*vis* spectrum comparation of compounds **7**, **8**, **9** and **13** in DCM at $1x10^{-5}$ M.
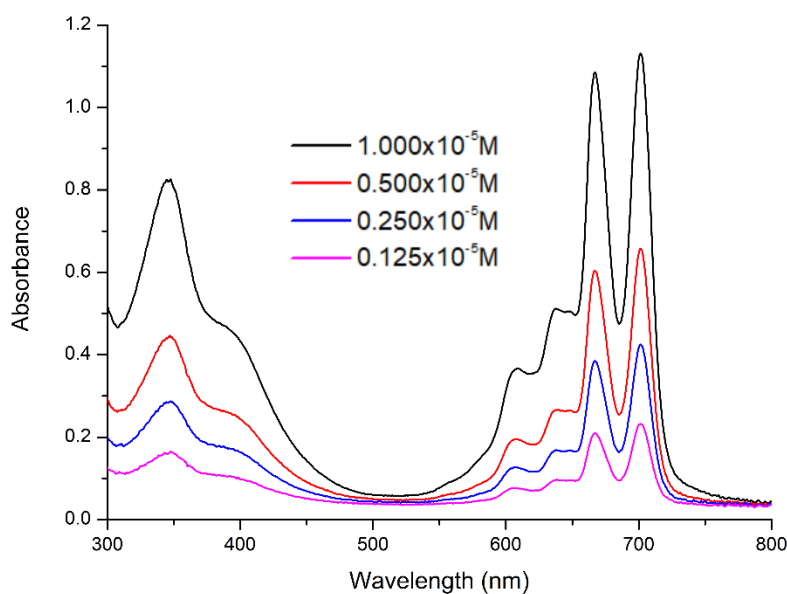
Figure 4.3. UV-*vis* spectrum of H$_2$Pc (**6**) at different concentrations in DCM.
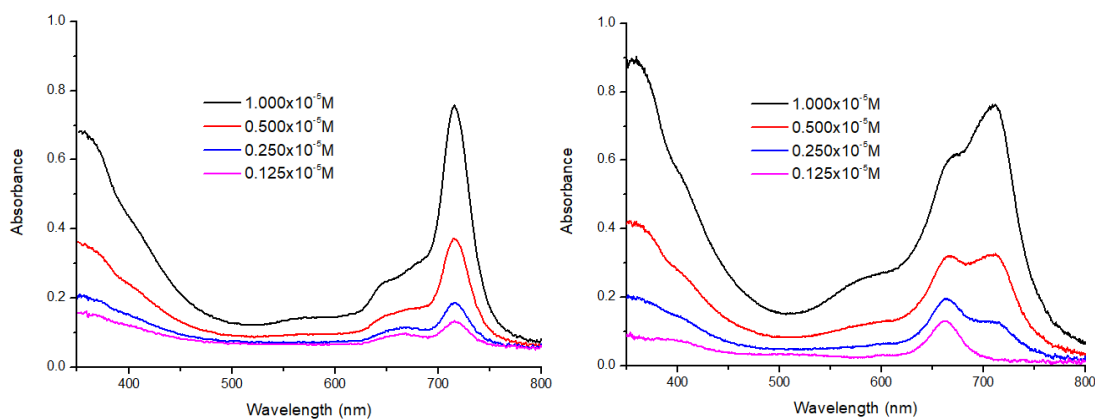
Figure 4.4. UV-*vis* spectra of FePc from two different fractions of column chromatography (**9**) in DCM.

4.2. Photochemical and photophysical studies of Pcs 6, 10, 11, 12 and 14.

Our investigations further continued with the synthesis of different metal analogs of H_2Pc **6**. We have prepared several MPcs with metals; indium (**10**), lutetium (**11**), magnesium (**12**) and zinc (**14**) to investigate their photophysical-photochemical characteristics and their potential for PDT.

4.2.1. Aggregation studies

First of all, we have studied aggregation properties of these Pcs at the concentration of $1\times10^{-5}M$ in different solvents (Figures 4.5-4.9).
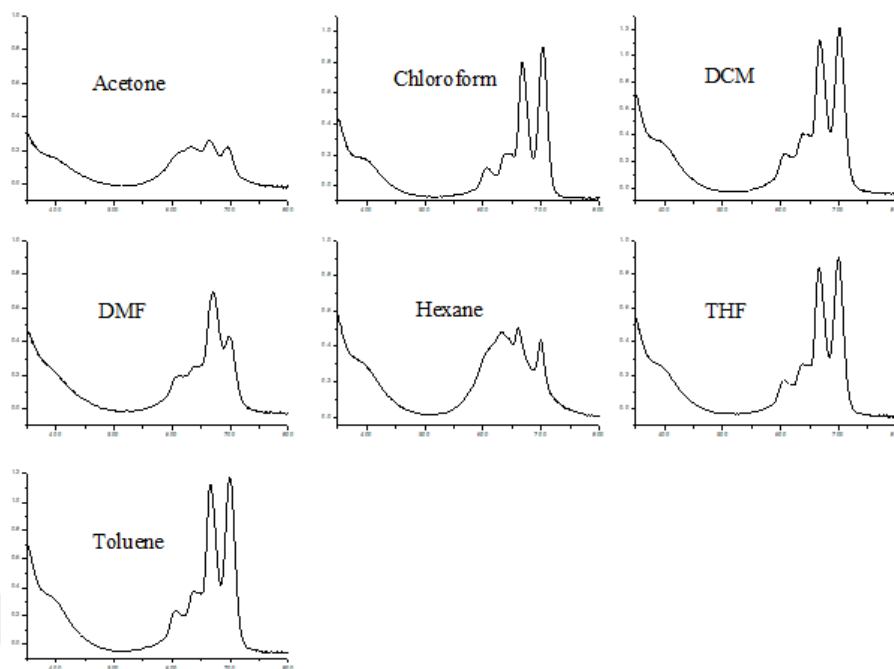
Figure 4.5. UV-*vis* spectra of 2,9,16,23-tetrachloro-3,10,17,24-tetrakis(2-isopropyl-5-methylphenoxy)phthalocyanine (**6**) in different solvents at 1×10^{-5}M.

Figure 4.6. UV-*vis* spectra of 2,9,16,23-tetrachloro-3,10,17,24-tetrakis(2-isopropyl-5-methylphenoxy)phthalocyaninato indium (III) acetate (**10**) in different solvents at 1×10^{-5}M.

Figure 4.7. UV-*vis* spectra of 2,9,16,23-tetrachloro-3,10,17,24-tetrakis(2-isopropyl-5-methylphenoxy)phthalocyaninato lutetium (III) acetate (**11**) in different solvents at 1×10^{-5}M.

Figure 4.8. UV-*vis* spectra of 2,9,16,23-tetrachloro-3,10,17,24-tetrakis(2-isopropyl-5-methylphenoxy)phthalocyaninato magnesium (**12**) in different solvents at 1×10^{-5}M.

Figure 4.9. UV-*vis* spectra of 2,9,16,23-tetrachloro-3,10,17,24-tetrakis(2-isopropyl-5-methylphenoxy)phthalocyaninato zinc (**14**) in different solvents at 1×10^{-5}M.

H_2Pc (**6**) aggregates in acetone and hexane and gets deprotonated in DMF (Figure 4.5). It is also not completely soluble in EtOH. InOAcPc (**10**) and MgPc (**12**) slightly aggregate in EtOH but ZnPc (**14**) aggregates more in EtOH. Furthermore, ZnPc (**14**) slightly aggregates in DMSO and hexane (Figure 4.9). *J* aggregation of MgPc (**12**) takes place in chloroform (Figure 4.8).

A suitable solvent was DMF for the Pcs. We have investigated their aggregation properties at different concentrations in DMF (Figures 4.10-4.14). Any of the Pcs do not aggregate in DMF. H_2Pc (**6**) deprotonated in DMF.
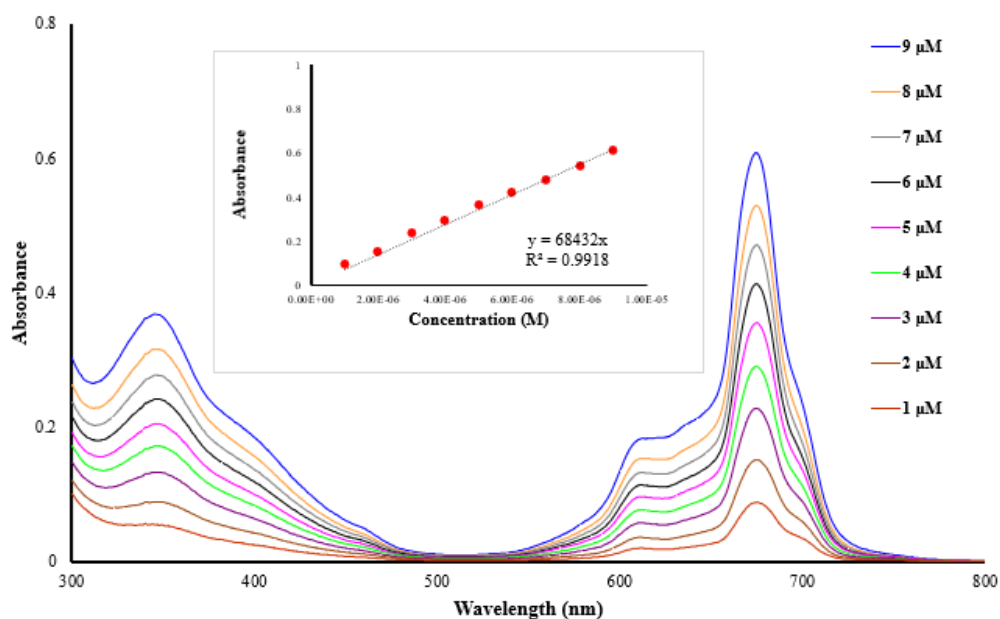
Figure 4.10. UV-*vis* spectrum of 2,9,16,23-tetrachloro-3,10,17,24-tetrakis(2-isopropyl-5-methylphenoxy)phthalocyanine (**6**) at different concentrations in DMF.
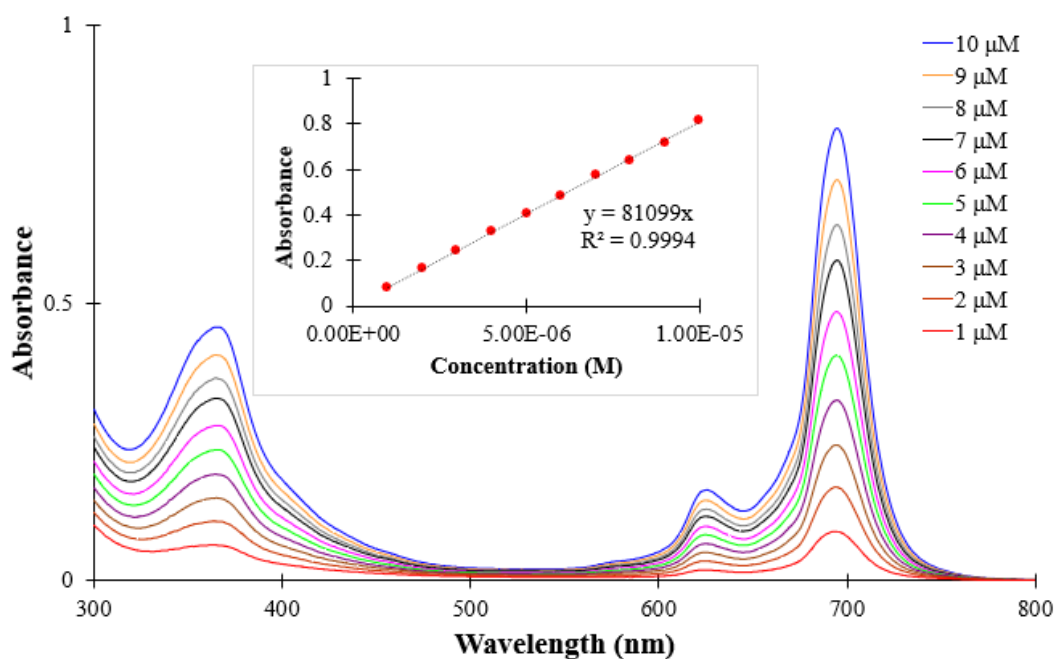
Figure 4.11. UV-*vis* spectrum of 2,9,16,23-tetrachloro-3,10,17,24-tetrakis(2-isopropyl-5-methylphenoxy)phthalocyaninato indium (III) acetate (**10**) at different concentrations in DMF.
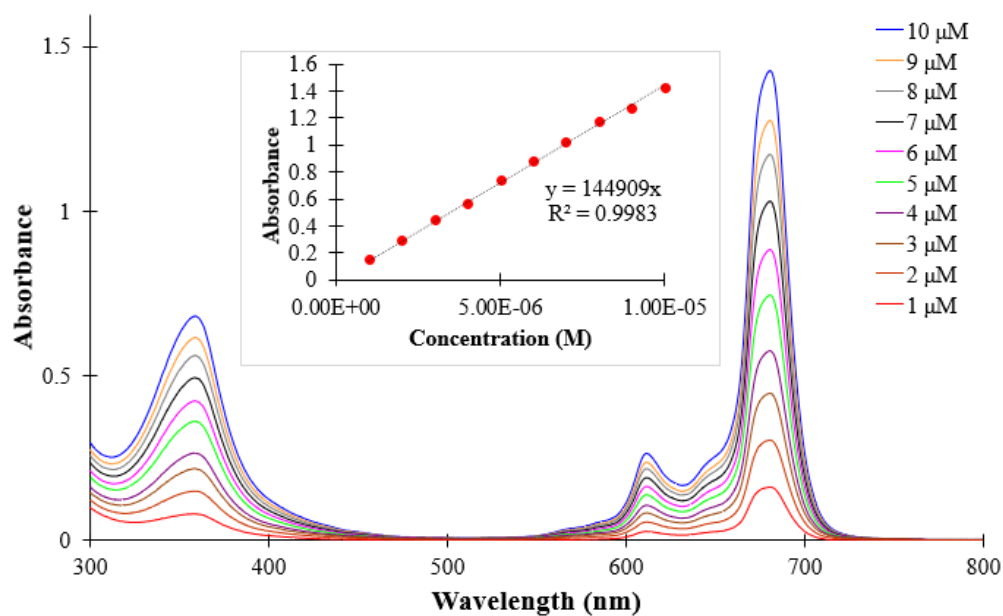
Figure 4.12. UV-*vis* spectrum of 2,9,16,23-tetrachloro-3,10,17,24-tetrakis(2-isopropyl-5-methylphenoxy)phthalocyaninato lutetium (III) acetate (**11**) at different concentrations in DMF.
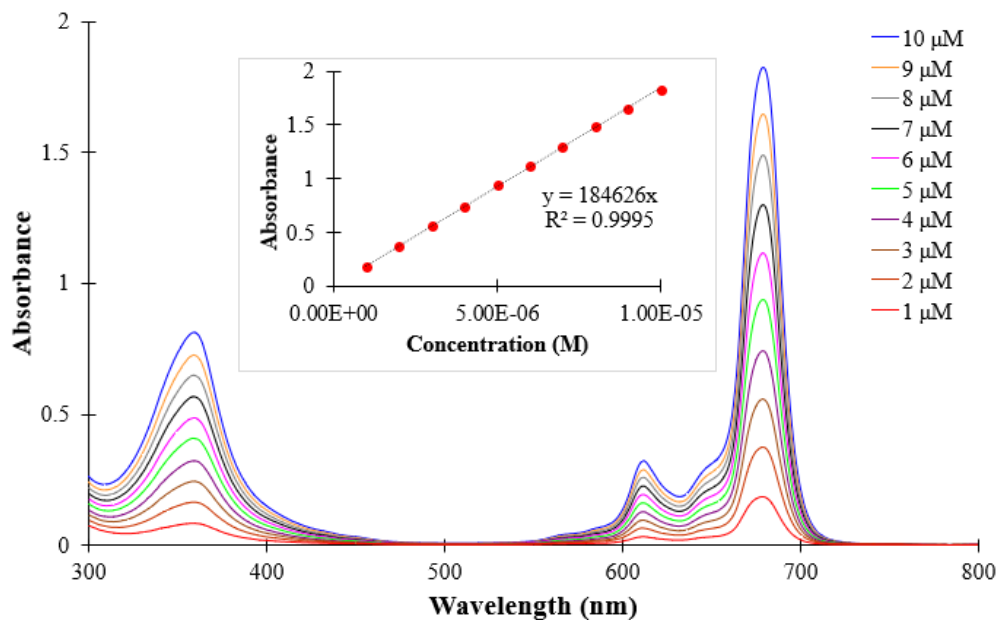
Figure 4.13. UV-*vis* spectrum of 2,9,16,23-tetrachloro-3,10,17,24-tetrakis(2-isopropyl-5-methylphenoxy)phthalocyaninato magnesium (**12**) at different concentrations in DMF.
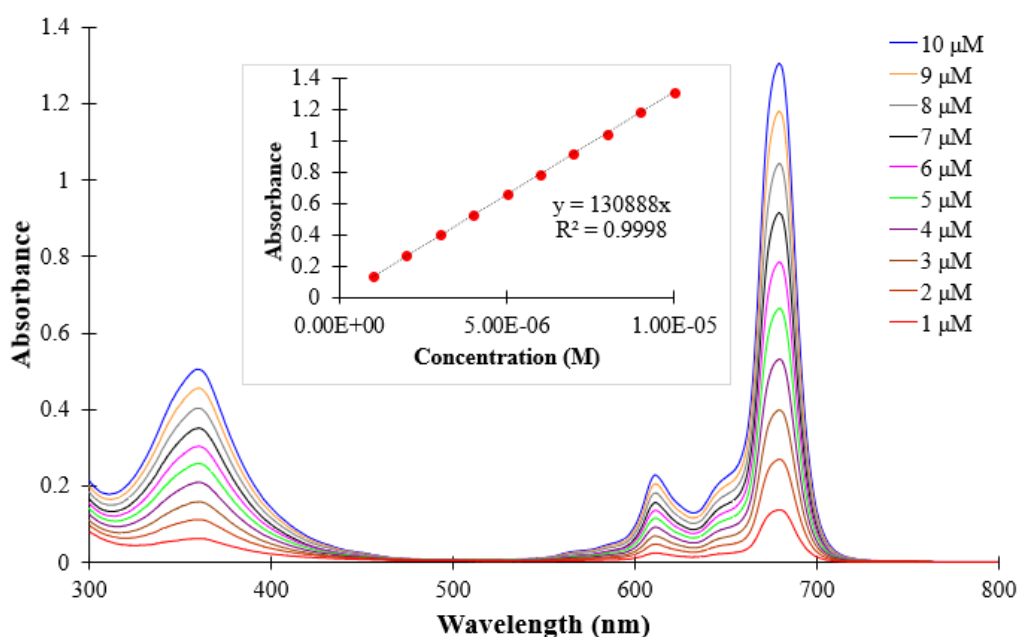
Figure 4.14. UV-*vis* spectrum of 2,9,16,23-tetrachloro-3,10,17,24-tetrakis(2-isopropyl-5-methylphenoxy)phthalocyaninato zinc (**14**) at different concentrations in DMF.

4.2.2. Singlet oxygen quantum yield (Φ_Δ)

The speed of the reaction depends on the amount of singlet oxygen formed per time. The quantum yield can be determined by considering the light energy supplied in the absorption maximum of the photosensitizer. The singlet oxygen quantum yield depends on the solvent used. A suitable solvent was DMF, which on the one hand met the conditions required for the photosensitizers and on the other hand was already used in the literature for the determination of singlet oxygen quantum yields.
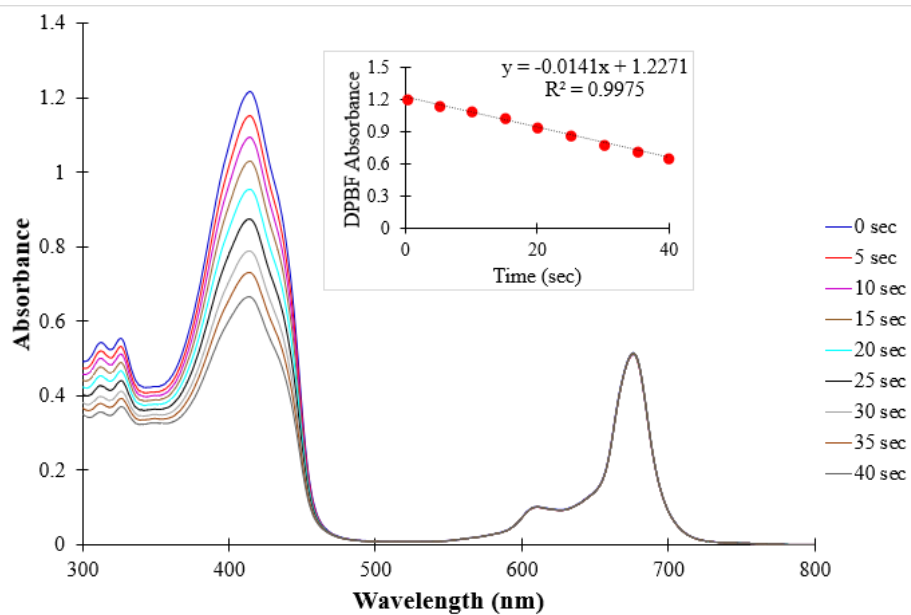
Figure 4.15. UV-*vis* spectrum changes of 2,9,16,23-tetrachloro-3,10,17,24-tetrakis(2-isopropyl-5-methylphenoxy)phthalocyanine (**6**) along with the singlet oxygen quantum yield (Solvent: DMF, C=1x10^{-5}M).
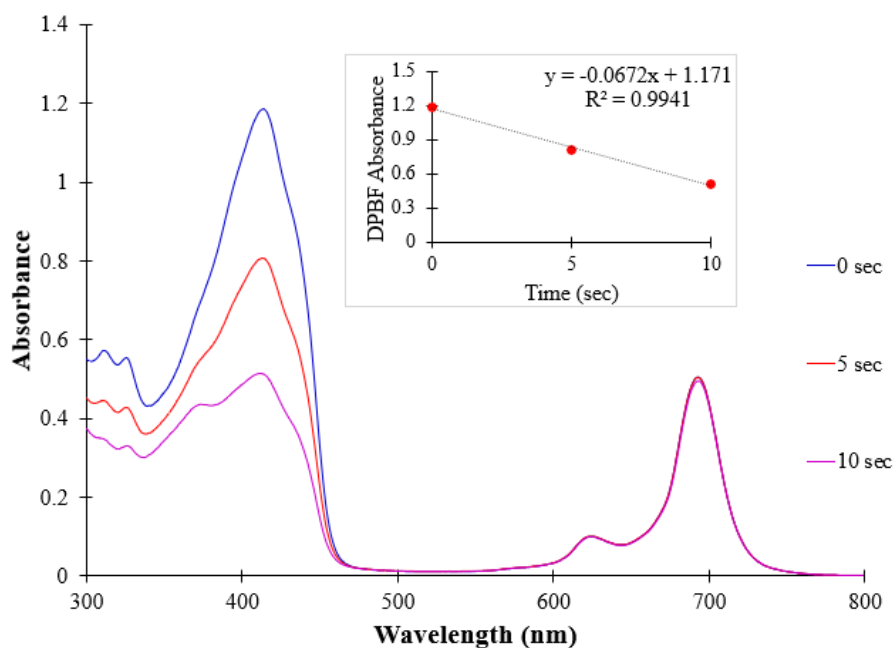
Figure 4.16. UV-*vis* spectrum changes of 2,9,16,23-tetrachloro-3,10,17,24-tetrakis(2-isopropyl-5-methylphenoxy)phthalocyaninato indium (III) acetate (**10**) along with the singlet oxygen quantum yield (Solvent: DMF, C=1x10^{-5}M).
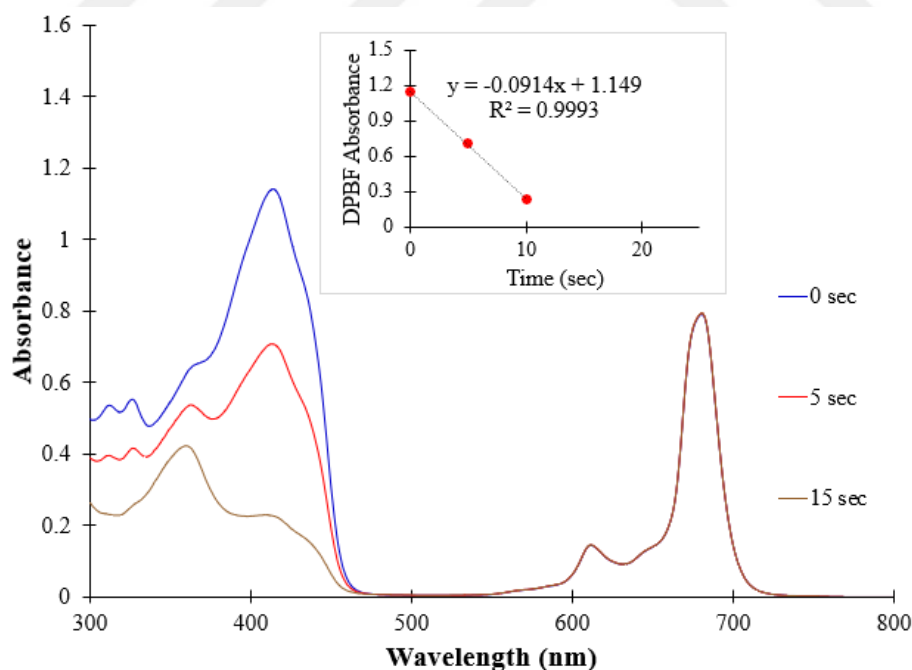
Figure 4.17. UV-*vis* spectrum changes of 2,9,16,23-tetrachloro-3,10,17,24-tetrakis(2-isopropyl-5-methylphenoxy)phthalocyaninato lutetium (III) acetate (**11**) along with the singlet oxygen quantum yield (Solvent: DMF, C=1x10^{-5}M).
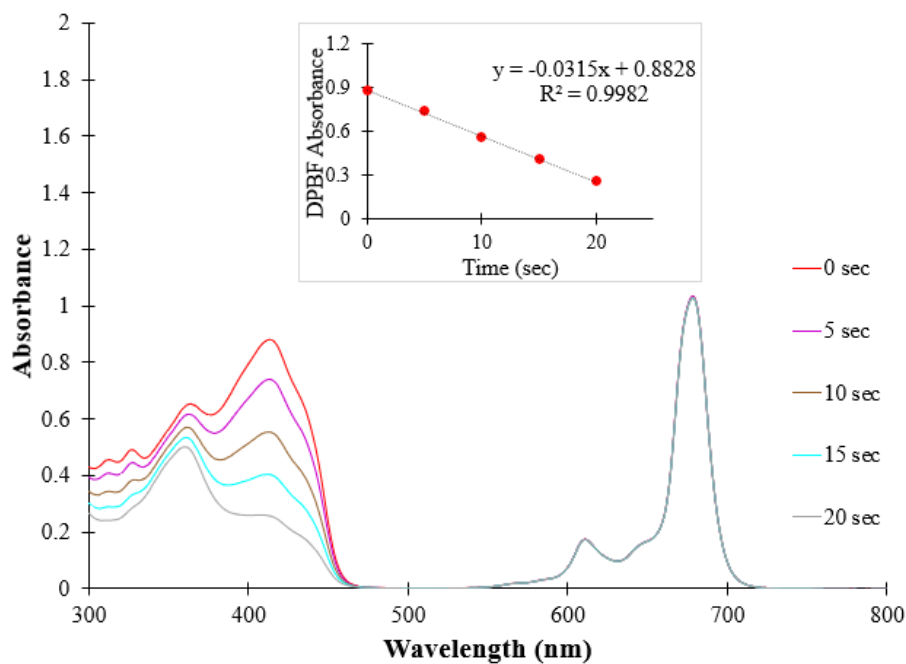
Figure 4.18. UV-*vis* spectrum changes of 2,9,16,23-tetrachloro-3,10,17,24-tetrakis(2-isopropyl-5-methylphenoxy)phthalocyaninato magnesium (**12**) along with the singlet oxygen quantum yield (Solvent: DMF, C=1x10^{-5}M).
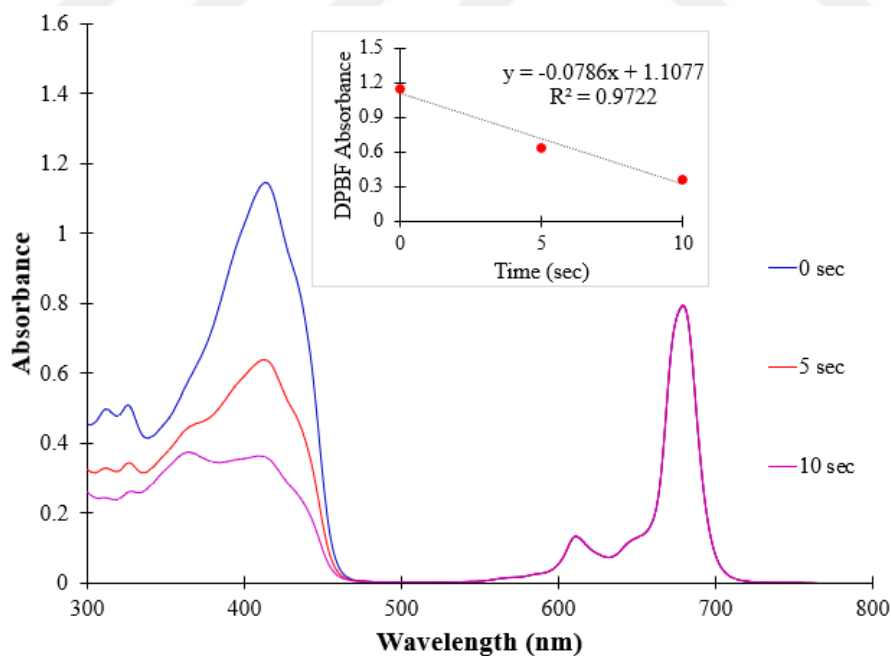
Figure 4.19. UV-*vis* spectrum changes of 2,9,16,23-tetrachloro-3,10,17,24-tetrakis(2-isopropyl-5-methylphenoxy)phthalocyaninato zinc (**14**) along with the singlet oxygen quantum yield (Solvent: DMF, C=1x10^{-5}M).

4.2.3. Photodegradation quantum yield (Φ_d)

Photostability of a Pc molecule under different wavelengths of light is essential for the photocatalytic reactions such as PDT. Photosensitizers (PS) for PDT are expected to be stable and not decompose until they accomplish their photodynamic activities within the cell. Photodegradation quantum yield (Φ_d) calculations help us to interpret PS's stability when they exposed to light. Photodegradation quantum yields of stable ZnPcs are around 10^{-6} and it is around 10^{-3} for unstable ones [125].

Here we have investigated photodegradation quantum yields of Pcs **6**, **10**, **11**, **12** and **14** through observation of the changes on Q bands after exposure of the light with the intensity of 7.05×10^{15} foton/(s.cm^2) (Figures 4.20-4.24).
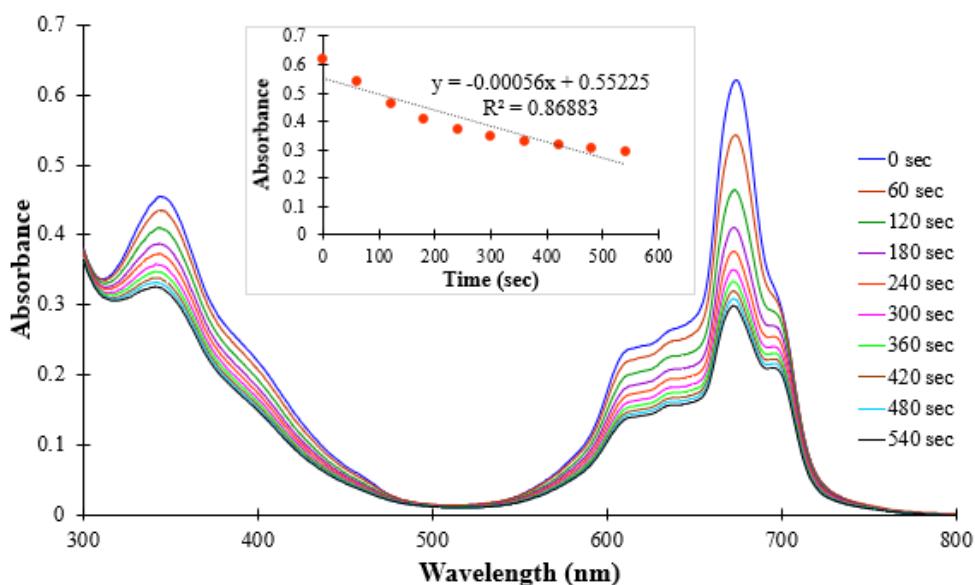
Figure 4.20. UV-*vis* spectrum changes of 2,9,16,23-tetrachloro-3,10,17,24-tetrakis(2-isopropyl-5-methylphenoxy)phthalocyanine (**6**) along with the photodegradation quantum yield (Solvent: DMF, C=1x10^{-5}M).
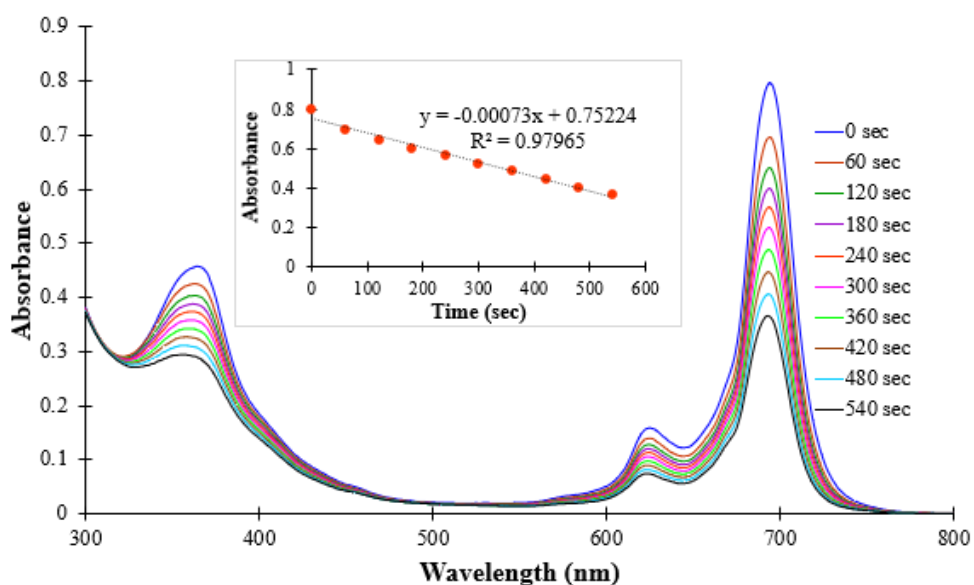
Figure 4.21. UV-*vis* spectrum changes of 2,9,16,23-tetrachloro-3,10,17,24-tetrakis(2-isopropyl-5-methylphenoxy)phthalocyaninato indium (III) acetate (**10**) along with the photodegradation quantum yield (Solvent: DMF, C=1x10^{-5}M).
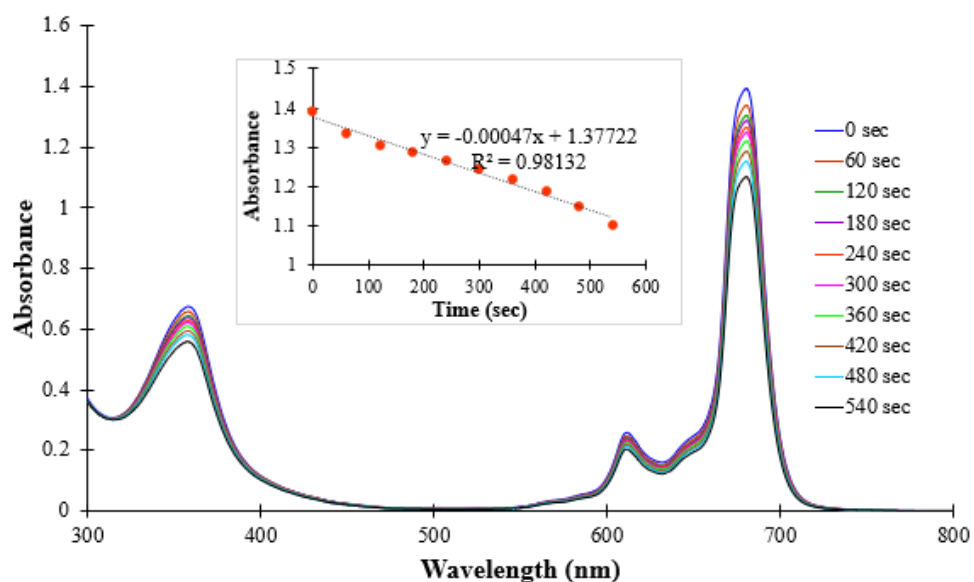
Figure 4.22. UV-*vis* spectrum changes of 2,9,16,23-tetrachloro-3,10,17,24-tetrakis(2-isopropyl-5-methylphenoxy)phthalocyaninato lutetium (III) acetate (**11**) along with the photodegradation quantum yield (Solvent: DMF, C=1x10^{-5}M).
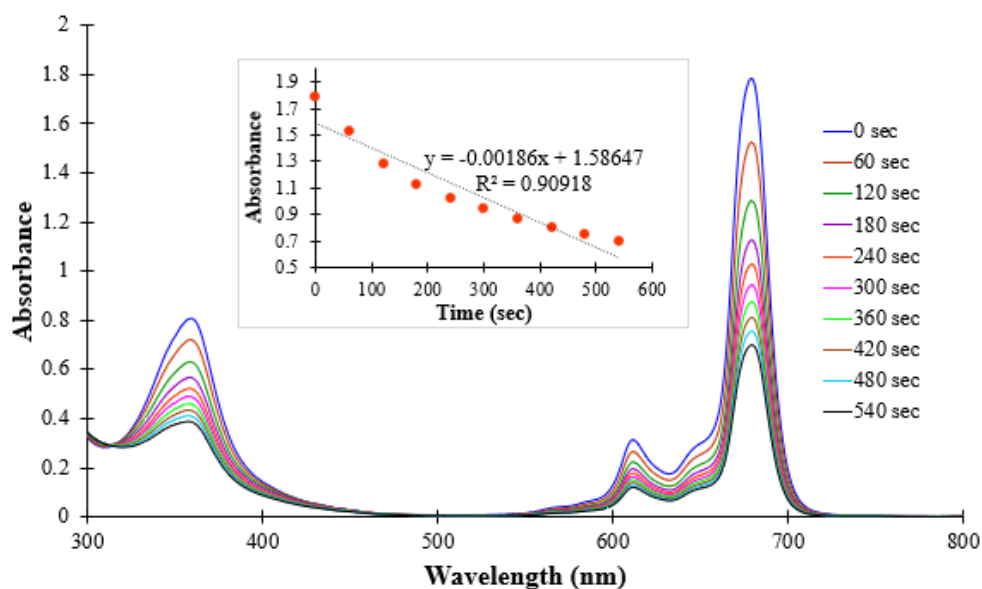
Figure 4.23. UV-*vis* spectrum changes of 2,9,16,23-tetrachloro-3,10,17,24-tetrakis(2-isopropyl-5-methylphenoxy)phthalocyaninato magnesium (**12**) along with the photodegradation quantum yield (Solvent: DMF, C=1x10⁻⁵M).
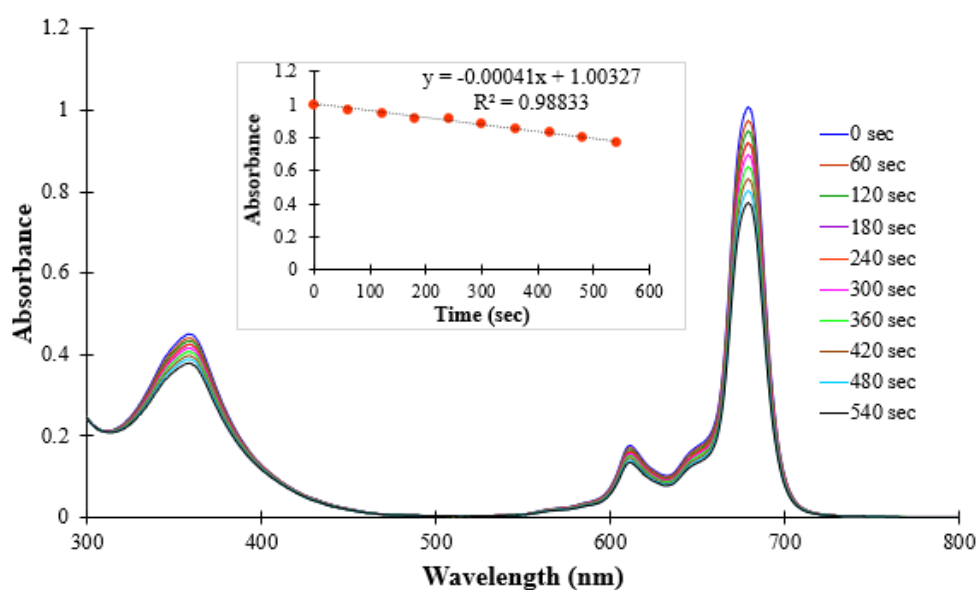
Figure 4.24. UV-*vis* spectrum changes of 2,9,16,23-tetrachloro-3,10,17,24-tetrakis(2-isopropyl-5-methylphenoxy)phthalocyaninato zinc (**14**) along with the photodegradation quantum yield (Solvent: DMF, C=1x10⁻⁵M).

4.2.4. Fluorescence quantum yield (Φ_f)

Ideal photosensitizers should show some fluorescence behavior in order to be able to follow them in the body. Therefore, it is important to investigate their fluorescence quantum yield (Φ_f) characteristics for PDT studies.
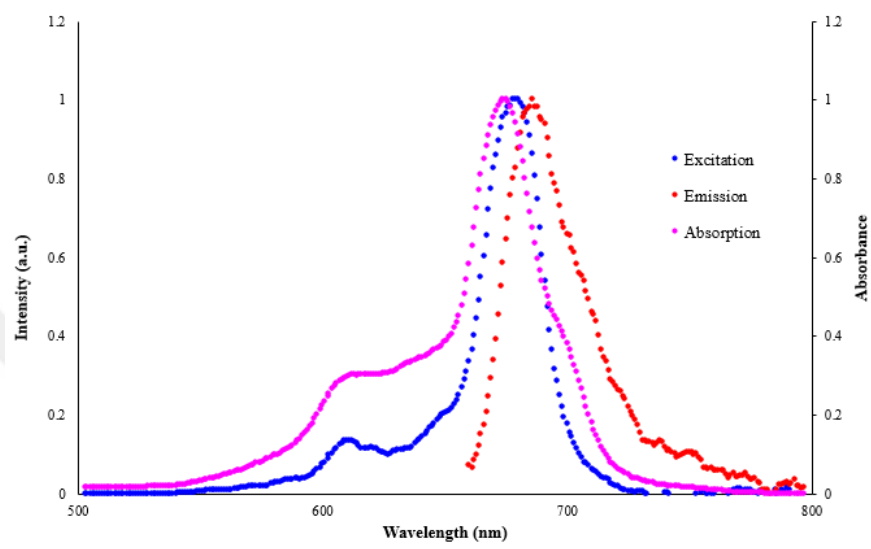
Figure 4.25. Excitation, emission and absorption spectra of 2,9,16,23-tetrachloro-3,10,17,24-tetrakis(2-isopropyl-5-methylphenoxy)phthalocyanine (**6**) (Solvent: DMF, C=1x10^{-6}M).
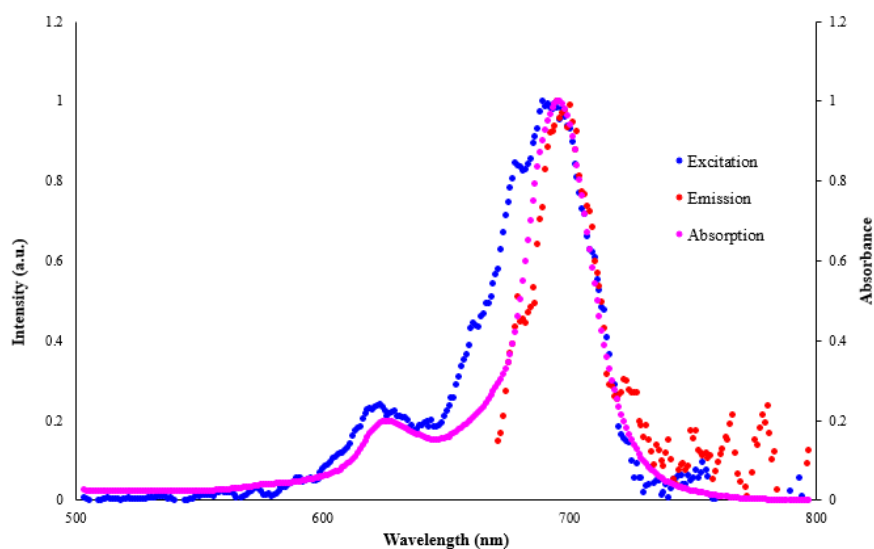
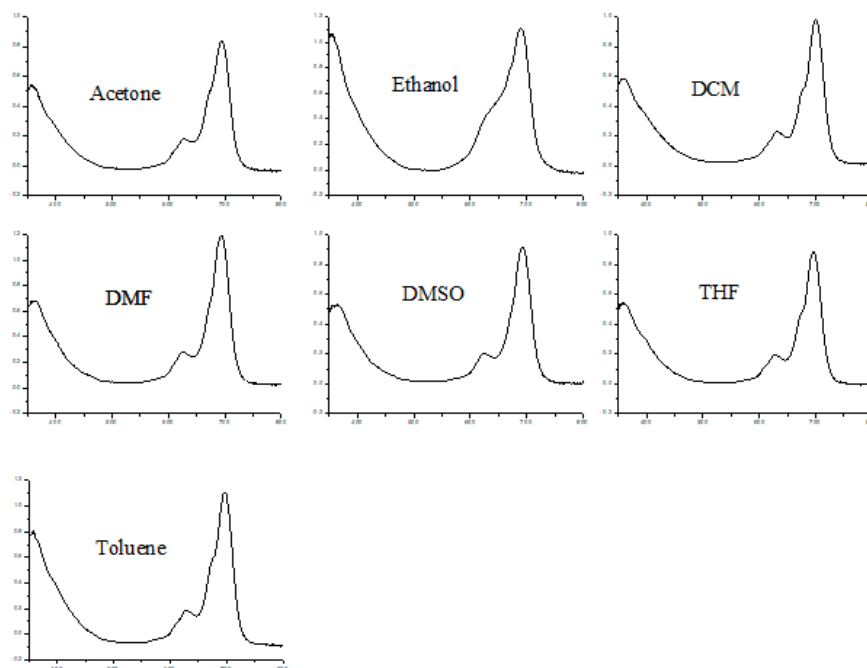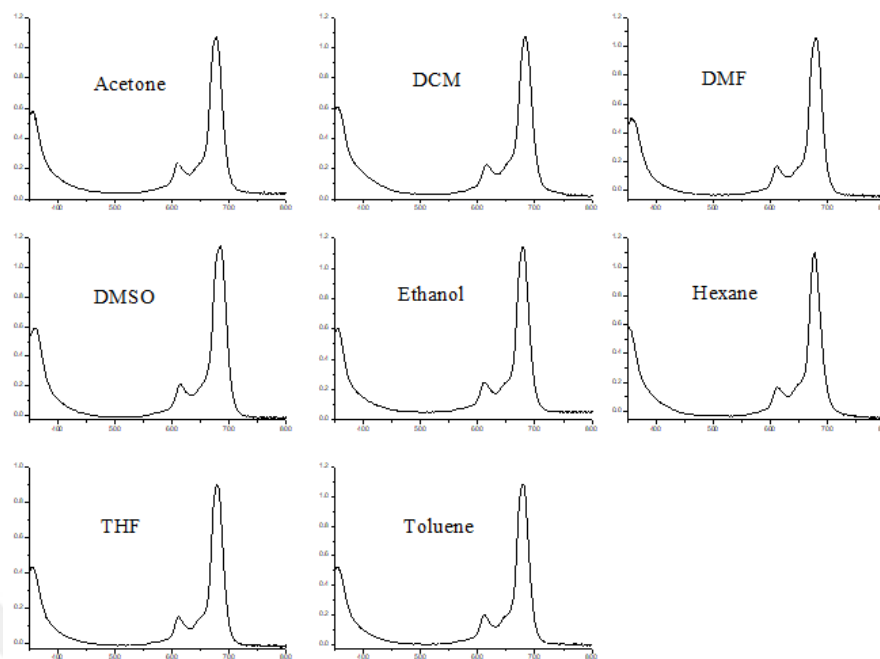**Figure 4.26.** Excitation, emission and absorption spectra of 2,9,16,23-tetrachloro-3,10,17,24-tetrakis(2-isopropyl-5-methylphenoxy)phthalocyaninato indium (III) acetate (**10**) (Solvent: DMF, C=1x10^{-6}M).
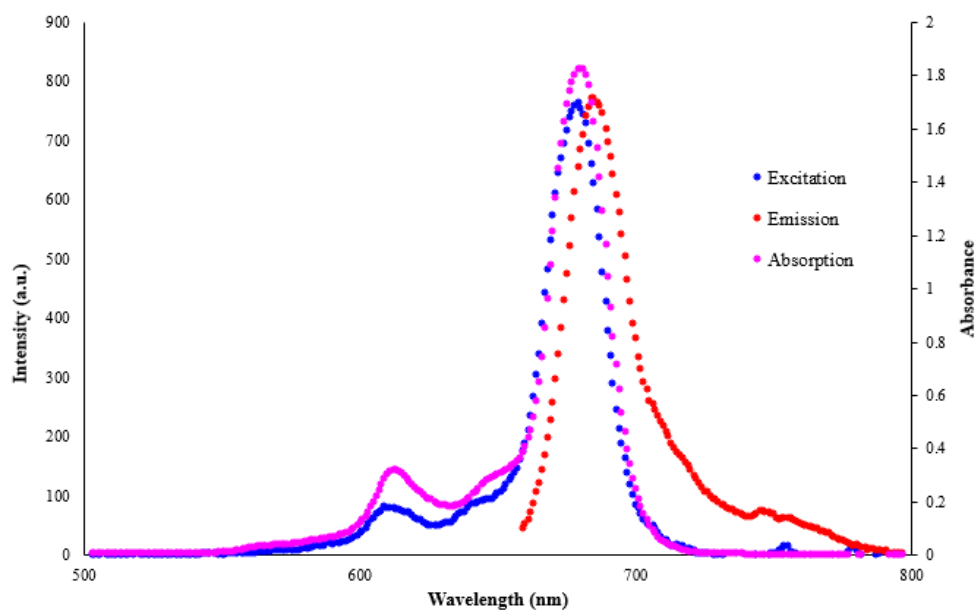
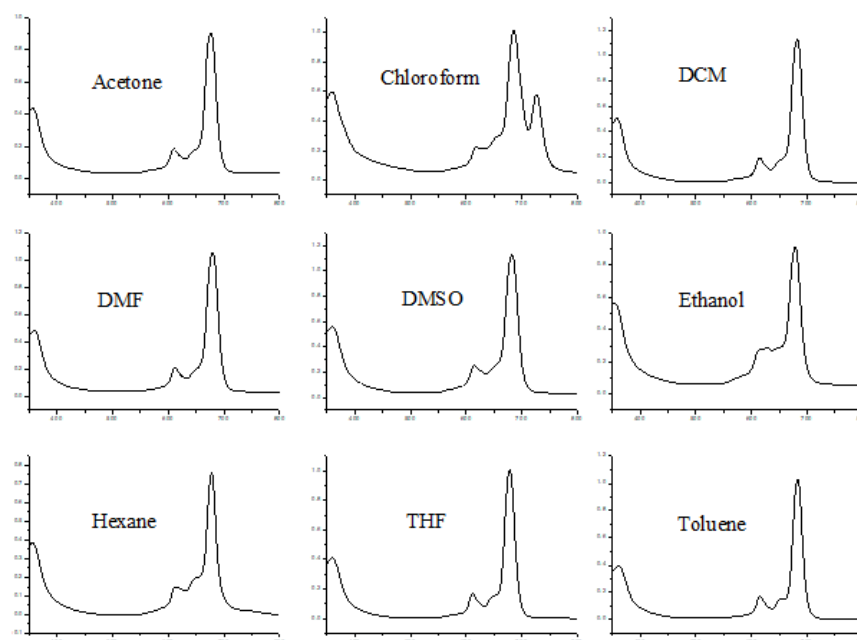**Figure 4.27.** Excitation, emission and absorption spectra of 2,9,16,23-tetrachloro-3,10,17,24-tetrakis(2-isopropyl-5-methylphenoxy)phthalocyaninato magnesium (**12**) (Solvent: DMF, C=1x10^{-6}M).
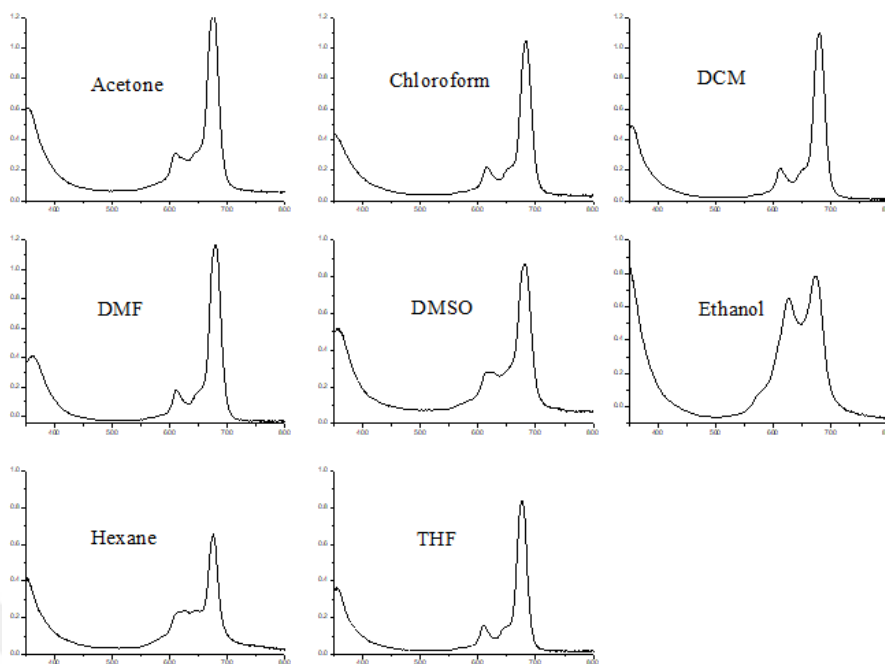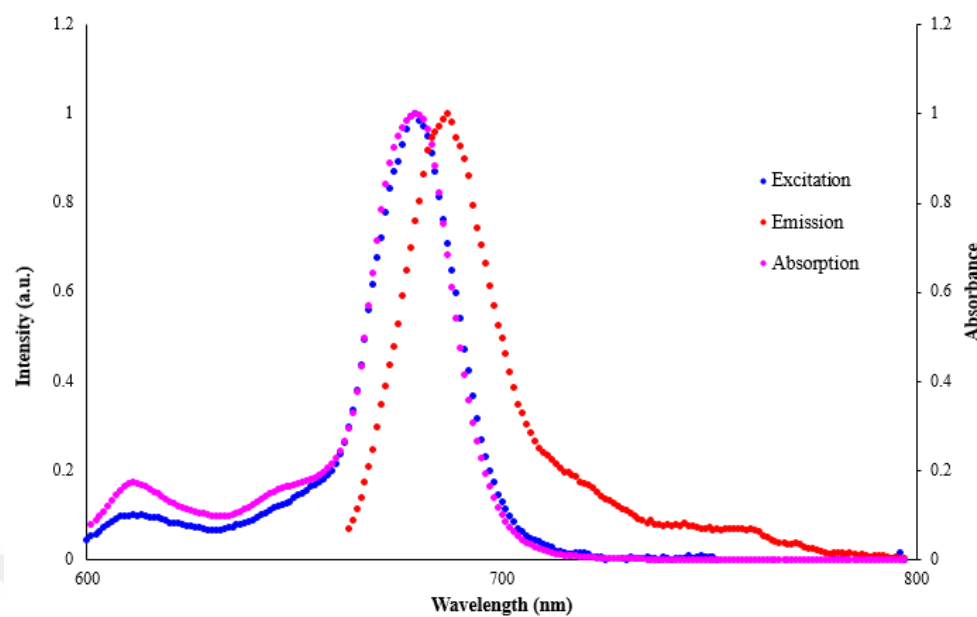
Figure 4.28. Excitation, emission and absorption spectra of 2,9,16,23-tetrachloro-3,10,17,24-tetrakis(2-isopropyl-5-methylphenoxy)phthalocyaninato zinc (**14**) (Solvent: DMF, C=1x10^{-6}M).

Evaluation of data

In order to examine the photophysical and photochemical properties of the compounds **6**, **10**, **11**, **12** and **14**, several measurements were carried out in DMF; including singlet oxygen quantum yield (Φ_Δ), photodegradation quantum yield (Φ_d), fluorescence quantum yield (Φ_F) and lifetimes (Υ_F). Unsubstituted ZnPc was used as standard.

Satisfactory results have been obtained for the use of phthalocyanines in PDT applications. Both InOAcPc (**10**) and ZnPc (**14**) showed higher singlet oxygen yield compared to standard unsubstituted zinc phthalocyanine. InOAcPc (**10**) showed the highest singlet oxygen quantum yield. This is due to the heavy metal effect.

The stability of the compounds is determined by irradiation of molecules. This is particularly important for molecules suitable for use in PDT. A photosensitizer should be able to remain in the body without degradation until the desired photodynamic process. On the other hand, after the PDT action is completed, within the optimum period, PS should be removed from the body to avoid side effects. Photodegradation studies have shown that complexes have reasonable photodegradation.

Among others, ZnPc (**14**) has considerably better fluorescence and triplet lifetimes, properties especially suitable for PDT.

The results are given in Table 1 and 2.

113

Compound	Q band l_{max}, (nm)	(log ε)	Excitation l_{Ex}, (nm)	Emission l_{Em}, (nm)	Stokes Shift Δ_{Stokes}, (nm)
H$_2$Pc (**6**)	674	4.78	679	686	7
ZnPc (**14**)	678	5.11	678	687	9
MgPc (**12**)	678	5.26	678	685	7
In(OAc)Pc (**10**)	691	4.91	689	699	10
Std-ZnPc [a]	670	5.37	670	676	6

Table 1. Absorption, excitation and emission spectral data of the Pcs.

Compound	Φ_F	T_F (ns)	Φ_d (x10^{-4})	Φ_Δ
H$_2$Pc (**6**)	0.075	3.79	2.49	0.130
ZnPc (**14**)	0.138	2.84	1.1	0.697
MgPc (**12**)	0.345	5.30	73.0	0.259
In(OAc)Pc (**10**)	0.051	0.15 (%75), 2.89 (%24)	2.45	0.837
Std-ZnPc[139]	0.170	1.03	2.61	0.560

Table 2. Photophysical and photochemical data of the Pcs.

4.3. Spectroscopic properties of octa thymol substituted Pcs and azo bridged Pcs.

In addition to the previously discussed Pcs, we have also synthesized octa-substituted (**15** and **16**) and azo bridged (**17** and **18**) analogs of the H_2Pc **6** and ZnPc **14** respectively, as described in the parts between 3.3.3-3.3.7.

There was not significant difference in the UV-*vis* spectra of the tetra- and -octa thymol substituted analogs, but in the UV-*vis* spectrum of the azo bridged Pcs we could observe clear bathochromic shift.
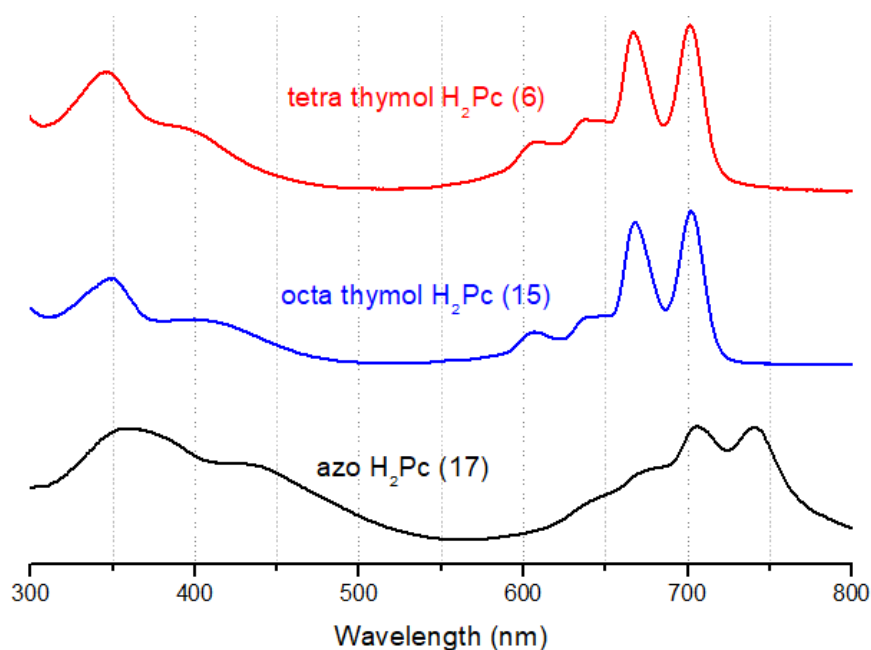
Figure 4.29. Comparation of the UV-*vis* spectra of the Pcs **6**, **15** and **17** in DCM $(1x10^{-5}M)$.
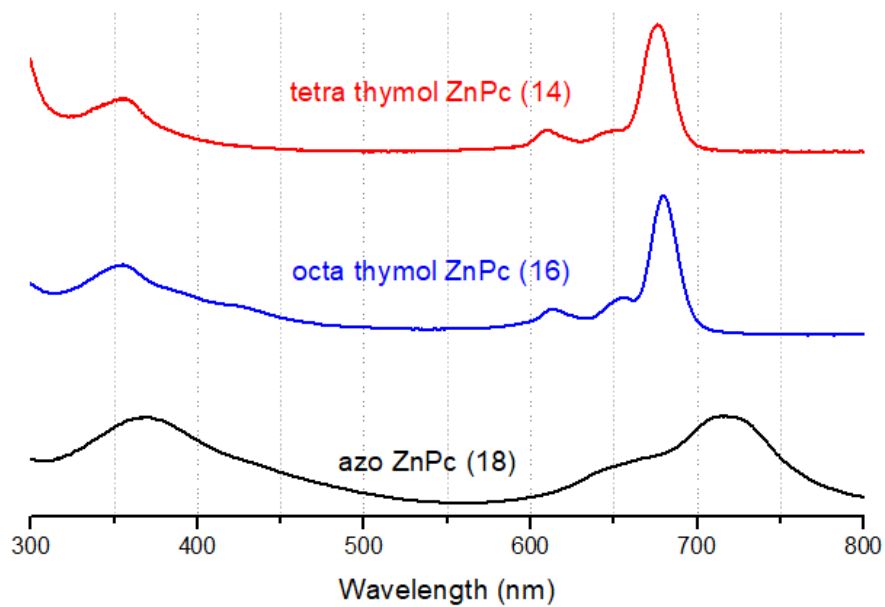
Figure 4.30. Comparation of the UV-*vis* spectra of the Pcs **14**, **16** and **18** in DCM (1x10^{-5}M).

4.4. Spectroscopic properties of subphthalocyanine 19

Last part of the experimental section describes the synthesis of the subphthalocyanine analog of the Pc **6**. Around 200 nm long hypsochromic shift can be observed if we compare UV-*vis* spectrum of the SubPc (**19**) with its H$_2$Pc analog (**6**).
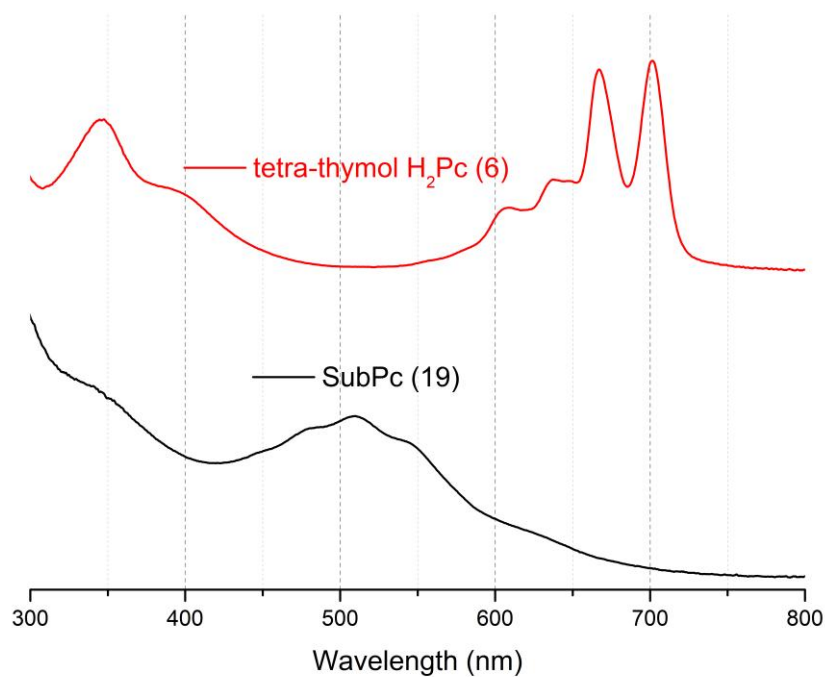
Figure 4.31. Comparation of the UV-*vis* spectra of the H$_2$Pc **6** and SubPc **19** in DCM (1x10^{-5}M).

SUMMARY

In this thesis work, we have synthesized Pc compounds substituted with thymol via oxo and azo bridges. We have obtained tetra- and octa substituted derivatives of oxo bridged Pcs as well as subphthalocyanine analog. These Pc complexes characterized with spectroscopic methods including UV-*Vis*, FT-IR, NMR and MALDI-TOF MS.

We have synthesized Pc molecules with Co, Cu, Mn and Fe metals in order to investigate their electrochemical properties. We have synthesized InOAcPc, LuOAcPc, MgPc and ZnPc and investigated their photophysical and photochemical properties to study their potential for PDT applications.

Throughout this thesis it has been shown that Pcs are among the most versatile and interesting compounds within molecular materials. Although technological applications based on these compounds already exist in the market, the design of Pcs with suitable properties for specific applications will continue to be studied due to the possibilities of improvement and the appearance of new properties and applications of these compounds.

REFERENCES

[1] Claessens, C. G., Blau, W. J., Cook, M., Hanack, M., Nolte, R. J., Torres, T., & Wöhrle, D. (2001). Phthalocyanines and phthalocyanine analogues: the quest for applicable optical properties. Monatshefte für Chemie/ Chemical Monthly, 132(1), 3-11.

[2] Kumbhar, P. P., & Dewang, P. M. (2001). Eco-friendly pest management using monoterpenoids. I. Antifungal efficacy of thymol derivatives.

[3] Li, Y., Wen, J. M., Du, C. J., Hu, S. M., Chen, J. X., Zhang, S. G., ... & Miyamoto, H. (2017). Thymol inhibits bladder cancer cell proliferation via inducing cell cycle arrest and apoptosis. Biochemical and biophysical research communications, 491(2), 530-536.

[4] Botelho, M. A., Nogueira, N. A. P., Bastos, G. M., Fonseca, S. G. C., Lemos, T. L. G., Matos, F. J. A., Brito, G. A. C. (2007). Antimicrobial activity of the essential oil from Lippia sidoides, carvacrol and thymol against oral pathogens. Brazilian Journal of Medical and Biological Research, 40(3), 349-356.

[5] Braga, P. C., Dal Sasso, M., Culici, M., Bianchi, T., Bordoni, L., & Marabini, L. (2006). Anti-inflammatory activity of thymol: inhibitory effect on the release of human neutrophil elastase. Pharmacology, 77(3), 130-136.

[6] Aeschbach, R., Löliger, J., Scott, B. C., Murcia, A., Butler, J., Halliwell, B., & Aruoma, O. I. (1994). Antioxidant actions of thymol, carvacrol, 6-gingerol, zingerone and hydroxytyrosol. Food and Chemical Toxicology, 32(1), 31-36.

[7] Flom, S. R. (2003). Nonlinear optical properties of phthalocyanines. In The porphyrin handbook (pp. 179-190). Academic Press.

[8] Wöhrle, D., & Schnurpfeil, G. (2003). Porphyrins and Phthalocyanines in Macromolecules. The porphyrin handbook (pp. 177-246).

[9] Tanaka, M. (2009). Phthalocyanines—High performance pigments and their applications. High performance pigments, 275-291.

[10] Claessens, C. G., Hahn, U., & Torres, T. (2008). Phthalocyanines: From outstanding electronic properties to emerging applications. The Chemical Record, 8(2), 75-97.

[11] Erk, P., & Hengelsberg, H. (2003). Phthalocyanine dyes and pigments. In The porphyrin handbook (pp. 105-149). Academic Press.

[12] Han, M., Zhang, X., Zhang, X., Liao, C., Zhu, B., & Li, Q. (2015). Azo-coupled zinc phthalocyanines: Towards broad absorption and application in dye-sensitized solar cells. Polyhedron, 85, 864-873.

[13] Braun, A. V., & Tcherniac, J. (1907). Über die produkte der einwirkung von acetanhydrid auf phthalamid. Berichte der deutschen chemischen Gesellschaft, 40(2), 2709-2714.

[14] De Diesbach, H., & Von Der Weid, E. (1927). Some salt complexes of o-dinitriles with copper and pyridine. Helvetica Chim. Acta,(10), 886-888.

[15] McKeown, N. B. (1998). Phthalocyanine materials: synthesis, structure and function (No. 6). Cambridge University Press.

[16] Dahlen, M. A. (1939). The phthalocyanines a new class of synthetic pigments and dyes. Industrial & Engineering Chemistry, 31(7), 839-847.

[17] Linstead, R. P. (1934). Phthalocyanines. Part I. A new type of synthetic colouring matters. Journal of the Chemical Society (Resumed), 1016-1017.

[18] Linstead, R. P., & Lowe, A. R. (1934). Phthalocyanines. Part III. Preliminary experiments on the preparation of phthalocyanines from phthalonitrile. Journal of the Chemical Society (Resumed), 1022-1027.

[19] Linstead, R. P., & Lowe, A. R. (1934). Phthalocyanines. Part V. The molecular weight of magnesium phthalocyanine. Journal of the Chemical Society (Resumed), 1031-1033.

[20] Linstead, R. P., Noble, E. G., & Wright, J. M. (1937). Phthalocyanines. Part IX. Derivatives of thiophen, thionaphthen, pyridine, and pyrazine, and a note on the nomenclature. Journal of the Chemical Society (Resumed), 911-921.

[21] Byrne, G. T., Linstead, R. P., & Lowe, A. R. (1934). Phthalocyanines. Part II. The preparation of phthalocyanine and some metallic derivatives from o-cyanobenzamide and phthalimide. Journal of the Chemical Society (Resumed), 1017-1022.

[22] Dent, C. E., Linstead, R. P., & Lowe, A. R. (1934). Phthalocyanines. Part VI. The structure of the phthalocyanines. Journal of the Chemical Society (Resumed), 1033-1039.

[23] a) Robertson, J. M., & An, X. (1935). ray study of the structure of the phthalocyanines: the metal‐ free, nickel, copper and platinum complexes. In

Chem Soc (Vol. 615, p. 621). b) Robertson, J. M. (1936). An X-ray study of the phthalocyanines. Part II. Quantitative structure determination of the metal-free compound. Journal of the Chemical Society (Resumed), 1195-1209. c) Crucius, G. (2013). Synthesen nichtperipher glykokonjugierter Zink (II) phthalocyanine (Doctoral dissertation).

[24] a) Mortimer, C. E., & Müller, U. Chemie: das Basiswissen der Chemie. (2003). Stuttgart, Thieme Verlag, 8, 458. b) Janiak, C., Klapötke, T., Meyer, H. J., Alsfasser, R., & Riedel, E. (2007). Moderne Anorganische Chemie. 3. Auf. ed.

[25] a) Reynolds, P. A., & Figgis, B. N. (1991). Metal phthalocyanine ground states: covalence and ab initio calculation of spin and charge densities. Inorganic Chemistry, 30(10), 2294-2300. b) Rosa, A., & Baerends, E. J. (1994). Metal-macrocycle interaction in phthalocyanines: density functional calculations of ground and excited states. Inorganic Chemistry, 33(3), 584-595.

[26] a) Kadish, K., Smith, K. M., & Guilard, R. (Eds.). (2000). The Porphyrin Handbook: Phthalocyanines: Properties and Materials (Vol. 17). Elsevier. b) Mckeown, N. B. Science of Synthesis, Vol. 17, Georg Thieme Verlag, Stuttgart, New York, 2004.

[27] a) Wöhrle, D., Schnurpfeil, G., Makarov, S., & Suvora, O. (2012). Phthalocyanine: Von Farbmitteln zu Materialien für Optik und Photoelektronik. Chemie in unserer Zeit, 46(1), 12-24. b) Crucius, G. (2013). Synthesen nichtperipher glykokonjugierter Zink (II) phthalocyanine (Doctoral dissertation). c) Glebe, U. (2012). Selbstassemblierte Monolagen und magnetisch strukturierte Submonolagen mit dia-und paramagnetischen Molekülen sowie Einzelmolekülmagneten auf Phthalocyanin-und Subphthalocyanin-Basis (Doctoral dissertation).

[28] Mckeown, N. B. (2003). in Science of Synthesis, Vol 17, Thieme Stuttgart.

[29] Brumfield, S. N., Mays, B. C., & Thomas, A. L. (1964). Formation of copper phthalocyanine. The Journal of Organic Chemistry, 29(8), 2484-2486.

[30] Stillman, M. J., Nyokong, T., Leznoff, C. C., & Lever, A. B. P. (1989). Phthalocyanines: properties and applications. by CC Leznoff and ABP Lever, VCH, New York, 1, 133.

[31] Ashida, M., Ueda, Y., Yanagi, H., Uyeda, N., Fujiyoshi, Y., & Fryer, J. R. (1988). Formation and structure of a 2,3,9,10,16,17,23,24-octacyanophthalocyanine–

potassium complex in thin film. Acta Crystallographica Section B: Structural Science, 44(2), 146-151.

[32] a) Tomoda, H., Saito, S., & Shiraishi, S. (1983). Synthesis of metallophthalocyanines from phthalonitrile with strong organic bases. Chemistry Letters, 12(3), 313-316. b) Tomoda, H., Saito, S., Ogawa, S., & Shiraishi, S. (1980). Synthesis of phthalocyanines from phthalonitrile with organic strong bases. Chemistry Letters, 9(10), 1277-1280. c) D. Wöhrle, D., Schnurpfeil, G., & Knothe, G. (1992). Efficient synthesis of phthalocyanines and related macrocyclic compounds in the presence of organic bases. Dyes and Pigments, 18(2), 91-102. d) Seikel, E. (2012). Axial funktionalisierte Metallophthalocyanine und-porphyrazine als Funktionsmoleküle für optoelektronische Anwendungen (Doctoral dissertation, Philipps-Universität Marburg).

[33] Snow, A. W., Kadish, K. M., Smith, K. M., & Guilard, R. (2003). The porphyrin handbook. Phthalocyanine Aggregation, Elsevier Science, Amsterdam, 17, 129-173.

[34] a) Baumann, F., Bienert, B., Rösch, G., Vollmann, H., & Wolf, W. (1956). Isoindolenine als Zwischenprodukte der Phthalocyanin- Synthese. Angewandte Chemie, 68(4), 133-150. b) Allen, F. H., Kennard, O., Watson, D. G., Brammer, L., Orpen, A. G., & Taylor, R. (1987). Tables of bond lengths determined by X-ray and neutron diffraction. Part 1. Bond lengths in organic compounds. Journal of the Chemical Society, Perkin Transactions 2, (12), 1-19. c) Gaspard, S., & Maillard, P. (1987). Structure des phtalocyanines tetra tertio-butylees: mecanisme de la synthese. Tetrahedron, 43(6), 1083-1090. d) Gray, G. W., Hird, M., Lacey, D., & Toyne, K. J. (1989). The synthesis and transition temperatures of some 4, 4 ″-dialkyl-and 4, 4 ″-alkoxyalkyl-1, 1′: 4′, 1 ″-terphenyls with 2, 3-or 2′, 3′-difluoro substituents and of their biphenyl analogues. Journal of the Chemical Society, Perkin Transactions 2, (12), 2041-2053.

[35] Hurley, T. J., Robinson, M. A., & Trotz, S. I. (1967). Complexes derived from 1, 3-diiminoisoindoline-containing ligands. II. Stepwise formation of nickel phthalocyanine. Inorganic Chemistry, 6(2), 389-392.

[36] a) Meller, A., & Ossko, A. (1972). Phthalocyaninartige bor-komplexe. Monatshefte für Chemie/Chemical Monthly, 103(1), 150-155. b) Kietaibl, H. (1974). Die

Kristall-und Molekülstruktur eines neuratigen phthalocyaninähnlichen Borkomplexes. Monatshefte für Chemie/Chemical Monthly, 105(2), 405-418.

[37] a) Kobayashi, N. (1999). Synthesis, optical properties, structures and molecular orbital calculations of subazaporphyrins, subphthalocyanines, subnaphthalocyanines and related compounds. Journal of Porphyrins and Phthalocyanines, 3(6- 7), 453-467. b) Medina, A., & Claessens, C. G. (2009). Subphthalocyanines: synthesis, self-organization, properties and applications. Journal of Porphyrins and Phthalocyanines, 13(04), 446-454.

[38] Geyer, M., Plenzig, F., Rauschnabel, J., Hanack, M., Del Rey, B., Sastre, A., & Torres, T. (1996). Subphthalocyanines: preparation, reactivity and physical properties. Synthesis, 1996(09), 1139-1151.

[39] Claessens, C. G., González-Rodríguez, D., & Torres, T. (2002). Subphthalocyanines: singular nonplanar aromatic compounds synthesis, reactivity, and physical properties. Chemical reviews, 102(3), 835-854.

[40] Torres, T. (2006). From subphthalocyanines to subporphyrins. Angewandte Chemie International Edition, 45(18), 2834-2837.

[41] Claessens, C. G., González- Rodríguez, D., del Rey, B., Torres, T., Mark, G., Schuchmann, H. P., Nohr, R. S. (2003). Highly Efficient Synthesis of Chloro- and Phenoxy- Substituted Subphthalocyanines. European Journal of Organic Chemistry, 2003(14), 2547-2551.

[42] Claessens, C. G., González-Rodríguez, D., McCallum, C. M., Nohr, R. S., Schuchmann, H. P., & Torres, T. (2007). On the mechanism of boron-subphthalocyanine chloride formation. Journal of Porphyrins and Phthalocyanines, 11(03), 181-188.

[43] a) Kobayashi, N., Ishizaki, T., Ishii, K., & Konami, H. (1999). Synthesis, spectroscopy, and molecular orbital calculations of subazaporphyrins, subphthalocyanines, subnaphthalocyanines, and compounds derived therefrom by ring expansion1. Journal of the American Chemical Society, 121(39), 9096-9110. b) Stork, J. R., Potucek, R. J., Durfee, W. S., & Noll, B. C. (1999). The synthesis and structure of mixed subphthalocyaninesubnaphthalocyanine complexes. Tetrahedron letters, 40(46), 8055-8058.

[44] Geyer, M., Plenzig, F., Rauschnabel, J., Hanack, M., Del Rey, B., Sastre, A., & Torres, T. (1996). Subphthalocyanines: preparation, reactivity and physical properties. Synthesis, 1996(09), 1139-1151.

[45] Claessens, C. G., González-Rodríguez, D., & Torres, T. (2002). Subphthalocyanines: singular nonplanar aromatic compounds synthesis, reactivity, and physical properties. Chemical reviews, 102(3), 835-854.

[46] Medina, A., & Claessens, C. G. (2009). Subphthalocyanines: synthesis, self-organization, properties and applications. Journal of Porphyrins and Phthalocyanines, 13(04), 446-454.

[47] Guilard, R., Kadish, K. M., Smith, K. M., & Guilard, R. (2003). The porphyrin handbook (Vol. 18, pp. 303-349). New York: Academic Press.

[48] Barrett, P. A., Frye, D. A., & Linstead, R. P. (1938). Phthalocyanines and associated compounds. Part XIV. Further investigations of metallic derivatives. Journal of the Chemical Society (Resumed), 1157-1163.

[49] Dolphin, D., Sams, J. R., Tsin, T. B., Ittel, S. D., & Cushing Jr, M. A. (1980). Metallophthalocyanins and Benzoporphines. Inorganic Syntheses, 20, 155-161.

[50] Barrett, P. A., Dent, C. E., & Linstead, R. P. (1936). 382. Phthalocyanines. Part VII. Phthalocyanine as a co-ordinating group. A general investigation of the metallic derivatives. Journal of the Chemical Society (Resumed), 1719-1736.

[51] Tomoda, H., Saito, S., & Shiraishi, S. (1983). Synthesis of metallophthalocyanines from phthalonitrile with strong organic bases. Chemistry Letters, 12(3), 313-316.

[52] Paillaud, J. L., Drillon, M., Decian, A., Fischer, J., Weiss, R., Poinsot, R., & Herr, A. (1991). Organic ferromagnetic chain in the yttrium diphthalocyanine [YPc2]· CH2Cl2: X-ray structure and magnetic behavior. Physica B: Condensed Matter, 175(4), 337-348.

[53] Iwase, A., Harnoode, C., & Kameda, Y. (1993). Synthesis and electrochemistry of double-decker lanthanoid (III) phthalocyanine complexes. Journal of alloys and compounds, 192(1-2), 280-283.

[54] Jiang, J., Xie, J., Choi, M. T., Yan, Y., Sun, S., & Ng, D. K. (1999). Double-decker yttrium (III) complexes with phthalocyaninato and porphyrinato ligands. Journal of Porphyrins and Phthalocyanines, 3(4), 322-328.

[55] Jiang, J., Xie, J., Ng, D. K., & Yan, Y. (1999). Synthesis, spectroscopic, and electrochemical properties of homoleptic bis (substituted-phthalocyaninato) cerium (IV) complexes. Molecular Crystals and Liquid Crystals Science and Technology. Section A. Molecular Crystals and Liquid Crystals, 337(1), 385-388.

[56] Linsky, J. P., Paul, T. R., Nohr, R. S., & Kenney, M. E. (1980). Studies of a series of haloaluminum,-gallium, and-indium phthalocyanines. Inorganic Chemistry, 19(10), 3131-3135.

[57] Napier, A., & Collins, R. A. (1994). FTIR characteristics of halogenated phthalocyanines exhibiting polymorphism. Thin solid films, 248(2), 166-177.

[58] Ejsmont, K., & Kubiak, R. (1997). Isostructural Complexes of Diiodo (phthalocyaninato) germanium (IV) and Diiodo (phthalocyaninato) tin (IV). Acta Crystallographica Section C: Crystal Structure Communications, 53(8), 1051-1054.

[59] Edmondson, S. J., & Mitchell, P. C. (1986). Molybdenum phthalocyanine. Polyhedron, 5(1-2), 315-317.

[60] Tomoda, H., Saito, S., & Shiraishi, S. (1983). Synthesis of metallophthalocyanines from phthalonitrile with strong organic bases. Chemistry Letters, 12(3), 313-316.

[61] Münz, X., & Hanack, M. (1988). Synthese von (Phthalocyaninato) rhodium (III)-Komplexen. Chemische Berichte, 121(2), 239-242.

[62] de la Torre, G., Claessens, C. G., & Torres, T. (2000). Phthalocyanines: The need for selective synthetic approaches. European Journal of Organic Chemistry, 2000(16), 2821-2830.

[63] Kadish, K., Smith, K. M., & Guilard, R. (Eds.). (2003). The Porphyrin Handbook: Phthalocyanines: Properties and Materials (Vol. 17). Elsevier.

[64] McKeown, N. B. (2003). Science of Synthesis, vol. 17. Thieme Stuttgart.

[65] Mack, J., & Kobayashi, N. (2010). Low symmetry phthalocyanines and their analogues. Chemical reviews, 111(2), 281-321.

[66] Kadish, K., Smith, K. M., & Guilard, R. (2003). The Porphyrin Handbook Vol. 20, Elsevier Science, San Diego, California, USA.

[67] De La Torre, G. E. M. A., Vazquez, P., Agullo-Lopez, F., & Torres, T. (1998). Phthalocyanines and related compounds: organic targets for nonlinear optical applications. Journal of Materials Chemistry, 8(8), 1671-1683.

[68] Kobayashi, N., Kondo, R., Nakajima, S., & Osa, T. (1990). New route to unsymmetrical phthalocyanine analogs by the use of structurally distorted subphthalocyanines. Journal of the American Chemical Society, 112(26), 9640-9641.

[69] Leznoff, C. C., & Hall, T. W. (1982). The synthesis of a soluble, unsymmetrical phthalocyanine on a polymer support. Tetrahedron Letters, 23(30), 3023-3026.

[70] Nolan, K. J. M., Hu, M., & Leznoff, C. C. (1997). Not Logged In Login. Synlett, 1997(5), 593-594.

[71] Schweizer, H. R. (1964). Geschichtliches. In Künstliche Organische Farbstoffe und Ihre Zwischenprodukte (pp. 3-9). Springer, Berlin, Heidelberg.

[72] Buchler, J. W., & Dolphin, D. (1978). The Porphyrins. by D. Dolphin, Academic Press, New York, 1, 389.

[73] Schnurpfeil, G., Sobbi, A. K., Spiller, W., Kliesch, H., & Wöhrle, D. (1997). Photo-oxidative stability and its correlation with semi-empirical MO calculations of various tetraazaporphyrin derivatives in solution. Journal of Porphyrins and Phthalocyanines, 1(02), 159-167.

[74] Micali, N., Monsu'Scolaro, L., Romeo, A., & Mallamace, F. (1998). Fractal aggregation in aqueous solutions of porphyrins. Physica A: Statistical Mechanics and its Applications, 249(1-4), 501-510.

[75] Owens, J. W., Smith, R., Robinson, R., & Robins, M. (1998). Photophysical properties of porphyrins, phthalocyanines, and benzochlorins. Inorganica chimica acta, 279(2), 226-231.

[76] Kantekin, H., Rakap, M., Gök, Y., & Şahinbaş, H. Z. (2007). Synthesis and characterization of new metal-free and phthalocyanine nickel (II) complex containing macrocyclic moieties. Dyes and pigments, 74(1), 21-25.

[77] Wöhrle, D., Tausch, M. W., Stohrer, W.-D. (1998). „Photochemie", Konzepte, Methoden, Experimente. Weinheim: Wiley-VCH. S. 117.

[78] a) Wöhrle, D. (1993). Phthalocyanines: Properties and applications. Edited by CC Leznoff and ABP Lever, VCH, Weinheim. Volume 1, 1989, 436 pp., ISBN 3-527- 26955- X; Volume 2, 1993, 305 pp., DM 268, ISBN 3- 527- 89544- 2. Advanced Materials, 5(12), 942-943. b) Ballesteros Moyano, B. (2008). Nuevos

sistemas dador-aceptor ftalocianina-fullereno y ftalocianina-nanotubo: síntesis, caracterización y estudios fotofísicos.

[79] Ballesteros Moyano, B. (2008). Nuevos sistemas dador-aceptor ftalocianina-fullereno y ftalocianina-nanotubo: síntesis, caracterización y estudios fotofísicos.

[80] Piechocki, C., Simon, J., Skoulios, A., Guillon, D., & Weber, P. (1982). Annelides. 7. Discotic mesophases obtained from substituted metallophthalocyanines. Toward liquid crystalline one-dimensional conductors. Journal of the American Chemical Society, 104(19), 5245-5247.

[81] a) Van Nostrum, C. F., & Nolte, R. J. (1996). Functional supramolecular materials: self-assembly of phthalocyanines and porphyrazines. Chemical Communications, (21), 2385-2392. b) Hoogboom, J., Garcia, P. M., Otten, M. B., Elemans, J. A., Sly, J., Lazarenko, S. V., Nolte, R. J. (2005). Tunable command layers for liquid crystal alignment. Journal of the American Chemical Society, 127(31), 11047-11052.

[82] a) Collins, G. E., Williams, V. S., Chau, L. K., Nebesny, K. W., England, C., Lee, P. A., Armstrong, N. R. (1993). Epitaxial phthalocyanine thin films and phthalocyanine/C60 multilayers. Synthetic metals, 54(1-3), 351-362. b) Yoon, M. H., Facchetti, A., Stern, C. E., & Marks, T. J. (2006). Fluorocarbon-modified organic semiconductors: molecular architecture, electronic, and crystal structure tuning of arene-versus fluoroarene-thiophene oligomer thin-film properties. Journal of the American Chemical Society, 128(17), 5792-5801.

[83] a) Minami, N., Sasaki, K., & Tsuda, K. (1983). Improvement of the performance of particulate phthalocyanine photovoltaic cells by the use of polar polymer binders. Journal of applied physics, 54(11), 6764-6766. b) Ostuni, R., Larciprete, M. C., Leahu, G., Belardini, A., Sibilia, C., & Bertolotti, M. (2007). Optical limiting behavior of zinc phthalocyanines in polymeric matrix. Journal of applied physics, 101(3), 033116.

[84] a) Cook, M. J. (1996). Thin film formulations of substituted phthalocyanines. Journal of Materials Chemistry, 6(5), 677-689. b) Cook, M. J. (1999). Phthalocyanine thin films. Pure and Applied Chemistry, 71(11), 2145-2151. c) Xiao, S., Myers, M., Miao, Q., Sanaur, S., Pang, K., Steigerwald, M. L., & Nuckolls, C. (2005). Molecular wires from contorted aromatic compounds. Angewandte Chemie International Edition, 44(45), 7390-7394.

[85] a) Petty, M. C., & Barlow, W. A. (1990). In Langmuir–Blodgett Films, Ed. GG Roberts. b) Peterson, I. R. (1990). Langmuir-blodgett films. Journal of Physics D: Applied Physics, 23(4), 379. c) Ulman, A. (2013). An Introduction to Ultrathin Organic Films: From Langmuir--Blodgett to Self--Assembly. Academic press.

[86] a) Ulman, A. (1996). Formation and structure of self-assembled monolayers. Chemical reviews, 96(4), 1533-1554. b) Ulman, A. (1998). Self-Assembled Monolayers of Thiols. Academic Press, San Diego.

[87] a) Lever, A. P. (1965). The phthalocyanines. In Advances in Inorganic Chemistry and Radiochemistry (Vol. 7, pp. 27-114). Academic Press. b) de la Torre, G., Claessens, C. G., & Torres, T. (2007). Phthalocyanines: old dyes, new materials. Putting color in nanotechnology. Chemical communications, (20), 2000-2015.

[88] a) Hanack, M., & Lang, M. (1994). Conducting stacked metallophthalocyanines and related compounds. Advanced Materials, 6(11), 819-833. b) Cammidge, A. N., Nekelson, F., Helliwell, M., Heeney, M. J., & Cook, M. J. (2005). A capping methodology for the synthesis of lower μ-oxo-phthalocyaninato silicon oligomers. Journal of the American Chemical Society, 127(47), 16382-16383.

[89] a) Sly, J., Kasák, P., Gomar-Nadal, E., Rovira, C., Górriz, L., Thordarson, P., Nolte, R. J. (2005). Chiral molecular tapes from novel tetra (thiafulvalene-crown-ether)-substituted phthalocyanine building blocks. Chemical Communications, (10), 1255-1257. b) Kobayashi, N., Togashi, M., Osa, T., Ishii, K., Yamauchi, S., & Hino, H. (1996). Low symmetrical phthalocyanine analogues substituted with three crown ether voids and their cation-induced supermolecules. Journal of the American Chemical Society, 118(5), 1073-1085.

[90] Tong, W. Y., Djurišić, A. B., Xie, M. H., Ng, A. C. M., Cheung, K. Y., Chan, W. K., Gwo, S. (2006). Metal phthalocyanine nanoribbons and nanowires. The Journal of Physical Chemistry B, 110(35), 17406-17413.

[91] Tsaryova, O. (2006). Darstellung und Untersuchung der photochemischen und photosensibilisierenden Eigenschaften verschieden substituierter Zn (II)-Phthalocyanine (Doctoral dissertation, Staats-und Universitätsbibliothek [Host]).

[92] Ballesteros Moyano, B. (2008). Nuevos sistemas dador-aceptor ftalocianina-fullereno y ftalocianina-nanotubo: síntesis, caracterización y estudios fotofísicos.

[93] Wöhrle, D., Schnurpfeil, G., Makarov, S., & Suvorova, S. (2012). Von Farbmitteln zu Materialien für Optik und Photoelektronik Phthalocyanine. Chem. Unserer. Zeit, 46, 12-24.

[94] a) Erk, P., Hengelsberg, H., Kadish, K. M., Smith, K. M., & Guilard, R. (2003). The Porphyrin Handbook. Kadish, KM, 106-146. b) Löbbert, G. (1992). Phthalocyanines, Ullmann's Encyclopedia of Industrial Chemistry, Vol. A 20, S. 213–241.

[95] Kadish, K., Smith, K. M., & Guilard, R. (Eds.). (2003). The porphyrin handbook (Vol. 3). Elsevier Science, San Diego.

[96] a) Rager, C., Schmid, G., & Hanack, M. (1999). Influence of Substituents, Reaction Conditions and Central Metals on the Isomer Distributions of 1 (4)-Tetrasubstituted Phthalocyanines. Chemistry–A European Journal, 5(1), 280-288. b) Görlach, B., Dachtler, M., Glaser, T., Albert, K., & Hanack, M. (2001). Synthesis and Separation of Structural Isomers of 2 (3), 9 (10), 16 (17), 23 (24)-Tetrasubstituted Phthalocyanines. Chemistry–A European Journal, 7(11), 2459-2465.

[97] Makarov, S. G., Suvorova, O. N., & Wöhrle, D. (2011). Conjugated di-and trinuclear phthalocyanines and their analogs. Journal of Porphyrins and Phthalocyanines, 15(09), 791-808.

[98] a) Wang, Y., Deng, K., Gui, L., Tang, Y., Zhou, J., Cai, L., Wang, Y. (1999). Preparation and characterization of nanoscopic organic semiconductor of oxovanadium phthalocyanine. b) Wang, Y., & Liang, D. (2010). Solvent-Stabilized Photoconductive Metal Phthalocyanine Nanoparticles: Preparation and Application in Single- Layered Photoreceptors. Advanced Materials, 22(13), 1521-1525.

[99] Römer, M., & Becker, W. (2009). "Beitrag der Chemie zum flachen Fernseher: Die Welt wird flacher". Chem. Unserer Zeit, 43, 94-99.

[100] Demonstration der additiven Farbmittel: Techtower, www. techtower.de/subcontent/inf_experimente.php?zu=1&von=1#ziel (Juni 2011).

[101] a) Brabec, C. J., Cravino, A., Meissner, D., Sariciftci, N. S., Fromherz, T., Rispens, M. T., ... & Hummelen, J. C. (2001). Origin of the open circuit voltage of plastic solar cells. Advanced Functional Materials, 11(5), 374-380. b) Cravino, A.,

& Sariciftci, N. S. (2002). Double-cable polymers for fullerene based organic optoelectronic applications. Journal of Materials Chemistry, 12(7), 1931-1943. c) Winder, C., & Sariciftci, N. S. (2004). Low bandgap polymers for photon harvesting in bulk heterojunction solar cells. Journal of Materials Chemistry, 14(7), 1077-1086. d) Sariciftci, N. S. (2004). Plastic photovoltaic devices. Materials today, 7(9), 36-40.

[102] a) Deng, H., Mao, H., Lu, Z., Li, J., & Xu, H. (1997). Cosensitization of a nanostructured TiO2 electrode with tetrasulfonated gallium phthalocyanine and tetrasulfonated zinc porphyrin. Journal of Photochemistry and Photobiology A: Chemistry, 110(1), 47-52. b) Bach, U., Lupo, D., Comte, P., Moser, J. E., Weissörtel, F., Salbeck, J., Grätzel, M. (1998). Solid-state dye-sensitized mesoporous TiO$_2$ solar cells with high photon-to-electron conversion efficiencies. Nature, 395(6702), 583-585. c) Burke, A., Ito, S., Snaith, H., Bach, U., Kwiatkowski, J., & Grätzel, M. (2008). The function of a TiO$_2$ compact layer in dye-sensitized solar cells incorporating "planar" organic dyes. Nano letters, 8(4), 977-981. d) Grätzel, M. (2001). Photoelectrochemical cells. nature, 414(6861), 338.

[103] a) Kobayashi, N., Muranaka, A., & Ishii, K. (2000). Symmetry-Lowering of the Phthalocyanine Chromophore by a C 2 Type Axial Ligand. Inorganic chemistry, 39(11), 2256-2257. b) Odobel, F., & Zabri, H. (2005). Preparations and characterizations of bichromophoric systems composed of a ruthenium polypyridine complex connected to a difluoroborazaindacene or a zinc phthalocyanine chromophore. Inorganic chemistry, 44(16), 5600-5611. c) Pei, L., Zhang, J., & Kong, W. (2007). Electronic polarization spectroscopy of metal phthalocyanine chloride compounds in superfluid helium droplets. The Journal of chemical physics, 127(17), 174308.

[104] Halls, J. J. M., Walsh, C. A., Greenham, N. C., Marseglia, E. A., Friend, R. H., Moratti, S. C., & Holmes, A. B. (1995). Efficient photodiodes from interpenetrating polymer networks. Nature, 376(6540), 498-500.

[105] Sariciftci, N. S., Braun, D., Zhang, C., Srdanov, V. I., Heeger, A. J., Stucky, G., & Wudl, F. (1993). Semiconducting polymer- buckminsterfullerene heterojunctions: Diodes, photodiodes, and photovoltaic cells. Applied physics

letters, 62(6), 585-587. b) Yu, G., Gao, J., Hummelen, J. C., Wudl, F., & Heeger, A. J. (1995). Polymer photovoltaic cells: enhanced efficiencies via a network of internal donor-acceptor heterojunctions. Science, 270(5243), 1789-1791. c) Wienk, M. M., Kroon, J. M., Verhees, W. J., Knol, J., Hummelen, J. C., van Hal, P. A., & Janssen, R. A. (2003). Efficient methano [70] fullerene/MDMO- PPV bulk heterojunction photovoltaic cells. Angewandte Chemie International Edition, 42(29), 3371-3375.

[106] a) Tang, C. W. (1986). Two- layer organic photovoltaic cell. Applied physics letters, 48(2), 183-185. b) Siebentritt, S., Günster, S., & Meissner, D. (1991). Junction effects in phthalocyanine thin film solar cells. Synthetic Metals, 41(3), 1173-1176.

[107] Wöhrle, D., & Hild, O. R. (2010). Organische Solarzellen. Energie der Zukunft. Chemie in unserer Zeit, 44(3), 174-189.

[108] Fraunhofer Institut, www.ipms.fraunhofer.de/de/applications/ organic-electronics/photovoltaics.html (June 2011).

[109] Walzer, K., Maennig, B., Pfeiffer, M., & Leo, K. (2007). Highly efficient organic devices based on electrically doped transport layers. Chemical reviews, 107(4), 1233-1271.

[110] Crucius, G. (2013). Synthesen nichtperipher glykokonjugierter Zink (II) phthalocyanine (Doctoral dissertation).

[111] a) Josefsen, L. B., & Boyle, R. W. (2012). Unique diagnostic and therapeutic roles of porphyrins and phthalocyanines in photodynamic therapy, imaging and theranostics. Theranostics, 2(9), 916. b) Hamblin, M. R., & Hasan, T. (2004). Photodynamic therapy: a new antimicrobial approach to infectious disease?. Photochemical & Photobiological Sciences, 3(5), 436-450.

[112] Patrice, T. (Ed.). (2003). Photodynamic therapy (Vol. 2). Royal Society of Chemistry.

[113] Tappeiner, H. V., & Jodlbauer, A. (1904). Über die Wirkung der photodynamischen (fluoreszierenden) Stoffe auf Infusorien. Dtsch Arch Klin Med, 80, 427-487.

[114] Tappeiner, H. V. (1903). Therapeutische Versuche mit fluoreszierenden Stoffen. Munch Med Wochenschr, 1, 2042-2044.

[115] Jesionek, A., & Von Tappeiner, H. (1905). On the treatment of skin cancers with fluorescent substances. Arch Klin Med, 82, 223-227.

[116] Hirth, A., Michelsen, U., & Woehrle, D. (1999). Photodynamische tumortherapie. Chemie in unserer Zeit, 33(2), 84-94.

[117] a) Moan, J. (1986). Porphyrin photosensitization and phototherapy. Photochemistry and photobiology, 43(6), 681-690. b) Moan, J., & Berg, K. (1992). Photochemotherapy of cancer: experimental research. Photochemistry and Photobiology, 55(6), 931-948.

[118] Whitacre, C. M., Feyes, D. K., Satoh, T., Grossmann, J., Mulvihill, J. W., Mukhtar, H., & Oleinick, N. L. (2000). Photodynamic therapy with the phthalocyanine photosensitizer Pc 4 of SW480 human colon cancer xenografts in athymic mice. Clinical Cancer Research, 6(5), 2021-2027.

[119] a) Allen, C. M., Sharman, W. M., & Van Lier, J. E. (2001). Current status of phthalocyanines in the photodynamic therapy of cancer. Journal of Porphyrins and Phthalocyanines, 5(02), 161-169. b) Dolmans, D. E., Fukumura, D., & Jain, R. K. (2003). Photodynamic therapy for cancer. Nature reviews cancer, 3(5), 380.

[120] Brasseur, N. (2003). Sensitizers for PDT: phthalocyanines. Photodynamic Therapy. The Royal Society of Chemistry, 105-18.

[121] Glebe, U. (2012). Selbstassemblierte Monolagen und magnetisch strukturierte Submonolagen mit dia-und paramagnetischen Molekülen sowie Einzelmolekülmagneten auf Phthalocyanin-und Subphthalocyanin-Basis (Doctoral dissertation).

[122] Mckeown, N. B. (2004). Science of Synthesis, Vol. 17, Georg Thieme Verlag, Stuttgart, New York.

[123] Seikel, E. (2012). Axial funktionalisierte Metallophthalocyanine und-porphyrazine als Funktionsmoleküle für optoelektronische Anwendungen (Doctoral dissertation, Philipps-Universität Marburg).

[124] a) Wöhrle, D., Eskes, M., Shigehara, K., & Yamada, A. (1993). A Simple Synthesis of 4, 5-Disubstituted 1, 2-Dicyanobenzenes and 2, 3, 9, 10, 16, 17, 23, 24-Octasubstituted Phthalocyanines. Synthesis, 1993(02), 194-196. b) Atalay, Ş., Çoruh, U., Akdemir, N., & Ağar, E. (2004). C—H··· π interactions in 4, 5-bis (2-

isopropyl-5-methylphenoxy) phthalonitrile. Acta Crystallographica Section E: Structure Reports Online, 60(2), 303-305.

[125] Nyokong, T. (2007). Effects of substituents on the photochemical and photophysical properties of main group metal phthalocyanines. Coordination Chemistry Reviews, 251(13-14), 1707-1722.

[126] Becker, H. G., Böttcher, H., Dietz, F., Rehorek, D., Roewer, G., Schiller, K., & Timpe, H. J. (1983). Einführung in die Photochemie. Stuttgart, New York: Georg Thieme Verlag.

[127] Tsaryova, O. (2006). Darstellung und Untersuchung der photochemischen und photosensibilisierenden Eigenschaften verschieden substituierter Zn (II)-Phthalocyanine (Doctoral dissertation, Staats-und Universitätsbibliothek [Host]).

[128] Klessinger, M. (1989). Physikalische organische Chemie. Verlag Chemie.

[129] Freyer, W., & Minh, L. Q. (1986). Synthesis of Metal Complexes of Tetra(2, 3-anthra)tetraazaporphin and Comparison of Their Electronic Absorption Spectra with Other Linearly Annellated Tetraazaporphin Systems. Chemischer Informationsdienst, 17(34), no-no.

[130] Darwent, J. R., Douglas, P., Harriman, A., Porter, G., & Richoux, M. C. (1982). Metal phthalocyanines and porphyrins as photosensitizers for reduction of water to hydrogen. Coordination Chemistry Reviews, 44(1), 83-126.

[131] Wohrle, D., Weitemeyer, A., Sobbi, A. K., Michelsen, U., & Kliesch, H. (1996). Monofunctional phthalocyanine derivatives as potential sensitizers for PDT. In Photochemotherapy: Photodynamic Therapy and Other Modalities (Vol. 2625, pp. 319-327). International Society for Optics and Photonics.

[132] Freyer, W., & Minh, L. Q. (1986). Synthesis of Metal Complexes of Tetra- (2, 3- anthra)- tetraazaporphin and Comparison of Their Electronic Absorption Spectra with Other Linearly Annellated Tetraazaporphin Systems. Chemischer Informationsdienst, 17(34).

[133] Becker, H. G., Böttcher, H., Dietz, F., Rehorek, D., Roewer, G., Schiller, K., & Timpe, H. J. (1983). Einführung in die Photochemie. Stuttgart, New York: Georg Thieme Verlag.

[134] Klessinger, M. (1989). Physikalische organische Chemie. Verlag Chemie.

[135] Grofcsik, A., Baranyai, P., Bitter, I., Csokai, V., Kubinyi, M., Szegletes, K., Vidóczy, T. (2004). Triple state properties of tetrasubstituted zinc phthalocyanine derivatives. Journal of molecular structure, 704(1-3), 11-15.

[136] d'Alessandro, N., Tonucci, L., Morvillo, A., Dragani, L. K., Di Deo, M., & Bressan, M. (2005). Thermal stability and photostability of water solutions of sulfophthalocyanines of Ru (II), Cu (II), Ni (II), Fe (III) and Co (II). Journal of organometallic chemistry, 690(8), 2133-2141.

[137] Gerdes, R. (2000). Niedermolekulare und immobilisierte Phthalocyanintetrasulfonsäuren als Photosensibilisatoren für die Photooxidation von Phenol und Chlorphenolen. na.

[138] Sobbi, A. (1994). Niedermolekulare Porphyrine und ihre Kombination mit anorganischen Trägern: Synthese, Untersuchungen zur Stabilität und Eignung als Materialien zur optischen Datenspeicherung (Doctoral dissertation, Verlag nicht ermittelbar).

[139] Zorlu, Y., Dumoulin, F., Durmuş, M., & Ahsen, V. (2010). Comparative studies of photophysical and photochemical properties of solketal substituted platinum (II) and zinc (II) phthalocyanine sets. Tetrahedron, 66(17), 3248-3258.

CURRICULUM VITAE

Name & Surname: Rovshen Atajanov

Place / Date of Birth: 31.03.1995 / Dashoguz, Turkmenistan

Marital Status: Single

Contact: rovshenatajanov@gmail.com

Education

High School: Koneurgench City School Nr 8 (2008-2012)
Dashoguz / Turkmenistan

Bachelor's degree: Biology Education (2012-2017)
Marmara University, Istanbul / Turkey

Erasmus: Master's program in Organic Chemistry (2019)
Technische Universität Clausthal, Clausthal-Zellerfeld, Germany

Poster Presentations

Atajanov, R., Durmuş, M., Odabaş, Z. (2018, November). *Synthesis, characterization and photodynamic activity of new thymol substituted phthalocyanines.* PP-163/ 30.National Chemistry Congress, Famagusta / Northern Cyprus.

Atajanov, R., Odabas, Z. (2018, November). *Synthesis and spectral properties of new thymol substituted azo bridged phthalocyanines.* PP-163/ 30.National Chemistry congress, Famagusta / Northern Cyprus.

Huraibat, B., Atajanov, R., Orman, E. B., Odabaş, Z., Ozkaya, A. R. (2018, September). *Electrochemical, spectroelectrochemical, electrocolorimetric and electrocatalytic properties of new metal phthalocyanine compounds.* M19-PS3-20060 / 1st International Balkan Chemistry Congress, Edirne / Turkey.

Funded research projects
Marmara University BAPKO (Scientific Research Projects Unit)
Title: "*Antimikrobiyal ve antifungal özellikli terpenoidlerden olan timol ve türevi bileşiklerden, metalli ve metalsiz ftalosiyaninlerin sentezi ve karakterizasyonu*".
NO: FEN-C-YLP-120418-0164